# Spectral Decomposition in Fixed Income: Leveraging Principal Components for Portfolio Analysis and Macroeconomic Interpretation

Master's Thesis

submitted by **Robin Sell**

on December 20, 2023

Department of Mathematics and Computer Science
University of Cologne

Supervisor: Prof. Dr. Dr. Hanspeter Schmidli

**Acknowledgement**

I want to thank Prof. Dr. Dr. Schmidli for his support in realizing my conceptual ideas in the context of this Master's thesis. His responses to my queries played a crucial role in shaping and improving the quality of my thesis.

Furthermore, I thank Mr. Henning Mensch and Dr. Nicolas Vogelpoth for their significant contributions. With their extensive experience in fixed income investment banking, they provided invaluable insights and participated in thoughtful discussions that not only shaped the original structure of my thesis but also refined its content.

In addition, I would like to thank my colleague Mr. Mathis Markarski for constructive discussions that helped to improve ideas and their realization.

I am grateful for their support, which contributed to successfully completing my Master's thesis.

## Abstract

This thesis deals with the fixed income market and focuses on the challenges related to the interest rate curve. It initially divides the issue into three parts: Building a comprehensive historical context by combining multiple datasets, calculating this history in detail across different maturities, and uncovering the underlying patterns in yield curve changes for macroeconomic interpretations.

The study combines a dataset covering over 50 years by combining German government bonds, Deutsche Mark swaps, and Euro swaps. A Brownian bridge helps to generate daily data from monthly government bond yields. This thesis employs cubic interpolation and the Nelson-Siegel-Svensson (NSS) model to address inconsistent maturities in historical quotes, with the latter being used for further analysis. Principal Component Analysis (PCA) identifies the underlying patterns in the changes in the interest rate curve across the extended historical dataset and provides insights into macroeconomic relationships. For the practical example, three clusters of yield curve shapes are identified, and specific portfolios consisting of individual forward rate swaps are analyzed for their sensitivity to macroeconomic changes using delta buckets and the previously calculated principal components.

The dataset is also clustered using different yield curve shapes to analyze various macroeconomic environments and to be able to make implied adjustments. Linking the generated principal components with portfolio sensitivities enables portfolio managers to tailor the allocation of derivatives in risk analyses. This approach serves as a dynamic instrument for constructing portfolios with explicit exposures and offers a variety of potential use cases.

In essence, this thesis provides concrete applications and valuable insights but also creates a flexible framework that can be easily applied to interest rate markets outside of the European market examined in this study. This illustrates the versatility and broader applicability of the implications of this thesis. The entire framework code of this thesis can be found in the appendix.

# Contents

# List of Figures

# List of Tables

# 1. Introduction

This thesis navigates one of the core challenges in the fixed income market: Establishing a link between classical macroeconomic shifts and the yield curve. Starting from a mathematical basis in the first chapter, three interrelated topics are systematically addressed: Creating a large historical context by combining different datasets, calculating swap rates over different maturities, and identifying yield curve patterns. Notably, a carefully crafted 50-year dataset, cluster-based analysis of swap curve shapes, and the linkage of principal components to portfolio sensitivities contribute to insightful applications. This compact journey aims to unveil the dynamics connecting classical macroeconomics and the yield curve, offering valuable perspectives for both theoretical understanding and practical portfolio management.

## 1.1. Financial Instruments: Bonds, Interest Rate Swaps and Forward Swaps

In modern finance, the concept of interest rates is a crucial element and embodies the time-value relationship inherent in the financial markets. An interest rate ($r$) represents the cost of borrowing capital or the return on investment over a specified period, typically expressed as a percentage. This fundamental financial parameter serves as the principal instrument in pricing financial assets, from debt securities to derivative contracts.

Mathematically, interest rates are defined as the ratio of the interest earned or paid ($I$) to the principal amount ($P$) over a given time interval ($t$). In its simplest form, this is defined by $I = P \times r \times t$, where $r$ denotes the nominal interest rate. Often, this interest rate is compounded periodically within a year. This is expressed by the discrete compound interest formula

$$A = P\left(1+\frac{r}{n}\right)^{nt} \quad , \tag{1.1}$$

where $A$ signifies the future value of the investment and $n$ denotes the number of compounding periods per annum.

To obtain the continuous compound interest formula, we aim to approach the limit as $n$ tends towards infinity:

$$\lim_{n\to\infty} P\left(1+\frac{r}{n}\right)^{nt} \quad . \tag{1.2}$$

Leveraging the representation of the $e$ function as a limit of a sequence

$$e = \lim_{m\to\infty}\left(1+\frac{1}{m}\right)^{m} \quad , \tag{1.3}$$

setting $n = mr$ and separating the exponent by parenthesizing accordingly, we arrive at:

$$P\left(\lim_{m\to\infty}\left(1+\frac{1}{m}\right)^{m}\right)^{rt} \quad . \tag{1.4}$$

Simplifying, we get the expression for the continuous compounded future value:

$$A = Pe^{rt} \quad . \tag{1.5}$$

The concept of continuous compounding smoothly integrates interest rates. It is used to such a great extent in pricing derivatives that it is often used in textbooks to explain different mathematical concepts in the financial market. For practical purposes, continuous compounding aligns closely with daily compounding, facilitating ease of understanding and application within financial calculations [34]. To transition between discrete and continuous compounding, a pivotal approach is to equate the formulas (1.1) and (1.5):

$$Pe^{r_c t} = P\left(1+\frac{r_n}{n}\right)^{nt} \quad . \tag{1.6}$$

This equation enables the flawless conversion of interest rates $r_c$ compounded continuously and those $r_n$ compounded $n$ times per annum, resulting in

$$r_c = n\ln\left(1+\frac{r_n}{n}\right) \qquad \text{and} \qquad r_n = n\left(e^{r_c/n}-1\right) \quad . \tag{1.7}$$

Interest rates play a central role in the labyrinth of financial markets and serve as the central driver for the dynamics of asset pricing, portfolio allocation, and risk management.

The profound role of interest rates can be accurately encapsulated through the Future Value ($FV$) and the Present Value ($PV$):

$$FV = PV\left(1+\frac{r}{n}\right)^{nt} \qquad \text{resp.} \qquad FV = PVe^{r_c t} \quad . \tag{1.8}$$

For determining the investment required today to achieve a desired Future Value, we utilize the inverse form of the above equations:

$$PV = \frac{FV}{(1+\frac{r_n}{n})^{nt}} \qquad \text{resp.} \qquad PV = FVe^{-r_c t} \quad . \tag{1.9}$$

If $FV = 1$, this results in the concept of the Discount Factor $d$

$$d(t_0, t) = PV = \frac{1}{(1+\frac{r_n}{n})^{nt}} \qquad \text{resp.} \qquad d = e^{-r_c t} \quad , \tag{1.10}$$

which represents the present value of a unit of currency to be received at a future time $t$, considering different compounding frequencies or continuous compounding [54]. These simple yet meaningful equations underscore the inverse relationship between the discount rate and the present value of future cash flows. As interest rates fluctuate, the present value of future cash flows adjusts correspondingly, forming the basis for asset valuation across various financial instruments.

As a brief perspective, the dividend discount model (DDM) offers a mathematical manifestation of this effect [38]. The model is based on the notion that the stock's present-day price, when discounted back to its present value, represents the value of all of its potential future dividends. Regardless of the market's state, the DDM aims to determine a stock's fair value. The stock is undervalued if the DDM value exceeds the market price. The inverse is true if the DDM value is smaller. For a dividend $D$ and an anticipated growth rate for dividends $g$ of any period, the equity value $V_{eq}$ is defined as

$$V_{eq} = \frac{D}{d-g} \quad . \tag{1.11}$$

Assuming a perpetuity of constant dividends $D$ with a growth rate of $g = 0$, it is evident that a higher discount rate $d$ results in a lower equity value, showcasing the sensitivity of equity prices to fluctuations in interest rates.

Turning back to the fixed income markets, the impact of interest rates is deeply rooted in the relationship between bond prices, yields, and the time value of money. As debt instruments, bonds promise periodic coupon payments and a bond's principal, also known as face value, upon maturity. The present value of these future cash flows, discounted at the prevailing interest rate, determines the bond's price.

Introducing the zero-coupon interest rate, wherein no intermediate payments are made, is of central importance. This rate, often called the spot rate or zero rate, is critical. For instance, envision a 3-year zero rate with continuous compounding, quoted at 4% per annum. If 100€ are invested, this grows to 100€ $\times e^{0.04\times 3} = 112.75$€.

Most bonds follow a pattern of periodic coupon payments throughout their lifespan, culminating in the repayment of their face value at maturity. As established earlier, the theoretical bond price is computed as the sum of all expected future cash flows, mathematically expressed as

$$PV = \sum_{i=1}^{N} c_i d_i \quad , \tag{1.12}$$

where $c_i$ is the future cash flows, and $d_i$ is the discount factor for each corresponding payment. To provide a concrete illustration for (1.12), let us assume a 1-year bond with a face value of 100€ and quarterly coupon payments at a rate of 4% per annum. The requisite zero rates for maturities of $[0.25, 0.5, 0.75, 1]$ are given by $[3.5\%, 4.0\%, 4.4\%, 4.7\%]$ respectively. Consequently, the theoretical bond price is calculated as follows:

$$1 \cdot e^{-0.035\times 0.25} + 1 \cdot e^{-0.040\times 0.50} + 1 \cdot e^{-0.044\times 0.75} + 101 \cdot e^{-0.047\times 1.00} = 99.30[€] \quad . \tag{1.13}$$

Assuming that this theoretical price aligns with the market value, the goal is to determine the bond yield, the single discount rate applied to all cash flows, often called yield to maturity (YTM). This involves solving the equation

$$1 \cdot e^{-y\times 0.25} + 1 \cdot e^{-y\times 0.50} + 1 \cdot e^{-y\times 0.75} + 101 \cdot e^{-y\times 1.00} = 99.30[€] \tag{1.14}$$

resulting in $y = 4.69\%$.

Furthermore, the quest for the par yield, which equalizes the bond price with its par value, is pursued. We reintroduce the zero rates while allowing the previously assumed

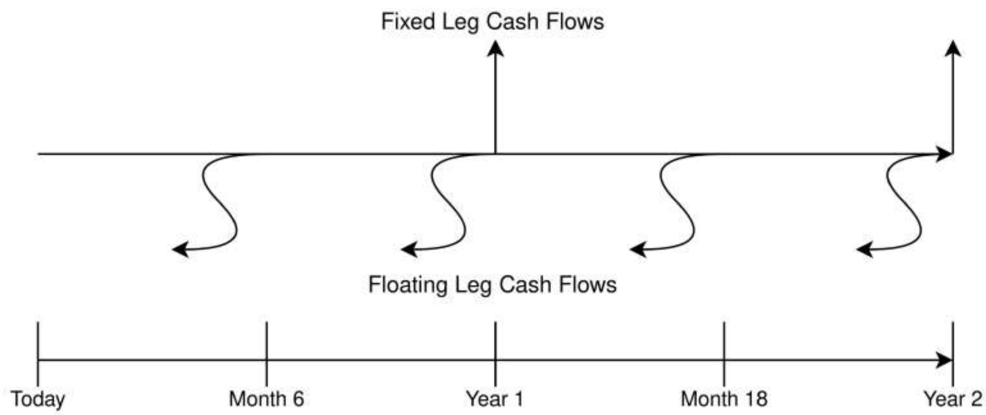


Figure 1.1.: Fixed vs. Floating Cash Flows for a Typical 2-Year Euro Swap

coupon rate of 4% to be denoted as variable $c$, leading to the equation:

$$\frac{c}{4} \cdot e^{-0.035\times0.25} + \frac{c}{4} \cdot e^{-0.040\times0.50} + \frac{c}{4} \cdot e^{-0.044\times0.75} + \left(100 + \frac{c}{4}\right) \cdot e^{-0.047\times1.00} = 100[\text{€}] \quad . \tag{1.15}$$

Solving this equation straightforwardly gives the par yield $c = 4.72\%$.

Let us now look at the concept of interest rate derivatives. The simplest derivative is a Forward Rate Agreement (FRA). An FRA is an over-the-counter (OTC) financial contract that allows two parties to reach an agreement today on the interest rate to be either paid or received on a specific date in the future. The FRA contract includes several key parameters, including the notional amount (which represents the investment amount), the agreed interest rate, the fixing date (when the reference rate is observed), and the settlement date (when the actual payment is made). FRAs fulfill a dual purpose, as they are used for both hedging and speculative transactions on the interest rate markets. With this financial instrument, a party can secure a predetermined interest rate for the future and thus hedge against potential interest rate fluctuations.

Moving on, there is also the concept of a plain-vanilla fixed-for-floating Interest Rate Swap (IRS). Extending the idea of an FRA, an IRS is a more extensive agreement for the

| | $t = 0$ | $t = 1$ | $t = 2$ | ... | $t = n$ |
|---|---|---|---|---|---|
| Rolling Investment | 0 | $1 + \text{Euribor}(1)$ | $1 + \text{Euribor}(2)$ | ... | $1 + \text{Euribor}(n)$ |
| | $-1$ | $-1$ | $-1$ | ... | 0 |
| Sum | $-1$ | Euribor(1) | Euribor(2) | ... | $1 + \text{Euribor}(n)$ |

Table 1.1.: Replicating Cash Flows for the Floating Leg

exchange of interest payments that allows counterparties to manage interest rate risk over a longer time. An IRS is an OTC agreement that provides for the regular exchange of interest payments between two counterparties. One counterparty, known as the fixed-rate payer, makes periodic payments at a predetermined fixed interest rate, while the other counterparty, the floating rate payer, makes variable payments periodically reset based on a benchmark interest rate index. Unlike FRAs, neither counterparty makes notional payments at the beginning or end of the agreement. The amount stated in the contract is still referred to as the nominal amount [45].

The party receiving the fixed rate is termed the receiver, while the other counterparty is the payer. Conceptually, a receiver swap is comparable to a long position in a bond, which involves receiving periodic coupons and making periodic payments of interest [54]. Conversely, the payer is essentially short a bond. As illustrated in Figure 1.1, each swap consists of two legs - a fixed leg and a floating leg. Each leg has an effective date (start date) and a maturity date (end date). In a typical Euro interest rate swap, payments on the fixed leg are made annually, while payments on the floating leg are made every six months. Obviously, the interest payments are based on the nominal value of the swap. In order to value an IRS, the net present value of both the fixed and floating leg has to be calculated. The valuation of the fixed leg is straightforward, as all cash flows are known.

On the other hand, pricing the floating leg presents a more tricky challenge. The future cash flows for the floating leg with an initial investment of 1[EUR] are detailed in Table 1.1. In general, the present value would be the sum of all discounted future cash flows. As we only know the value of Euribor(1) on the date of agreement, this approach is not feasible.

To solve this problem, we first introduce a fundamental principle known as the no-arbitrage concept. Arbitrage strategies, which are characterized by being riskless and profitable, are incompatible with an efficient market [53]. This, in turn, means there can be no risk-free profit. Since the Euribor rate is paid at each point in time $t$ and the remaining 1[EUR] is reinvested at every step, only the final amount at time $t = n$ has to be discounted. This replication of future cash flows relies on the assumption of no-arbitrage.

As a result, we only need the corresponding discount factor or, equivalently, the discount curve. This means that for $s_{0:n}$ denoting the swap rate with maturity $n$, we are now able to define both the present value of the fixed leg

$$PV_{fix} = s_{0:n} \sum_{i=1}^{n} d(t_0, t_i) \tag{1.16}$$

and the floating leg

$$PV_{float} = 1 - d(t_0, t_n) \quad . \tag{1.17}$$

In the context of the no-arbitrage concept, it should be pointed out that the discount curve should always show a monotonically falling trend. Any deviation from this pattern would potentially create an arbitrage opportunity.

As evident, the critical requirement is the discount curve, or equivalently, the zero rate curve. It would be convenient if the market directly quoted this curve, significantly simplifying the process and saving market participants a lot of grief [54]. However, in reality, this is not the case. In this thesis, we use swap rates as the data basis. A common approach to compute the discount curve from there is through bootstrapping [26]. Starting with the shortest maturity to obtain the first discount rate using Equation (1.10). Subsequently, we iteratively determine the next discount factor. Assuming the swap rates are aligned with maturities from the natural numbers and no maturity is missing, we can define the following formulas for the bootstrap method. Initially, we set:

$$d(t_0, t_0) = 1 \quad . \tag{1.18}$$

Let $s_{0:1}$ denote the first given swap rate with maturity 1. This allows us to derive the following:

$$d(t_0, t_1) = \frac{1}{1 + s_{0:1}} \quad . \tag{1.19}$$

We can now formally define the bootstrapping method:

$$d(t_0, t_i) = \frac{1 - s_{0:i} \times \sum_{k=1}^{i-1} d(t_0, t_k)}{1 + s_{0:i}} \quad \text{for} \quad i = 2, \ldots, n \in \mathbb{N}. \tag{1.20}$$

So far, we have concentrated on derivatives with a start date in the present. Now, we want to look at derivatives whose start date is in the future. Therefore, since all discounting factors are known, we can introduce forward interest rates, often referred to as forward rates. A forward rate represents the market expectation for the future interest rate for a certain period. It is an interest rate that is agreed today for an investment that begins at a later date. The forward rates are characterized by three distinct time points: The time $t$ at which the rate is considered, the effective date $m$, and its maturity date $n$, where $t \leq m \leq n$. In an FRA, at maturity $n$, a fixed payment based on a fixed rate is exchanged against a floating payment dependent on the spot rate resetting at $m$ and maturing at $n$ [8].

The forward rate can then be calculated as follows:

$$s_{m:n} = \frac{d(t_0, t_m) - d(t_0, t_n)}{\sum_{i=1}^{n-m} d(t_0, t_{m+i})} \quad . \tag{1.21}$$

Following the sequential approach of calculating the discount curve, computing the forward rates can be done as previously introduced, but now in parallel, which is essential for computing performances. In Chapter 5, these forward rates will be of immense significance, as an in-depth exploration will be undertaken to derive derivatives based on forward rates, thereby constructing portfolios that will then undergo a comprehensive analysis.

Finally, as before with an IRS, we can now also specify the fixed leg

$$PV_{fix} = s_{m:n} \sum_{i=1}^{n-m} d(t_0, t_{m+i}) \tag{1.22}$$

and the floating leg

$$PV_{float} = d(t_0, t_m) - d(t_0, t_n) \tag{1.23}$$

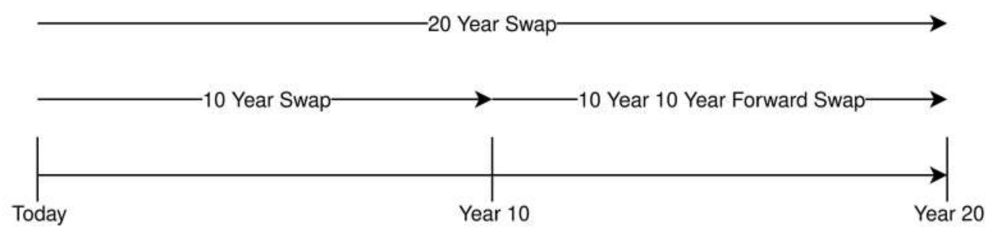


Figure 1.2.: Example of a 10-Year Swap starting in 10 Years

for a Forward Receiver Swap (FWD). To avoid arbitrage, the present value of a portfolio consisting of a 10-year and a 10-year-10-year forward swap must be equal to the present value of a 20-year swap, as shown in Figure 1.2. This means that the 10-year forward rate is the one that makes the forward curve arbitrage-free.

## 1.2. The Yield Curve Shape and Influencing Factors

Having examined the application and significance of interest rates in financial markets, we now address the yield curve. The yield curve is a graphical representation of yields for a range of maturities, offering insights into market expectations. Yield curve shapes, such as steep, inverted, or flat, indicate economic conditions and market sentiment, influencing investment strategies and risk management. The normal yield curve, characterized by increasing yields with longer maturities, typically signifies an expanding economy and expectations of future interest rate hikes. Conversely, an inverted yield curve, where short-term yields are higher than long-term yields, often anticipates an economic slowdown or recession, prompting monetary policy adjustments. Yield curves can be represented using various models, such as the Nelson-Siegel or Svensson models, to derive smooth yield curve surfaces that accurately help price bonds and derivatives. Alternatively, many interpolation techniques, such as cubic interpolation, approximate missing yield curve maturities, each bearing its own set of advantages and disadvantages [29]. It is important to emphasize that a yield curve is a versatile concept applicable to a wide range of debt instruments and financial products - from government bonds and treasury bills to interest rate swaps - offering valuable insights into the pricing dynamics and expectations across various sectors of the financial markets.

In the book by Belke et al. [5] (section 1.5.4), a comparison is made between the 3-month and 10-year yields in Germany/Europe and the US, spanning from January 1978 to April 2007. On average, long-term yields were found to surpass short-term interest rates. The authors highlight that bond yields generally exhibit an upward trend as maturities lengthen, resulting in a positively sloped yield curve. This behavior is underpinned by the principle that longer-term bonds entail higher risk for investors. Consequently, investors demand a higher yield to compensate for this elevated risk. Hence, it seems abnormal when the yield curve is inverted, implying that investors accept a lower return for a higher risk. However, economic considerations and central bank decisions may lead investors to believe that the currently restrictive monetary policy will be short-lived, followed by rate reductions.

This implies that the dynamics of yield curves have profound implications for any portfolio, especially in the fixed income market. Portfolio managers use yield curve strategies to optimize portfolio duration and maximize returns while managing interest rate risk. Understanding yield curve shapes and shifts is fundamental for effectively implementing these strategies. Therefore, it is crucial to understand the financial market behavior affected by government policies and central bank actions.

Central banks use monetary policy tools to achieve economic objectives, such as buying/selling government securities in the open market, adjusting reserve requirements for banks, or signaling future monetary policy intentions to influence market expectations [30]. Primarily, central banks act by altering the policy (or target) refinancing rate to impact the overall level of interest rates in the economy. They also rely on other monetary policy instruments to achieve economic goals, such as buying/selling government securities on the open market, adjusting the minimum reserve requirements for banks, or signaling future monetary policy intentions to influence market expectations [30].

Above all, the central bank uses the key interest rate to target the overnight rate, a rate at which banks can borrow money directly. It also significantly influences the interbank market, where banks lend money to each other. This way, they can manipulate short-term interest rates throughout the economy and change the cost of borrowing and lending. In monetary terms, the relationship in the interbank market can be represented as follows

$$R_{\mathrm{IB}} = R_{\mathrm{CB}} + \mathrm{Spread} \quad , \tag{1.24}$$

where $R_{\mathrm{IB}}$ is the overnight interbank interest rate, $R_{\mathrm{CB}}$ denotes the central bank's policy rate, and the Spread represents the banks' fee for lending money in excess of the policy rate. Given the main focus of this thesis is on the European market, the European Central Bank and its challenges as a monetary union, including its instruments to select between multiple aims and business cycle developments in the Eurozone, are of crucial relevance. It is therefore advisable to read the detailed explanations by Paul De Grauwe [20].

In general, changes in the policy rate ($R_{\mathrm{CB}}$) of the central bank have consequences on the entire interest rate structure in the economy, including rates on swaps, loans, mortgages, and other financial instruments. For example, when central banks increase the policy rate (e.g. during a tightening cycle), short-term rates rise, potentially flattening the yield curve. Short-term yields converge to or may exceed long-term yields, reflecting expectations of economic slowdown or future rate cuts. Conversely, during a rate-cutting cycle, short-term rates fall, potentially resulting in a steepening yield curve. Short-term yields decline relative to long-term yields, indicating market expectations of economic stimulus and potential future rate hikes.

In this context, economic factors also play a tremendous role. Inflation, in particular, is one of the most important determinants. The Fisher equation establishes the relationship between nominal interest rates ($r_{\mathrm{nom}}$), real interest rates ($r_{\mathrm{real}}$), and inflation ($\pi$)

$$r_{\mathrm{nom}} = r_{\mathrm{real}} + \pi \tag{1.25}$$

since central banks often set policy rates aiming to achieve a target inflation rate of around 2% per annum, thus having an impact on both nominal and real interest rates.

Other drivers include the unemployment rate or economic growth, which immensely echoes credit demand or foreign exchange rates, as captured by the interest rate parity (IRP), which is expressed as follows:

$$\frac{F}{S} = \frac{1 + r_f}{1 + r_d} \quad . \tag{1.26}$$

Here, $F$ stands for the forward exchange rate, $S$ for the spot exchange rate, $r_f$ for the foreign interest rate, and $r_d$ for the domestic interest rate. Similarly, global economic circumstances, trade policies, geopolitical events, and international financial stability affect interest rates. These multifaceted influences, alongside their expectations, bear considerable significance and serve as prominent catalysts in shaping the forward rates, which, as mentioned before, play an immense role in the practical example later in this thesis.

## 1.3. An Outline of the Thesis

In Chapter 2, we focus on combining key datasets crucial for a comprehensive analysis of historical swap rates in the fixed income market. The chapter explores the evolution of financial landscapes, beginning with German government bonds (1972-1989) as a correlated substitute for interest rate swaps, followed by German interest rate swaps (1989-1998), and ending with Euro interest rate swaps after 1998. The challenge of only having government bonds available every month is solved so that a dataset based on daily resolution can be used for further analysis in subsequent chapters.

Chapter 3 deals with the challenge of constructing a comprehensive yield curve, ensuring the inclusion of all necessary maturities crucial for subsequent analyses. The literature review explores existing methodologies, leading to the selection of two methods whose mathematical foundations are explained. Both methods are presented and implemented in detail, followed by a thorough comparison of their advantages and weaknesses. The overarching objective is to choose a robust approach that allows a nuanced analysis of the multiple swap curve shapes observed in historical data.

In Chapter 4, the priority is to simplify the complexity of the established dataset. A key challenge addressed is the high correlation among absolute returns of daily swap rate changes across different maturities. The chapter introduces the Spectral Decomposition theorem as a fundamental principle, paving the way for the exploration and application of Principal Component Analysis (PCA). The narrative is guided by its overall goal of identifying and capturing the predominant sources of variation. Consequently, we unveil their interpretation of central bank decisions directing the swap curve in conjunction with their implications on prevailing economic paradigms.

Chapter 5 aims to apply the previously explored framework to practical use by examining different economic paradigms throughout history, mainly focusing on the distinctive forms of swap curves — flat, steep, and inverse. Through identifying and analyzing these clusters, the chapter quantifies the impact of each principal component on portfolio sensitivity. This then facilitates quantifying principal component influence on two exemplary portfolios, concluding with thoroughly examining these measures in a broader macroeconomic context.

# 2. Data Integration

## 2.1. Introduction

In order to undertake a thorough examination of the following methods in this thesis, an analysis of historical swap rates and government bonds is essential. The latter is used here to extend the existing history of swap rates.

This chapter details the process of integrating the key datasets essential to the comprehensive analytical investigation in subsequent chapters. The datasets examined include three distinct but interrelated components: German government bonds (1972-1989), German interest rate swaps (1989-1998), and Euro interest rate swaps.

The introduction of the Euro as a single currency on the 1st of January in 1999 marks the onset of utilizing Euro interest rate swaps as a foundational data source. To ensure an in-depth and well-founded analysis in the later chapters, we also use German interest rates from the 6th of October 1989 to the 31st of December 1998. At that time, Germany, the largest European economy, hosted many companies actively involved in trading and financial transactions denominated in the German currency. Consequently, these companies were significantly exposed to interest rate risks in this particular economic landscape, rendering it the most liquid one in Europe and, hence, suitable as an extension of the Euro interest rate swaps. In 1997, the central banks of Austria, Belgium, Germany, Italy, the Netherlands, Australia, and Switzerland exchanged swaps against either the U.S. dollar or the Deutsche Mark (or both) [4], strongly affirming the previously presented rationale.

To further strengthen the analysis, the dataset is extended to include German government bonds from the 1st of September 1972 to the 1st of September 1989. This extension is due to the strong correlation between swap rates and government bond yields. A detailed analysis of both rates from the 1st of January 1999 and over more than 20 years using correlation statistics has revealed a remarkable correlation that illustrates the highly synchronized nature of these financial instruments. Thus, the Pearson correlation coefficient, calculated by

$$r = \frac{\sum_{i=1}^{n}(x_i - \bar{x})(y_i - \bar{y})}{\sqrt{\sum_{i=1}^{n}(x_i - \bar{x})^2 \sum_{i=1}^{n}(y_i - \bar{y})^2}} \quad , \tag{2.1}$$

where $x_i$ and $y_i$ are the individual data points of variables $X$ and $Y$ - in our case, the swap rates and the bond yields - as well as $\bar{x}$ and $\bar{y}$ are the mean values of variables $X$ and $Y$, respectively, yielded a value of 0.9947. This indicates a very high linear correlation. Spearman's rank correlation coefficient, which is given by

$$\rho = 1 - \frac{6 \sum d_i^2}{n(n^2 - 1)} \quad , \tag{2.2}$$

where $d_i$ is the difference between the ranks of corresponding elements in the two variables, a value of 0.9950 returned. This suggests a strong monotonic relationship, meaning that as one variable increases, the other also tends to increase (or decrease). Considering all the results, extending the data by adding government bonds seems reasonable.

The focus now shifts to the detailed exploration of each individual dataset, outlining the steps involved in its preparation, meaningful augmentation, and precise processing. The ultimate goal during this preparation process is to ensure that the resulting integrated dataset maintains high consistency and usability for all subsequent analyses. This strategic integration of datasets forms the basis for the analytical quality of the insights to be gained and the resulting conclusions of this thesis.

## 2.2. Brownian Bridge

In the upcoming sections, it becomes clear that one dataset provides only monthly information and that a smooth transition between the three different datasets must be ensured. The concept of a Brownian bridge is first introduced to facilitate the transitions without sudden interruptions and to obtain daily information.

The Brownian bridge is designed to be calculated between two given data points, with the first date as the initial reference point and the subsequent one as a fixed endpoint, referred to as $T$. To begin, we introduce a continuous-time stochastic process denoted as $W_n(t)t \geq 0$ through the following equation:

$$W_n(t) = \frac{1}{\sqrt{n}} \sum_{1 \leq j \leq \lfloor nt \rfloor} \xi_j, \quad n \in \mathbb{N}. \tag{2.3}$$

This random step function exhibits increments of size $\pm\frac{1}{\sqrt{n}}$. The increments are independent due to $\xi_j$, which form a sequence of independent, identically distributed random variables with a mean of 0 and a variance of 1. From this derives the definition of Brownian motion $W(t)$, which is defined as the limit when $n \to \infty$ in Equation (2.3). The crucial difference is that $W_n(t)$ has a natural time step and linear properties within these intervals, whereas Brownian motion has no such linearity.

The Brownian bridge is a stochastic process similar to Brownian motion but with the distinctive feature that, with probability one, it reaches a fixed endpoint. As defined in [59], the Brownian bridge from 0 to 0 over the interval $[0, T]$ follows the same distribution as the subsequent process:

$$X(t) = W(t) - \frac{t}{T}W(T), \quad 0 \leq t \leq T. \tag{2.4}$$

This definition ensures that $X(0) = X(T) = 0$. Furthermore, we can extend this definition to establish the Brownian bridge from $a$ to $b$ over the interval $[0, T]$:

$$X^{a \to b}(t) = a + \frac{(b-a)t}{T} + X(t), \quad 0 \leq t \leq T, \tag{2.5}$$

where $X(t) = X^{0 \to 0}$ aligns with the definition presented in Equation (2.4). This new interpretation naturally affects the mean function, as the expected value of $X(t)$ is zero. Consequently, the term $a + \frac{(b-a)t}{T}$ in Equation (2.5) represents the mean value. Nevertheless, this adjustment does not influence the covariance concerning its prior definition in Equation (2.4), which remains as $c^{a \to b}(s, t) = s \wedge t - \frac{st}{T}$, with $s \wedge t$ denoting the minimum of $s$ and $t$ [59]. In the next sections, this methodology will be applied multiple times.

| Time Period | | German Government Bonds | | | | | | | | | | | | | |
|---|---|---|---|---|---|---|---|---|---|---|---|---|---|---|---|
| Start Date | End Date | 1 | 2 | 3 | 4 | 5 | 6 | 7 | 8 | 9 | 10 | 15 | 20 | 30 | 50 |
| 1972-09-01 | 1989-10-01 | ✓ | ✓ | ✓ | ✓ | ✓ | ✓ | ✓ | ✓ | ✓ | ✓ | C | C | C | C |

Table 2.1.: Available German Government Bonds

## 2.3. German Government Bonds (1972-1989)

The dataset on German government bonds, which covers the years 1972 to 1989, is made available online by the Deutsche Bundesbank[1], presents a unique challenge. Observations are available only once per month and are limited to maturities up to 10 years marked with ✓ in Table 2.1. A robust approach is required to augment the dataset for maturities up to 60 years, particularly in addressing two fundamental issues. One is to obtain reasonable values for extended maturities, and the other is to achieve a daily data resolution.

To address the challenge of extending maturities, the idea is to calculate approximated rates for maturities 15, 20, 30, and 50 (marked with a $C$ in Table 2.1). This step is crucial because past research has demonstrated that no parametric model or interpolation technique can generate meaningful results without these additional support points, resulting in an ill-defined yield curve. To find these support points, an initial comparative analysis of bond yields for 2-year and 10-year maturities is conducted, denoted as $Y_{10}$ and $Y_2$. In particular, the average difference between those two values is calculated as

$$\Delta Y_{2s10s,i} = (Y_{10,i} - Y_{2,i}) \quad , \quad i = 1, \ldots, N, \tag{2.6}$$

where $N$ signifies the total number of dates with available data. This analysis provides a foundation for deducing relationships and dependencies. Following this, the difference between maturities of 10 and 15, 10 and 20, 10 and 30, as well as 10 and 50 years are calculated:

$$\Delta Y_{10sXs,i} = (Y_{X,i} - Y_{10,i}) \quad , \quad i = 1, \ldots, N. \tag{2.7}$$

[1]Visit https://www.bundesbank.de/en/statistics/money-and-capital-markets/interest-rates-and-yields

This exploration utilizes the complete historical dataset from the German or the Euro swap rates, but only once the corresponding maturity data is available. Additionally, a clustering approach is adopted to categorize instances where $\Delta Y_{2s10s,i}$ shows a positive or negative value. For each category, we compute a distinct average yield difference denoted as $\Delta\overline{Y}_{10sXs}$, where $X$ represents various maturities (e.g., 15, 20, 30, 50 years). The computation is defined as follows:

$$\Delta\overline{Y}_{10sXs} = \frac{1}{N}\sum_{i=1}^{N}\frac{\Delta Y_{10sXs,i}}{\Delta Y_{2s10s,i}} \quad , \tag{2.8}$$

Here, $N$ aggregates dates based on whether $\Delta Y_{2s10s,i}$ is positive or negative (set $N = N_{\text{pos}}$ or $N = N_{\text{neg}}$). Subsequently, we establish a fundamental equation from which all new yield values are derived:

$$Y_{X,i} = Y_{10,i} + \Delta\overline{Y}_{10sXs} * \Delta Y_{2s10s,i} \quad . \tag{2.9}$$

In this formulation, $Y_{X,i}$ and $Y_{10,i}$ represent the yields for maturities $X$ and 10 at date $i$. This method offers an approach for estimating yields for maturities 15, 20, 30, and 50 years. It draws upon the observed relationship between 2-year and 10-year yields, considering historical data and their average yield differences to adjust the 10-year yield for different maturities.

In total, there are 206 months of government data, resulting in 206 distinct yield curves. Each curve underwent careful examination for structural and behavioral coherence to achieve natural and plausible curve shapes.

Several approaches can be explored to overcome the challenge of working with monthly data points and achieve daily resolution. One potential method involves seeking a correlated dataset with daily resolution and leveraging its intra-month volatility as an approximation. The procedure can be summarized as follows: Each month, the cumulative difference in proximity is calculated and subtracted from the monthly cumulative difference of the German government bonds. This difference is then divided by the number of trading days in the respective month, providing the daily volatility. Finally, the cumulative daily return of the German government bond must be computed.

As a proximity measure, an analysis of U.S. government bonds around the same period was conducted. Analyzing the data revealed that the highest monthly Pearson correlation, denoted in Equation (2.1), reached a value of 0.53 when using the monthly data from the 1st of October 1972 to the 1st of November 1989. Since U.S. government bonds are available in daily resolution, they present a feasible option. However, despite these calculations and ideas, the relatively low correlation limited the practicality of the results, suggesting the need to explore alternative approaches.

An alternative approach employs the previously introduced Brownian Bridge concept detailed in Section 2.2. This bridge should be formed between each of the provided monthly data points. Given our objective to transition from monthly data to daily resolution, we will apply the defined Brownian bridge by utilizing the discrete stochastic process $W_n(t)$ as defined in Equation (2.3). This approach introduces a scaling challenge to ensure realistic movements. To address this, we examine the day-to-day variations in the 1, 10, 20, and 50 year swap rates spanning the period from 1989 to 2023. This analysis provides insights into the distribution that underlies each maturity, allowing us to determine the most suitable distribution for our purpose. The research indicates that a normal distribution best fits the data.

In light of this, we need to adapt Equation (2.3). In that equation, a standard normal distribution was employed and scaled by $\frac{1}{\sqrt{n}}$, with $n$ representing the size of the interval. However, in our case, the size of each interval is not a reliable indicator of daily variations occurring within a month. Instead, we calculate the standard deviation for all four maturities and compute their average. The average standard deviation $\bar{\sigma} = 0.00041$ is applied to adjust Equation (2.3). In this adjustment, $\xi_j$ is replaced with a sequence of independent samples drawn from a normal distribution with a mean of 0 and a standard deviation of $1.5 \cdot \bar{\sigma}$, requiring no additional scaling. This modification guarantees the generation of nuanced and realistic daily changes for the given and calculated maturities listed in Table 2.1. The 1.5 factor accounted for tail risk and generated realistic movements comparable to the daily data from 1989 onwards. The resulting effect is illustrated in Figure 2.1.

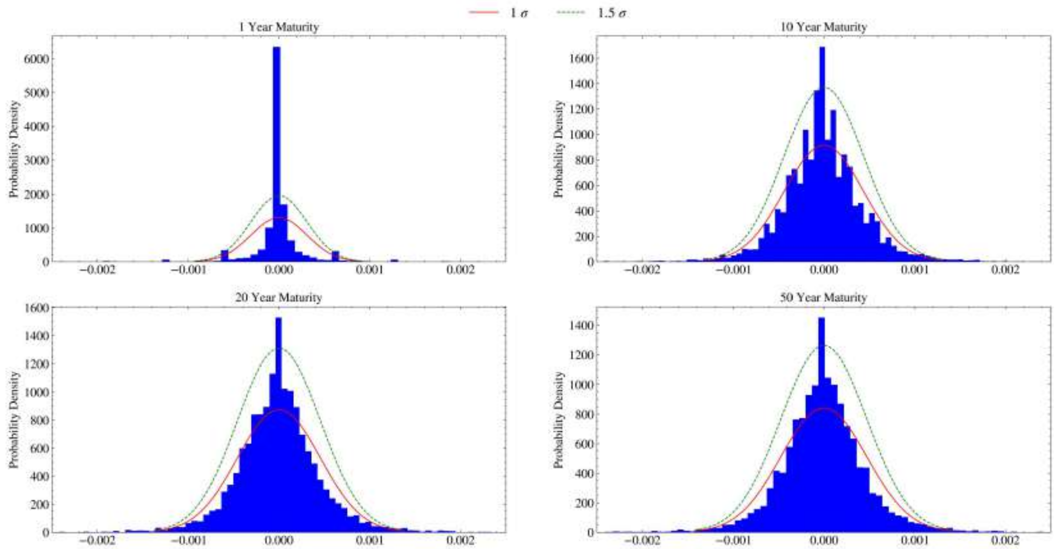


Figure 2.1.: Distributions of Daily Swap Rate Changes for Different Maturities

The final alternative in this thesis involves the simple application of linear interpolation, a practical and efficient method. Given a pair of data points ($x_1$,$y_1$) and ($x_2$,$y_2$), where $x_1$ and $x_2$ represent consecutive given monthly days, and $y_1$ and $y_2$ the corresponding yields, the linearly interpolated yield ($Y_{\text{int}}(x)$) for a specific trading day $x$ between $x_1$ and $x_2$ can be calculated as follows:

$$Y_{\text{int}}(x) = y_1 + \frac{(x - x_1)(y_2 - y_1)}{(x_2 - x_1)} \quad . \tag{2.10}$$

This method offers a straightforward approach for estimating daily yields and bridging the gap between monthly data points.

## 2.4. Deutsche Mark Interest Rate Swaps (1989-1998)

The dataset concerning German interest rate swaps from 1989 to 1998 was acquired from Bloomberg, a prominent global provider of financial news and information. This dataset offers daily resolution, unlike the monthly resolution found in government bond data. Similar to the available data in the preceding section for German government bonds, this

| Time Period | | Deutsche Mark Swaps | | | | | | | | | | | |
|---|---|---|---|---|---|---|---|---|---|---|---|---|---|
| Start Date | End Date | 1-5 | 6 | 7 | 8 | 9 | 10 | 12 | 15 | 20 | 25 | 30 | 50 |
| 1989-10-06 | 1996-01-01 | ✓ | | ✓ | | | ✓ | | C | C | | C | C |
| 1996-01-02 | 1998-02-11 | ✓ | ✓ | ✓ | | | ✓ | | C | C | | C | C |
| 1998-02-12 | 1998-12-31 | ✓ | ✓ | ✓ | | | ✓ | ✓ | C | C | ✓ | C | C |

Table 2.2.: Available Deutsche Mark Swap Rates

dataset also presents missing maturities, evident in the absence of entries or the entry of a C in Table 2.2. The previously developed methodology to analyze relationships among available maturities again estimates the missing values denoted by $C$.

## 2.5. Euro Interest Rate Swaps (1999-2023)

| Time Period | | Euro Mark Swaps | | | | | | | | | |
|---|---|---|---|---|---|---|---|---|---|---|---|
| Start Date | End Date | 1-10 | 11 | 12 | 15 | 20 | 25 | 30 | 40 | 50 | 60 |
| 1999-01-01 | 1999-10-18 | ✓ | | ✓ | ✓ | ✓ | | ✓ | | ✓ | |
| 1999-10-19 | 2000-01-31 | ✓ | | ✓ | ✓ | ✓ | ✓ | ✓ | | ✓ | |
| 2000-02-01 | 2001-06-25 | ✓ | ✓ | ✓ | ✓ | ✓ | ✓ | ✓ | | ✓ | |
| 2001-06-26 | 2020-11-06 | ✓ | ✓ | ✓ | ✓ | ✓ | ✓ | ✓ | ✓ | ✓ | |
| 2020-11-09 | 2023-12-15 | ✓ | ✓ | ✓ | ✓ | ✓ | ✓ | ✓ | ✓ | ✓ | ✓ |

Table 2.3.: Available Euro Swap Rates

The dataset relating to Euro interest rate swaps from 1999 to 2023 is sourced from Bloomberg, but this time, it relies on data provided by ICAP, a globally leading Inter-Dealer-Broker. A significant advantage of this dataset is the consistent daily resolution of data points available and its consistency over time, as seen in Table 2.3. Given this consistency, the manual calculation of missing maturities is no longer required. This

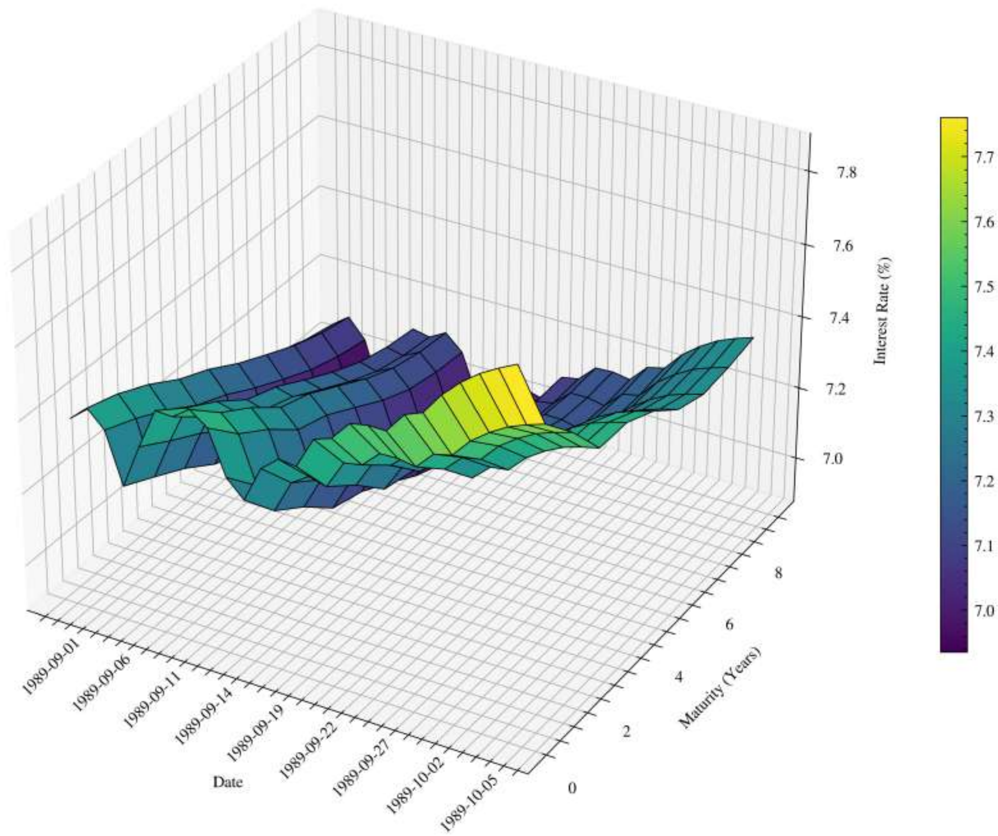


Figure 2.2.: Brownian Bridge Transition from Bonds to Swaps

aspect significantly enhances precision and augments the overall quality of the subsequent analytical endeavors. In addition, the 60-year point has also been available since the 9th of November in 2020.

## 2.6. Dataset Fusion and Transition Analysis

This section thoroughly integrates the previously introduced datasets: German government bonds, Deutsche Mark interest rate swaps, and Euro interest rate swaps. The objective is to create a seamless dataset that maintains data continuity and ensures a

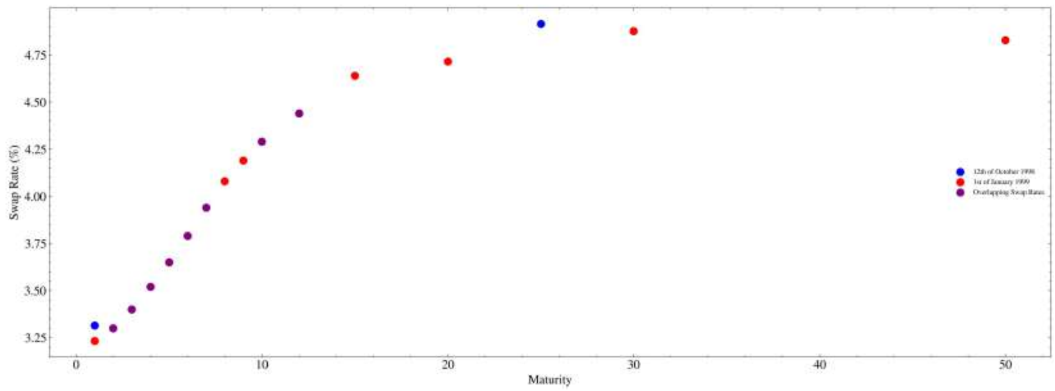


Figure 2.3.: Natural Transition from Deutsche Mark Swaps to Euro Swaps

smooth transition between the distinct components. Precise handling of these transitions is critical to prevent abrupt shifts in the dataset, which could adversely affect portfolio analysis and subsequent financial modeling. Two critical transitions have been identified, necessitating specific treatment to ensure a smooth merging process.

The Brownian bridge from Equation (2.5) is again implemented to manage the smooth transition from the German government bonds to the Deutsche Mark swap rates. The bond yield for the 1st of September 1989 and the German swap rate on the 6th of October 1989 serve as anchor points. This approach is instrumental in minimizing any abrupt jumps in the dataset. The result of the Brownian bridge for this transition is shown in Figure 2.2.

The transition between the Deutsche Mark to the Euro at the end of 1998 and the beginning of 1999 demonstrates an even smoother integration, requiring no specific handling. The swap rates for the 31st of December, 1998, and the 1st of January, 1999, align closely, confirming the appropriateness of employing German swap rates as a meaningful extension of Euro swap rates. Figure 2.3 underscores the minimal transition disparity between the Deutsche Mark and the Euro swap rates at the turn of 1999.

## 2.7. Data Quality Review, Limitations, and Future Research Directions

In this section, a thorough review of data quality is conducted, acknowledging encountered limitations and proposing potential routes for future research to improve the accuracy and precision of the dataset.

To bolster data quality, the dataset was cautiously expanded to include longer maturities, particularly in the historical context where such values were unavailable. However, the methodology employed for this augmentation was somewhat simplistic, though guided by fundamental principles. Leveraging subsequent maturity relationships, specifically divided by positive and negative $\Delta Y_{2s10s,i}$ values, is a reasonably straightforward approach. Even though this was complemented for the German government bonds by thoroughly analyzing all 206 yield curves to ensure data rationality, it could not be done for all Deutsche Mark swap curves.

A potential enhancement involves further categorization of $\Delta Y_{2s10s}$ values into strongly positive/negative and slightly positive/negative. This increased granularity could yield more accurate data points for longer maturities and refine the extended yield curve for comprehensive analyses. One challenge would be to find appropriate thresholds that ensure a certain level of data quality. The objective function could be represented as follows

$$Y_x = Y_{10} + \Delta Y_{2s10s} \times f(\Delta Y_{2s10s}) \quad , \tag{2.11}$$

where $Y_x$ denotes the newly created value for the different maturities $x = 15, 20, 30, 50$. $Y_{10}$ is the given value at maturity 10 and $f(\Delta Y_{2s10s})$ is defined by:

$$f(\Delta Y_{2s10s}) = \begin{cases} (\Delta Y^{++}_{10sXs}, 0, 0, 0) & \text{if } \Delta Y_{2s10s} \geq t_1 \\ (0, \Delta Y^{+}_{10sXs}, 0, 0) & \text{if } 0 < \Delta Y_{2s10s} < t_1 \\ (0, 0, \Delta Y^{-}_{10sXs}, 0) & \text{if } t_2 < \Delta Y_{2s10s} \leq 0 \\ (0, 0, 0, \Delta Y^{--}_{10sXs}) & \text{otherwise.} \end{cases} \tag{2.12}$$

In this formulation, $t_1$ and $t_2$ represent the thresholds to be optimized, and $Y_{10sXs}$ is the average difference calculated as in Equation (2.6) by adjusting the maturities according to the specified value of $x$. This approach can be extended with more thresholds to accommodate any needed complexity. Additionally, the combination of $\Delta Y_{2s10s}$ and $\Delta Y_{10s15s}$, once the data is computed, can be utilized for further enhancements in even longer maturities. The same strategy can be applied as more data becomes available over time.

The challenge of achieving daily resolution has also been explored, with criticism directed at the low correlation between monthly U.S. and German government bonds, rendering this data insufficient for substantiating its use. Two alternative approaches were considered: Linear interpolation and the Brownian bridge.

The linear interpolation, while more straightforward, presents a notable concern. In Chapter 4, the Principal Component Analysis (PCA) results will be identical every month for the respective maturity, in about 20 daily changes. This can potentially impact the quality of the PCA and thus influence the analysis in Chapter 5.

In contrast, the Brownian bridge offers a more sophisticated approach. It relies on a normal distribution with a mean of 0 and a standard deviation of $1.5 \cdot \bar{\sigma}$, derived from the average standard deviation of the swap rates spanning from 1989 to 2023 for maturities of 1, 10, 20, and 50. The primary challenge was to ensure the consistent construction of realistic yield curves on all trading days. To address this, a single Brownian bridge was applied to all maturities for each month. This approach diverged from constructing a unique Brownian bridge for each maturity, which often resulted in unrealistic shapes, especially during the first half of some months. The discrepancy resulted from the smaller movement in the second half of each month, ultimately converging with the following month's swap rates, which have an inherently realistic shape based on the values originally priced in the market.

Furthermore, the Brownian bridge was implemented to cover the first ten given maturities as well as the four supplementary calculated maturities (15, 20, 30, and 50 years). The distributions for the daily changes in the 20-year and 50-year maturities closely resembled that of the 10-year maturity, as demonstrated in Figure 2.1. This

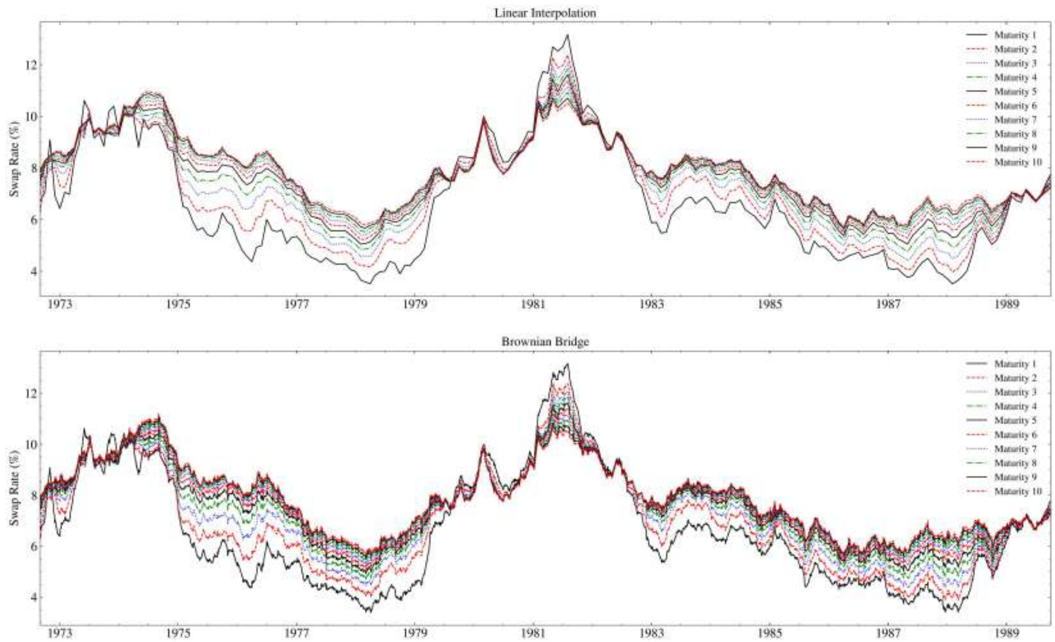


Figure 2.4.: Linear Interpolation vs. Brownian Bridge for Daily Resolution of Bonds

observation supports the idea of using a single distribution for sampling, although it can be seen that the distribution of daily swaps with a maturity of one year is not perfectly matched. The comprehensive validation process yielded satisfactory results, with all yield curves consistently showing a realistic shape. While a joint Brownian bridge may be helpful, different factors could be considered depending on each maturity.

This approach, particularly when contrasted with the simplicity of linear interpolation, introduced significant intra-month variations. The visual contrast between both methodologies for maturities ranging from 1 to 10 is demonstrated in Figure 2.4.

For a better understanding, Figure 2.5 serves as a comprehensive overview of the dynamic evolution of daily swap rates over the extensive period from 1989 to 2023, explicitly focusing on the first ten maturities again. This visual examination not only captures the historical trends but also provides a good comparison for the results obtained by using the Brownian bridge and the linear interpolation over the period from 1972 to 1989, as shown in Figure 2.4.

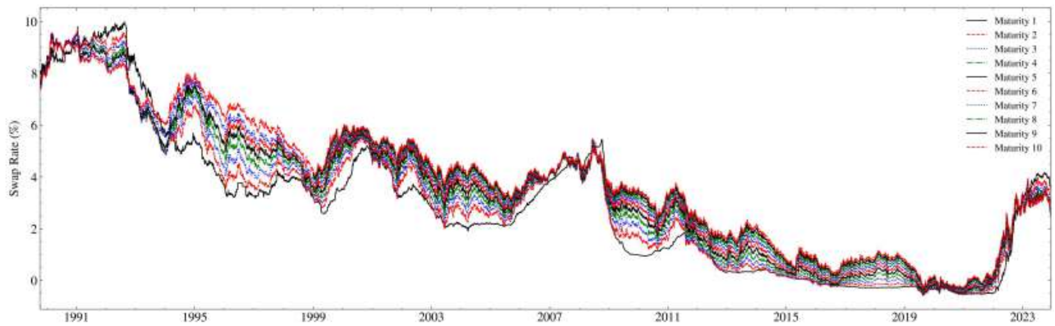


Figure 2.5.: Daily Resolution of Deutsche Mark and Euro Swaps

It is worth noting that, in general, daily changes decrease as maturity extends. While we utilize one distribution for sampling, it is already considered that lower maturities tend to exhibit higher variations in daily changes. This is because the higher movements observed in shorter maturities also lead to larger differences between the monthly data points. In Equation (2.5), this difference is reflected in the term $b - a$ in the numerator. However, it is essential to recognize that this difference can fluctuate significantly depending on the monthly data provided.

One potential approach to further enhance the Brownian bridge involves using a well-fitting distribution for all maturities while introducing additional scaling based on maturity and their respective confidence intervals from 1989 to 2023. This adjustment should be executed carefully to ensure that the resulting yield curve maintains a realistic shape at any time. The potential outcome is that later maturities exhibit reduced movement while earlier maturities display slightly more variability. Additionally, it may be worthwhile to investigate the possible influence of the overall swap rate level on these daily changes, as it could yield valuable insights and further enhance our understanding of the dynamics at play.

Alternative methodologies are bootstrapping and the use of Machine Learning models. In bootstrapping, the approach aims to reconstruct the yield curve using all accessible market data at a given time. The results will require subsequent smoothing and validation procedures to ensure realistic yield curves. Similarly, a Machine Learning model can be developed to aggregate relevant market data, particularly for 1989 to 2023, in conjunction with daily swap rates. The model aims to identify underlying patterns that can be used to generate daily curves for the period from 1972 to 1989. These possibilities are open for future research.

Another assumption in the data preparation in this thesis was the reliance on German government bonds and German interest rate swaps due to the higher liquidity of the German market during this period. This choice remains logical, especially in light of the transition from German to European swap rates in 1998/1999, but an interesting path for future research is to take a broader perspective. This could involve pooling swap rate data from the major European economies relative to their economic size, which could provide valuable insights into regional swap rate dynamics.

Mathematically, let $Y_{cou_i}$ represent the yield for a specific European country, and $S_{eco_i}$ denote the economic size of that country. A relative approach can be formulated as:

$$Y_{comb} = \sum_{i=1}^{n} \frac{Y_{cou_i}}{S_{eco_i}} \quad . \tag{2.13}$$

This method offers a glimpse into the potential of a more comprehensive, regionally representative yield curve. These future research areas promise to improve the dataset's quality further and open the way to potentially more accurate financial analysis and deeper insights.

# 3. Yield Curve Construction

## 3.1. Introduction

The accurate representation of interest rates is significant across various financial applications, such as pricing derivatives, evaluating risks, and assessing portfolios. Nevertheless, only a limited number of interest rates are usually quoted directly on the market, as already described in Chapter 2. Yet efforts to extend the maturities for swap rates have encountered problems because the cash flow data does not match the predefined finite time grid. This highlights the need to add additional data points to the curve in order to achieve a finer resolution.

The construction of yield curves holds considerable significance within the framework of numerous interest rate models. These models can be viewed as probabilistic representations illustrating the potential fluctuations in interest rates over time. This probabilistic framework enables portfolio managers to assess portfolio performance under plausible future scenarios, facilitating effective control of interest-rate risk. It is crucial to underscore that the global crisis from 2007 to 2009 triggered fundamental shifts in the foundations of interest rate modeling, particularly in curve construction and risk management. Before this crisis, a singular Libor discount curve was often considered sufficient; however, the landscape at the time required dealing with a challenge involving the compilation of interconnected curves. A comprehensive description of the impact observed at that time concerning quotations in February 2009 in comparing four Euribor swap curves can be found in the introduction of [6].

As explained in Section 1.1, the effectiveness of a constructed yield curve significantly impacts computations involving discount factors and forward rates, both of which play a central role in this thesis. Mathematically, the interest rate curve, generally referred to as a yield curve, is represented as a function $Y(t,T)$, where $t$ is the current time and $T$ is the time to maturity. This function describes the relationship between the time to maturity and the corresponding yield or interest rate for a specific point in time.

The overarching challenge of determining this term structure can be formulated through the following:

$$p = C\,d + \epsilon \quad . \tag{3.1}$$

Here, $p$ denotes a column vector containing $n$ market prices, while $C$ represents the associated cash flow matrix. The variable $d$ characterizes the corresponding discount function involving $N$ cash flow dates, and $\epsilon$ encapsulates a vector of pricing errors that necessitates minimization. These errors arise due to the inherent discrepancies in simultaneous market price quotations and the existence of bid-ask spreads. Consequently, including an error term within the model becomes essential.

In the European money market, the €STR and Euribor are frequently used for short maturities (from overnight to one, three, and six months). Euro Futures are generally taken for short maturities up to 3 or 4 years and swap rates for medium to longer maturities. However, these diverse instruments, chosen because they are the most liquid, are not uniformly priced for identical maturities, compounded by a shortage of usable securities. Consequently, the linear optimization problem aimed at minimizing $\epsilon$

$$\min_{d \in \mathbb{R}^N} \|p - Cd\|^2 \tag{3.2}$$

becomes ill-posed due to $n \ll N$, i.e. a significantly lower number of market prices in relation to different cash flow dates. Although adjusting $C$ to synchronize cash flows precisely at the same time, as suggested in Carleton and Cooper [9], fails to provide regularization to the regression model. The shortage of securities prompts the consideration of introducing "fictitious" securities by employing interpolation or extrapolation techniques. However, this approach might yield unconventional curve shapes [2].

Another viable approach involves utilizing a parametric functional form or a spline representation featuring $N$ user-selected knots typically placed at the maturity dates of benchmark securities. Determining the yield curve's level at these knots constitutes the $N$ unknowns to be resolved.

The final alternative involves exploring the solution space of (3.2) and selecting the optimal solution by employing smoothing splines. This method leverages the error term $\epsilon$ within a penalized least-squares optimization framework to achieve smoother transitions in the yield curve.

Within this thesis, our exclusive focus lies on swap rates. The forthcoming review and analysis of portfolios in Chapter 5 excludes any positions in the portfolio maturing in less than 3 years due to volatility considerations. Hence, the assumption to solely use swap rates appears justifiable. Our exploration will primarily focus on conventional techniques for single-curve construction, which also forms the basis for resolving the multidimensional problem. We will look at the historical research in this area and conduct a more detailed investigation into the aforementioned parametric approaches.

## 3.2. Literature Review

Across recent decades, a variety of methodologies have been developed to characterize the yield curve and extend its representation beyond observed maturities. The earliest attempt to model the discount curve dates back to McCulloch in 1971 and 1975 [41][42], applying polynomial splines (also observed in McCulloch and Kwon 1993 [43]). Regrettably, the polynomial structure led to a divergence in longer maturities, resulting in inadequate fits to yields that exhibit flattening trends with maturity, as shown by Shea in 1984 [57]. Such discrepancies prove especially troublesome given the data under examination in this thesis.

Vasicek and Fong introduced a refinement in modeling techniques in 1982 [66], employing exponential splines on U.S. Treasury securities. Their approach involved a negative transformation of maturities, ensuring that zero-coupon yields and forward rates converge to a fixed limit as maturity extends. This adaptation was more successful in fitting yields that demonstrate flat long ends. However, Shea (1985) [58] highlighted the potential for implied forward rates to exhibit implausible volatility despite these advancements.

Building upon this, Adams and Van Deventer [1] introduced an alternate objective, aiming to fit observable points on the yield curve with a function of time that generates the smoothest possible forward rate curve, abbreviated as the forward curve. They leveraged a standard mathematical definition of smoothness, often applied in engineering contexts to an interval $(0, T)$ characterized by $Z = \int_0^T f''(s)^2 ds$. Pursuing the smoothest forward curve led to the minimization of this function by employing a fourth-order spline, excluding the cubic term.

Alternatively, Fama and Bliss pioneered a bootstrapping method in 1987 [25], demonstrating high accuracy in representing the curve's front end but showcasing limited precision for maturities surpassing one year. Their iterative process assumes a constant forward curve between observed bond maturities, deriving a discount function that enables accurate pricing of in-sample bonds and generally reliable pricing for short-term out-of-sample contracts. While it is very accurate for in-sample bond pricing, its reliability for out-of-sample bonds is primarily constrained to shorter maturity contracts, which is particularly limiting for the maturity range discussed in this thesis.

As previously highlighted for the multidimensional problem, employing $N$-knot splines based on polynomial and exponential splines featuring varying degrees of differentiability appears reasonable. An instance involves crafting piecewise linear yields utilizing the formulation:

$$y(T) = y(T_i)\frac{T_{i+1} - T}{T_{i+1} - T_i} + y(T_{i+1})\frac{T - T_i}{T_{i+1} - T_i}, \quad T \in [T_i, T_{i+1}] \quad , \tag{3.3}$$

where $T_1, T_2, \ldots, T_N$ represent the various maturities. As showcased in section 6.2.1.1 of [2], an example demonstrates a continuously compounded forward curve exhibiting a discontinuous "saw-tooth" shape.

Another strategy involves assuming piecewise flat forward rates to derive the yield curve. This method, also detailed in [2], introduces discontinuities in forward curves, which seem unrealistic. Therefore, adopting once-differentiable yield curves ensuring continuous forward curves appears more pragmatic. To achieve this, leveraging Hermite cubic splines becomes feasible, particularly the Catmull-Tom spline, where derivatives $y'(T_i)$ are constructed via finite differences.

However, one problem persists: The forward curve remains non-differentiable, which runs contradictory to the desired smoothness. As a result, twice-differentiable cubic splines become a mandatory consideration, prompting a detailed exploration in Section 3.3.1.

Further interesting research areas are parametric models that use specific functional forms to fit the term structure appropriately. Pioneering work includes Cohen, Kramer, and Qaugh (1966) [16], who introduced a method involving multi-linear regression for U.S. government securities. They applied the yield regression concerning the days to maturity and the squared logarithm of days of maturity $T$. In 1976, Echols and Elliot [24] modified this technique into a linear regression model of the form $\ln(1 + r(T)) = a\frac{1}{T} + bT + c + \epsilon_T$.

One of the prominently applied parametric models was subsequently proposed by Nelson and Siegel in 1987, specifying a functional form for the instantaneous forward rates derived from the solution of a second-order differential equation. It is essential to emphasize that the three factors employed within this model align with the three factors of the term structure model introduced by Litterman and Scheinman in 1991 [40]: Level, slope, and curvature. These three factors serve as fundamental concepts in this thesis, forming the basis for all forthcoming chapters. The Nelson-Siegel (NS) model incorporates the most important characteristics of the forward curve, namely monotonic, humped, and S-shaped trends. Consequently, the yield curve can be readily extracted from this model.

It is notable that in 1994, Svensson [61] proposed an enhancement to the NS model featuring two humps by duplicating the respective term and introducing two additional parameters. Both these models will be inspected in Section 3.3.2.

## 3.3. Comparing Various Approaches

Within this section, we discuss two distinct approaches, each with its own set of advantages and drawbacks. Firstly, we examine the mathematical underpinnings of twice-differentiable cubic splines, then explore the underlying theory concerning the Nelson-Siegel (NS) and Nelson-Siegel Svensson (NSS) models. Subsequently, the calculation framework and the expected results are explained. The next step is to question the results, analyzing them independently and in the context of expectations. Finally, this section concludes by determining a singular method to proceed with.

### 3.3.1. Cubic Interpolation

As previously introduced, the use of twice-differentiable cubic splines has become a widespread approach, the mathematical clarification of which is presented here. The cubic spline interpolant manifests itself as piecewise linear in its second derivative, represented as

$$f''(T) = \frac{T_{i+1} - T}{T_{i+1} - T_i} f_i'' + \frac{T - T_i}{T_{i+1} - T_i} f_{i+1}'', \quad T \in [T_i, T_{i+1}], \tag{3.4}$$

where $f_i'' \mathrel{\widehat{=}} f''(T_i)$. It is worth noting that the second derivative maintains continuity across knot points:

$$lim_{T \downarrow T} f''(T) = lim_{T \uparrow T} f''(T) = f''(T_i) \quad . \tag{3.5}$$

If we integrate twice and make sure that the curve intersects the designated data points at maturity $T$, the key formula is obtained as

$$\begin{aligned} y(T) = \frac{(T_{i+1} - T_i)^3}{6h_i} y_i'' + \frac{(T - T_i)^3}{6h_i} y_{i+1}'' + (T_{i+1} - T) \left( \frac{y_i}{h_i} - \frac{h_i}{6} y_i'' \right) \\ + (T - T_i) \left( \frac{y_{i+1}}{h_i} - \frac{h_i}{6} y_{i+1}'' \right), \quad T \in [T_i, T_{i+1}], \end{aligned} \tag{3.6}$$

where $y_i'' = d^2 y(T_i)$, $y_i = y(T_i)$, and $h_i = T_{i+1} - T_i$.

To guarantee the continuity of the second derivative across all knots necessitates connecting $y_i''$ and $y_i$ through a tri-diagonal linear system of equations, defined as:

$$\frac{h_{i-1}}{6} f_{i-1}'' + \frac{h_{i-1} + h_i}{3} f_i'' + \frac{h_i}{6} f_{i+1}'' = \frac{f_{i+1} - f_i}{h_i} - \frac{f_i - f_{i-1}}{h_{i-1}} \quad . \tag{3.7}$$

Once the boundary conditions are given for $f_1''$ and $f_N''$, this tri-diagonal system can be resolved within $O(N-2)$ operations. As referenced in [2], the boundary condition typically employed is $f_1'' = f_N'' = 0$, creating the natural cubic spline.

### 3.3.2. Nelson-Siegel and Svensson Model

We will now take a closer look at parametric functional forms. It has been previously emphasized that the factor structure typically offers a highly accurate empirical representation of yield curve data. Chapter 4 will provide a more detailed exploration of the three systematic risks, illustrating how nearly all movements in the yield curve can be explained using this limited set of factors. While we will further discuss this in Chapter 4, the idea of employing a factor-based parametric approach appears logically sound at this stage.

The Nelson-Siegel model, as introduced in 1987, aims to define the instantaneous forward rate at maturity $T$, represented as $r(T)$. This model is based on the solution to a second-order differential equation

$$r(T) = \beta_0 + \beta_1 \cdot \exp\left(-\frac{T}{\tau_1}\right) + \beta_2 \cdot \exp\left(-\frac{T}{\tau_2}\right) \quad , \tag{3.8}$$

where $\tau_1$ and $\tau_2$ stand as time constants, while $\beta_0$, $\beta_1$, and $\beta_2$ are determined by initial conditions. The formulation's goal is to generate forward curves that exhibit characteristics such as monotonic, humped, or S-shaped profiles. However, experiments conducted by the authors revealed an issue of overparametrization. They established $\tau_1 = \tau_2$ to simplify the model, effectively presenting it as a constant combined with a Laguerre function. The Laguerre function consists of polynomials multiplied by exponential decay terms known for their approximation properties within the domain $[0, \infty)$, aligning with the term structure's domain.

To derive the yield as a function of maturity, integrating the model from zero to $T$ and dividing by $T$ results in:

$$R(T) = \beta_0 + (\beta_1 + \beta_2) \cdot \frac{1 - \exp(-T/\tau)}{T/\tau} - \beta_2 \cdot \exp(-T/\tau) \quad . \tag{3.9}$$

This expression, initially presented in the original paper, is now commonly articulated as:

$$R(T) = \beta_0 + \beta_1 \left(\frac{1 - \exp(-T/\tau)}{T/\tau}\right) + \beta_2 \left(\frac{1 - \exp(-T/\tau)}{T/\tau} - \exp(-T/\tau)\right) \quad . \tag{3.10}$$

The Nelson-Siegel (NS) model, based on four parameters, serves as a simple yet robust method for explaining various behaviors observed in the yield curve. This model presents appealing attributes, imposing essential constraints rooted in financial economic theory. Especially, even without using the bootstrapping method from Section 1.1, it ensures by itself that the corresponding discount curve satisfies $P(0) = 1$ and $\lim_{x\to\infty} P(\infty) = 0$, among other conditions.

Additionally, it offers a parsimonious approximation that fosters smoothness, guards against in-sample overfitting, crucial for producing reliable short-term forecasts, as commonly utilized in the Dynamic Nelson-Siegel model [22] or the No-Arbitrage Nelson-Siegel model [15], and encourages empirically tractable and reliable estimation.

In 1994, Svensson [61] introduced two additional parameters to the NS model due to its inability to account for yields across all maturities during stressful market conditions. To attain greater flexibility, Svensson incorporated the last term from (3.10) again with an additional $\beta$ and a new regularization parameter, leading to the expression:

$$\begin{aligned} R(T) = \beta_0 + \beta_1 \left( \frac{1 - \exp(-T/\tau_1)}{T/\tau_1} \right) + \beta_2 \left( \frac{1 - \exp(-T/\tau_1)}{T/\tau_1} - \exp(-T/\tau_1) \right) \\ + \beta_3 \left( \frac{1 - \exp(-T/\tau_2)}{T/\tau_2} - \exp(-T/\tau_2) \right). \end{aligned} \tag{3.11}$$

This modification allows for an additional hump, enabling a broader spectrum of potential forward curve shapes, such as flat, increasing, decreasing, U-shaped, or upside-down U-shaped.

Later, Bliss [7] introduced the Extended Nelson-Siegel method, which involves fitting an exponential approximation of the discount rate function directly to bond prices. This necessitates a more complex discussion, which is beyond the scope of this thesis. Further details, including a comprehensive discussion on a five-factor model designed to augment fitting flexibility, can be found in [21].

### 3.3.3. Expectations and Implementation

This section will outline the anticipated outcomes based on the theory we have just presented and the preceding literature review. Subsequently, we will detail the implementation of the various methods, providing the reader with the means to replicate the process.

Based on the cubic interpolation, the inherent twice differentiability of cubic splines ensures the differentiability of the forward curve itself. This characteristic guarantees the preservation of the original data points as the curve crosses these points. However, despite these advantages, cubic interpolation is burdened with a theoretical drawback, as it fails to uphold the monotonicity and convexity properties of the original dataset. Notably, it exhibits non-local behavior in extreme turns, leading to pronounced values of the second derivative $f''$ [2].

As emphasized in Hagan and West [29], cubic methods cannot ensure strictly positive forward rates and non-decreasing discount factors when applied directly to the discount factors, which can lead to arbitrage opportunities. The risk of inadvertently computing negative discount factors is also acknowledged in calculations [29]. Consequently, a comprehensive evaluation of these aspects is imperative, drawing insights from the results obtained through interpolating and extrapolating the provided dataset. Since we apply cubic interpolation directly to the swap sets, there should be no arbitrage issue.

Now, we will delve into the expectations associated with the Nelson-Siegel (NS) and Nelson-Siegel Svensson (NSS) models. As mentioned earlier, the NS model provides a straightforward yet robust approach to capturing various yield curve behaviors while satisfying essential settings for the discount curve. Both models are recognized for generating smooth curves, although this comes at the expense of precision, potentially leading to the loss of original data points.

The NS model exhibits limitations in addressing longer maturities, particularly in stressful market scenarios. This drawback is overcome by the NSS model, making it more suitable for applications involving very long maturities. If the second hump is not required, the additional parameter added to the NSS model can be set to a value close to zero. This means that this thesis will focus on the NSS model for implementation, where we are working with a long history of many stressful market scenarios.

A comparative study by Kazemie [37] compares linear interpolation with the bootstrapping method for calculating forward rates with the NSS model. The findings reveal that the NSS model provides accurate approximations for maturities ranging from 5 to

30 years, with differences of up to 2 basis points. However, it is acknowledged that the NSS model's approximation is less satisfactory for maturities shorter than one year. The study suggests a combination of spline and NSS approximation for improved accuracy in such cases. As we work with swap rates and they are only priced from a maturity of one year, this restriction is fortunately not relevant. Additionally, as the portfolio analysis in Chapter 5 does not extend to maturities lower than three years, this constraint does not impact the study.

It is worth noting that Kazemie's study employed the Excel solver, highlighting sensitivity to initial values in determining optimal parameter values. Given this thesis's more sophisticated optimization approach, such sensitivity is expected to be reduced.

Having discussed the anticipated outcomes of the two approaches, we will now briefly overview their implementation details. All code presented in this thesis has been developed using Python. In the case of cubic interpolation, the scipy package was instrumental, leveraging its pre-implemented Cubic Interpolation functionality. It is imperative to highlight the careful specification of boundary conditions to ensure the utilization of the natural cubic spline.

Conversely, implementing the Nelson-Siegel Svensson (NSS) model posed greater challenges. Simple approaches to optimization proved inadequate, terminating prematurely and yielding misleading results. Given the substantial historical dataset requiring optimization, run-time efficiency became a critical consideration. Therefore, an implementation strategy was developed in this thesis using a unique combination of the Adam optimizer and JAX, a library for numerical computations for automatic differentiation. This approach was chosen due to its effectiveness in handling the optimization complexity of the NSS model and ensuring accurate results. No evidence exists in the existing literature of a comparable combination of techniques tailored for this specific purpose, making this implementation a novel contribution to the field.

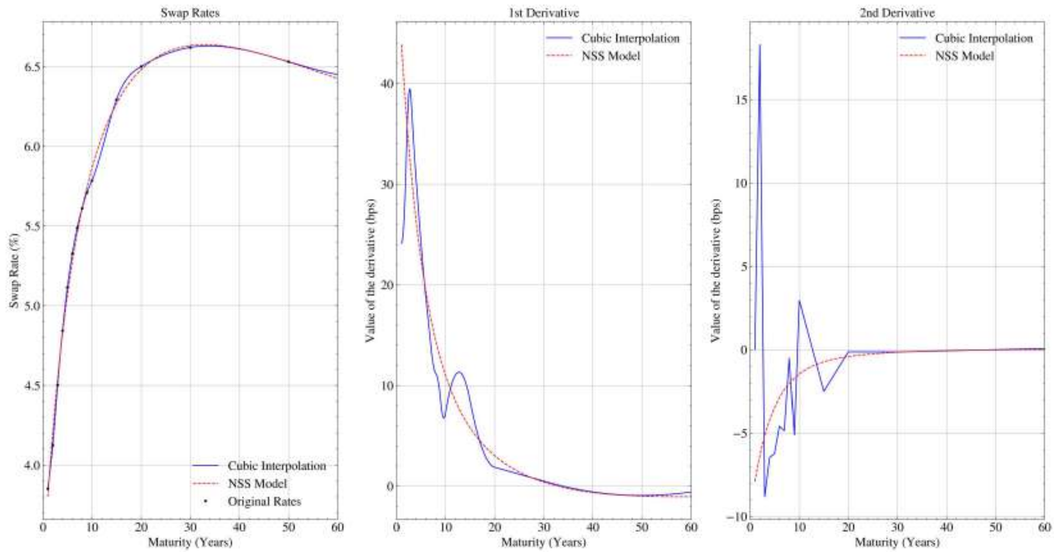


Figure 3.1.: Comparison: Cubic Interpolation vs. NSS Model (April 3, 1987)

### 3.3.4. Evaluation and Selection

We will now study the outcomes derived from the Cubic Interpolation and the Nelson-Siegel Svensson model applied to the prepared dataset generated in Chapter 2. For the analysis in Chapter 5, we will disregard results for maturities less than one year, as insufficient data was available for either method to yield meaningful outcomes. Given that none of this data is required for subsequent analyses, we can make this assumption.

To start the analysis, we focus on one illustrative historical date, comparing the results of both approaches along with their first and second derivative. Figure 3.1 illustrates this comparison. The constructed yield curve is presented on the left, showcasing its yields for maturities ranging from 1 to 60. Notably, subtle differences in convexity are apparent. Examining the gradient of the yield curve in the middle of Figure 3.1 provides a clearer view of the sensitivity of the yield curve. Additionally, the second derivative, which is a linear function in the case of cubic interpolation as seen in Equation (3.4), helps to examine the consistency of the curvature of the yield curve. In this instance, it is important to highlight that $f''$ was explicitly set to zero at maturity 1 and 50. This

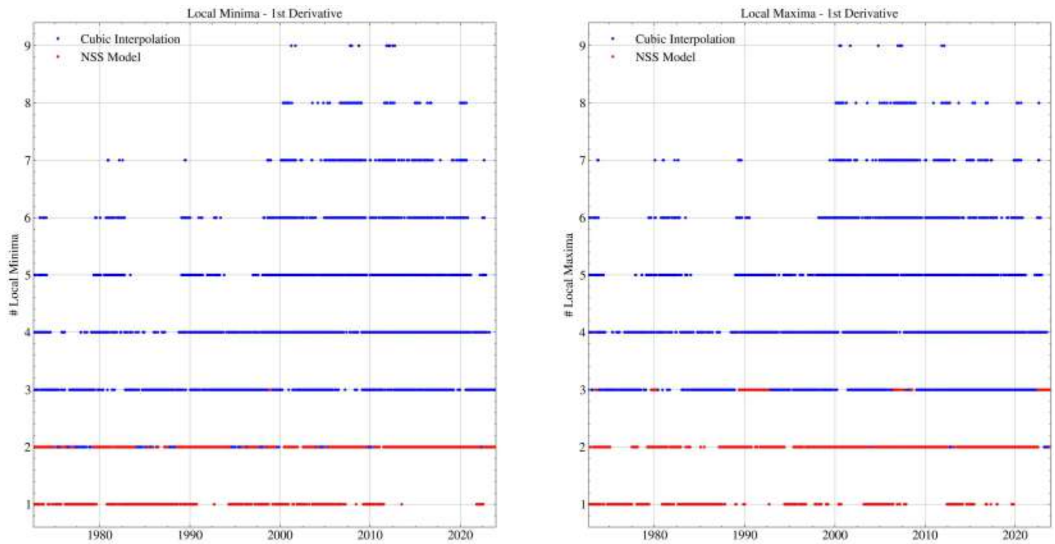


Figure 3.2.: Evolution of Critical Points

chosen boundary condition for the natural cubic spline aligns with the observed visual results.

For the 3rd of April in 1987, we observe, in alignment with the assertions made in the previous section, that the cubic interpolation fails to maintain convexity property. In contrast, as anticipated in the literature, the Nelson-Siegel Svensson (NSS) model yields a smooth curve with these desired characteristics. To extend this observation to the broader dataset, Figure 3.2 illustrates, on the left, the number of local minima in the first derivative for each date and, on the right, the number of local maxima. The visual representation affirms that the properties discussed for the specific date persist throughout the entire dataset.

Despite the literature's cautionary warnings regarding the potential risk of negative discount factors associated with natural cubic splines, our analysis, which directly applied the method to swap rates, did not encounter such issues. Curiously, negative discount factors were identified in the government bond dataset for specific lengthy maturities with an incorrect initial boundary condition after the bootstrapping method was applied. Instead of setting the second derivative to zero at these points, the "not-a-knot" condition

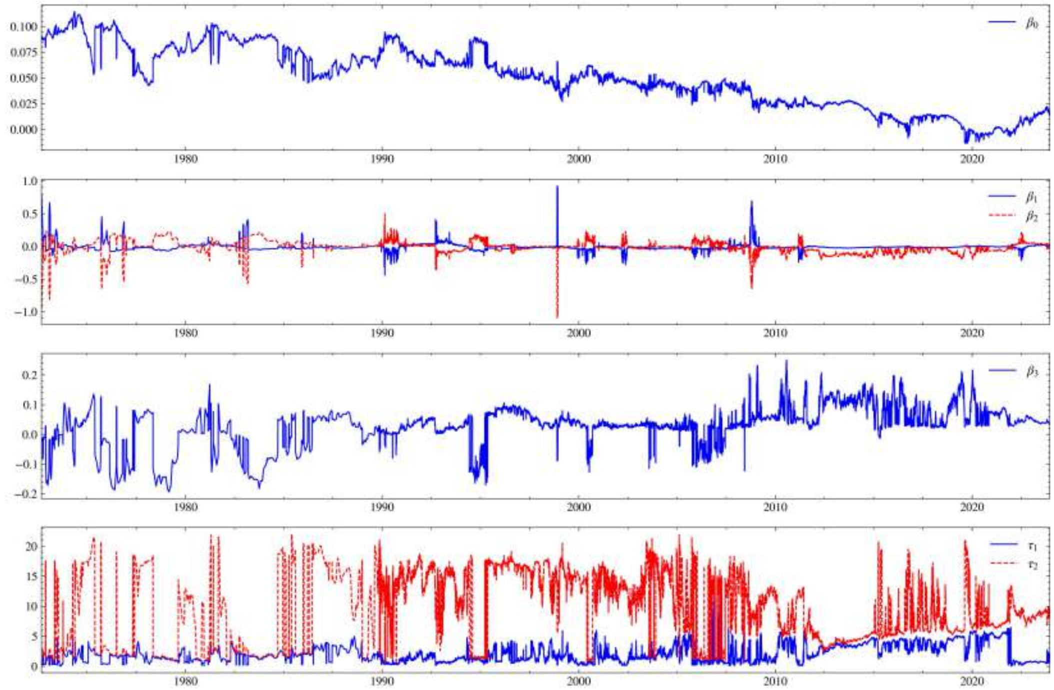


Figure 3.3.: Historical Dynamics of NSS Parameters

was employed, ensuring continuity even up to the third derivative at the first and last interior breaks. This underscores the importance of employing the correct boundary conditions, as suggested in [2].

A closer examination of the NSS model and its parameters, visualized in Figure 3.3, reveals some noteworthy insights. The $\beta_0$ parameter is particularly striking, as it shows a significant similarity to the overall trend of the yield curve over time. This similarity suggests that $\beta_0$ is instrumental in orchestrating the parallel movement of the curves.

Furthermore, the parameters $\beta_1$ and $\beta_2$ exhibit a negative correlation, implying that in Equation (3.11), we are effectively left with the $\beta_2$ parameter and the term $-\exp(-T/\tau_1)$. On the other hand, interpreting the parameters $\beta_3$, $\tau_1$, and $\tau_2$ proves more complicated. The small values of $\beta_3$ could suggest that when they approach zero, the NSS model approximates results similar to those of the Nelson-Siegel (NS) model. In stressed market scenarios, it appears that this second hump is activated, enhancing the model's

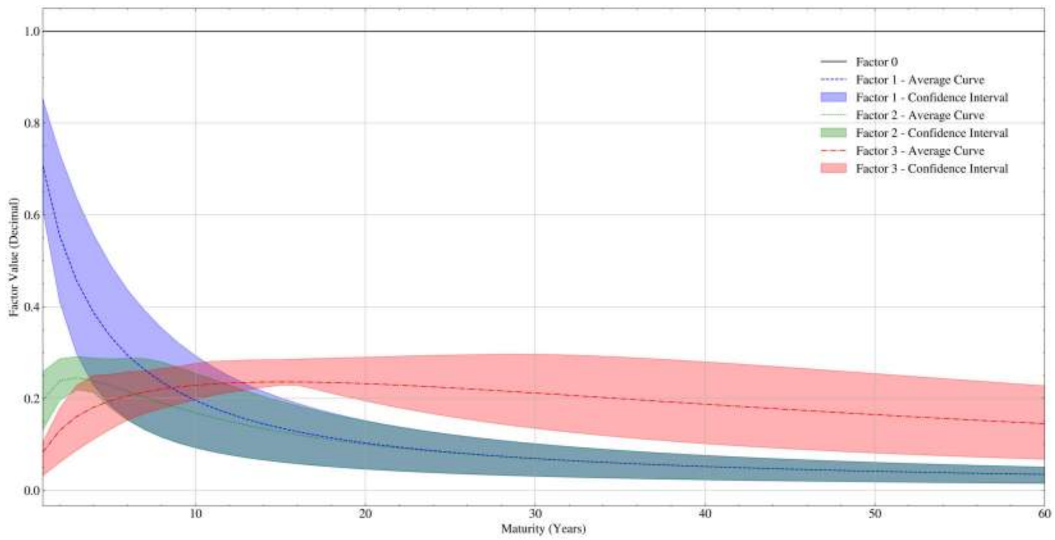


Figure 3.4.: Visualization of NSS Model Factor Loadings with [25%, 75%] CI

approximation capabilities. Future research possibilities may include exploring whether there is a significant correlation between $\beta_0$ and the 30-year long-term treasury yield, as well as whether $\beta_1$ correlates with the 2-year to 10-year treasury spread.

Despite the nuanced interpretations, the overall validity of all parameters is supported when compared to the outcomes of chapter 5 in [39]. In that work, a Genetic Algorithm was employed for parameter calculation, yielding bound constraints that align with the parameter ranges determined in this thesis. It is essential to underscore that the calibration involved an extensive 200.000 epochs. Interestingly, extending the calibration to one million epochs led to parameters that exceeded these constraints. These results were significantly inferior regarding smoothness, residual fit to the original points, and overall correctness.

For a more comprehensive understanding of the parameters, it is essential to examine Figure 3.4, which illustrates the distinct factors from Equation (3.11). It is trivial that $\beta_0$ retains a factor of 1 throughout, serving as the overarching interest level. The first and second factors are employed for changes in shorter maturities, which clarifies the interpretation of parameters $\beta_1$ and $\beta_2$. The occasionally negatively correlated behavior of these factors suggests that effects in mid and long maturities offset each other, contributing to a nuanced interpretation of shorter maturity behaviors.

The discussion often revolves around the introduction of a second hump in the NSS model. This is well visualized in factor 3 of Figure 3.4, showcasing an additional slope effect on longer maturities. This becomes particularly relevant given our focus on maturities up to 60. Assigning interpretations, factor 0 can be regarded as the level factor, factor 1 as the slope factor, factor 2 as the curvature, and factor 3 as an extra slope factor. This conceptualization sets the stage for the subsequent analysis in Chapter 4. The appropriateness of the overall behavior of these factors is evident when compared to the results obtained in section 3.3 of [37].

Revisiting the decision to prefer the NSS model over the NS model, our earlier discussions highlighted the advantageous incorporation of a second hump by the NSS model, contributing to improved performance, particularly in stressed market scenarios. In [10], section 1.6.2 suggests that some industry professionals are skeptical about the existence of a second hump. It is observed that, in general, smaller dimensions render the model more robust and less prone to instability.

After implementing the parameter calculation approach and thoroughly examining the parameters, no unstable behavior is indicated. The concerns about instability, as raised in [10], may be more relevant for smaller countries. Furthermore, countries such as Belgium, Canada, and France initially solved the four-dimensional optimization problem, utilized the obtained values as initial parameters, set $\beta_3 = 0$ and $\tau_2 = 1$ for the new parameters, and then minimized the loss function for the NSS model. Even in their case, the NSS model was only employed if the $\beta_3$ parameter significantly deviated from 0 and $\tau_2$ was not extremely large.

In the context of our training approach for the NSS model in this thesis, these concerns do not seem applicable. The robustness of our results is attributed to the quality of the data used, the liquidity in the swap rates and government bonds considered, and the parameter characteristics outlined in Figure 3.3. Additionally, an analysis of the behavior of $\beta_3$ in the NSS model reveals instances where it is nearly turned off, resembling

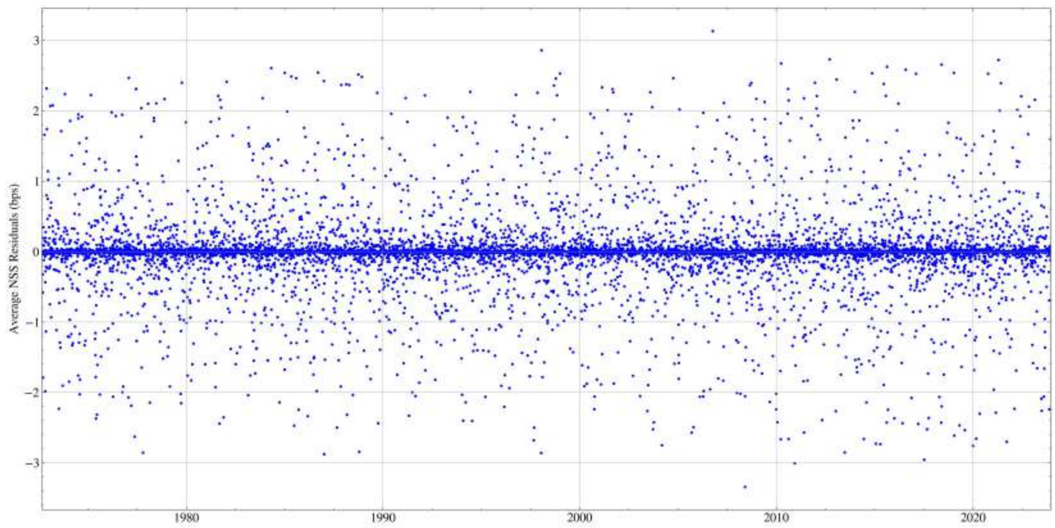


Figure 3.5.: Evolution of NSS Model Residuals Over Time

results that would have been obtained using the NS model. Based on this rationale, it is apparent that the decision to prefer the NSS model over the NS model was justified.

Finally, the disparity between the original rates and those derived from Cubic Interpolation and the NSS model must be questioned. Cubic interpolation inherently passes through the actual data points, necessitating the sole quantification of differences introduced by the NSS model. Figure 3.5 illustrates the averaged difference across all original data points over the historical period. The discrepancy can average up to 3 basis points (bps) for a given date.

The key decision in method selection revolves around striking a balance between smoothness and sensitivity for hedging and analytical purposes. Chapter 2 in [54] by Amir Sadr addresses this tradeoff and underscores the absence of a universally accepted curve-building method. He notes that the market is always considered correct for market-maker or flow-trading desks at a broker or dealer, where profit stems from the bid-offer spread of traded instruments. Consequently, the constructed curve must precisely fit all traded instruments, favoring interpolation techniques like cubic interpolation that pass through exact points. This ensures that each book is marked-to-market, theoretically enabling a correct valuation of the liquidation value. This rationale extends to investment boutiques engaged in derivatives trading, aiming to possess the same information as their broker to assess whether a particular price is excessively high.

On the flip side, the motivation might be determining the relative fair value of traded instruments, allowing for deviations. Proprietary traders often adopt this approach, aiding in determining where an instrument should trade relative to some benchmark instruments. Similarly, one can argue that backtesting analysis on a historical dataset, which focuses on relative behaviors of the term structure and prioritizes smoothness for safety, benefits from models like the NSS model.

## 3.4. Conclusion and Future Research

In this chapter, we addressed the challenge of accurately constructing yield curves. Beginning with an in-depth literature review, we explored the research history in this field. We delved into two prominent approaches: Cubic Interpolation and the Nelson-Siegel (NS) and Nelson-Siegel Svensson (NSS) model. After introducing their theoretical and mathematical backgrounds, we implemented the methodologies, outlining the anticipated results. A detailed analysis of the outcomes for each construction technique was then conducted using the prepared dataset from Chapter 2. We emphasized the tradeoff between smoothness and the correct inclusion of data points in the final curve, providing examples of typical users for each method.

Looking ahead to the analysis in Chapter 4 and 5, the emphasis shifts toward the importance of curve smoothness and the smoothness of forward rates. Given that we are examining historical trends and are more interested in diverse curve shapes over time rather than exact quotes at every point in time, the enhanced flexibility and smoothness provided by the addition of the second hump in the NSS model align with our objectives.

In [2], it is mentioned that forward rates obtained from cubic interpolation are differentiable. Still, twice differentiable cubic spline yield curves often exhibit oscillatory behavior, spurious inflection points, poor extrapolatory behavior, and non-local behavior when prices in the benchmark set are perturbed. A disturbance in a single benchmark price can lead to a slow-decaying "ringing" effect on the $C^2$ cubic yield curve, causing the perturbation's influence to extend across the entire yield curve. To overcome these limitations, [3] suggests introducing tension into the spline by employing the classical exponential tension spline construction method from [55]. Subsequently, this tension spline is directly applied for interpolating the discount curve.

In [28] and [29], a comprehensive analysis of various interpolation techniques, including cubic interpolation and a monotone-preserving cubic spline, is presented. A notable milestone in this exploration is the introduction of monotone convex interpolation directly applicable to forward rates. The paper by Jherek Healy [31] establishes that popular methods for directly interpolating forward rates correspond to classical interpolation methods on discount factors. The prominence of these discount factor methods increased following the impactful research conducted by Hagan and West in 2006 [28], where they developed monotone convex interpolation specifically for this application.

Du Preez [23] identified specific conditions under which the interpolation function of monotone convex interpolation could lead to discontinuities in forward rates. This discovery prompted the introduction of the monotone-preserving method of interpolation by Du Preez, which exhibits slightly improved stability and continuity of forward rates. However, this method possesses the characteristic of non-differentiability at knot points. Muthoni, Onyango, and Ongati proposed another modification [48], which addressed the non-differentiability at knot points by incorporating Hyman monotonicity constraints.

The implementation and analysis of these alternative approaches are left for future research. Given our focus on constructing the interest rate swap curve, abbreviated as the swap curve, for the analysis in Chapter 4 and 5, these methods may not be ideally suited for our current research objectives. Therefore, the theoretical quality of smoothness in the forward rates derived from the NSS model suffices for our present needs.

Moreover, additional insights are provided by Muthoni [47] through an exploration of a different market, where a parametric functional form was compared with cubic interpolation. Despite the different market conditions, Muthoni concludes that when considering the spot curve and the forward rates, the parametric functional form yields

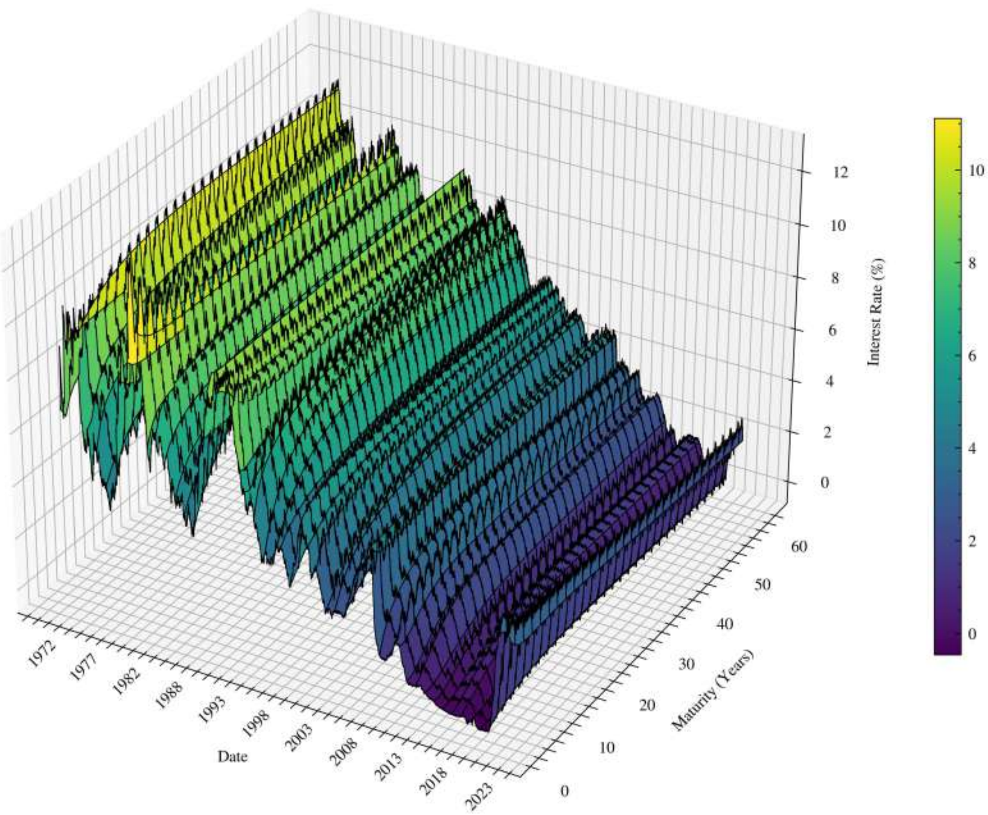


Figure 3.6.: Resultant Data from NSS Model

superior curves for pricing securities in a historical context. The significance of smoothness and monotonicity is particularly emphasized for maturities exceeding 25 years. This observation aligns with our decision to employ the NSS model in this thesis. Additionally, when recalling the approach from Section 2.3, where longer maturities were calculated through a heuristic method, using the NSS model ensures the creation of realistic shapes between 1972 and 1989.

It is important to reiterate that our analysis did not incorporate data preceding the one-year maturity point. To improve the results in this short-term range for both techniques presented, one could consider adding €STR overnight rates as well as one- and three-month Euribor rates and Euro futures for maturities up to three or four years to the dataset, as these are very liquid. Visualizing the yield curve ultimately constructed by the NSS model in Figure 3.6 provides a comprehensive representation of the yield curve's behavior, capturing nuances and complexities essential for understanding market dynamics. The details uncovered through this thorough evaluation pave the way for in-depth exploration and analysis in the upcoming sections, allowing us to delve deeper into the interest rate dynamics, risk assessment, and portfolio optimization.

As we conclude this chapter, several possibilities for future research have already been outlined. One noteworthy parametric approach for further analysis could also be the model introduced by Wiseman [68][69]. Recent research from 2022 [12] compared the Five Factor De Rezende-Ferreira model and a Feed Forward Neural Network applied to data from BRICS countries, yielding interesting results. Another area that justifies further investigation is exploring the support vector machine [46] for curve construction.

# 4. Principal Component Analysis (PCA)

The established dataset from the previous chapters covers daily swap rates from 1972 to 2023, transformed into a continuous yield curve using the Nelson-Siegel Svensson model. In pursuit of analyzing and simplifying the daily changes in swap rates for utilization in the subsequent portfolio analysis (Chapter 5), the focus shifts to addressing reducing dimensionality.

The high correlation among the absolute returns of daily swap rates across different maturities seen in Figure 4.1 characterizes the data's stationary. However, the increased correlation might introduce multicollinearity issues. This highlights the necessity to convert the data into a lower-dimensional set of linearly uncorrelated variables. The spectral decomposition principle provides a method to achieve this goal.

The spectral decomposition theorem establishes that for any symmetric matrix $Q \in \mathbb{R}^{n \times n}$, there exists a factorization such that:

$$Q = ALA^T \quad . \tag{4.1}$$

Here, $A$ signifies an orthogonal matrix composed of the normalized eigenvectors of $Q$, constituting an orthonormal basis of $\mathbb{R}^n$, $A^T$ represents the transpose of matrix $A$ and $L = \text{diag}(\lambda_1, \cdots, \lambda_n)$ symbolizes the diagonal matrix of eigenvalues of $Q$ with $\lambda_1 \geq \lambda_2 \geq \cdots \geq \lambda_n$ [44].

## 4.1. Introduction

This leads us to introduce Principal Component Analysis (PCA). PCA, initially introduced by Pearson in 1901 [49], has since emerged as one of the most preferred techniques for

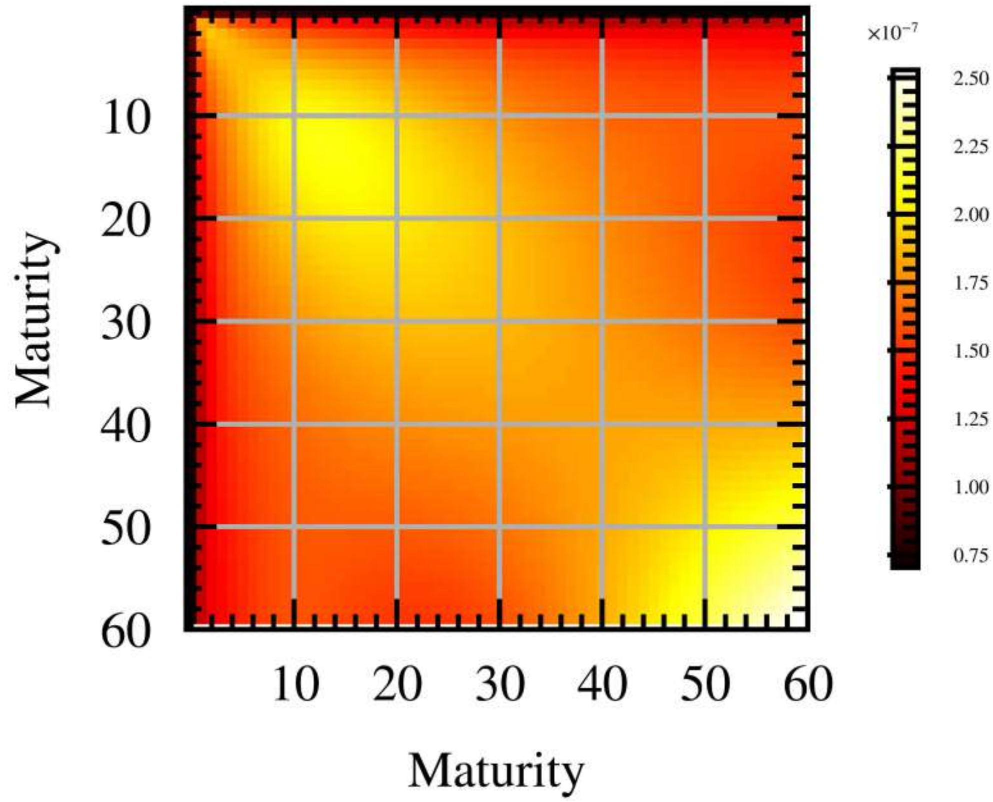


Figure 4.1.: Correlation Matrix for All Maturities

dimensionality reduction in various fields. A standard reference for this technique can be found in Jolliffe's work [35]. In a comparative analysis by Van Der Maaten and Hinton [64], PCA proves its efficiency in real-world applications, positioning it as a preferred choice for this study.

The primary objective of PCA is to identify the predominant sources of variation within a dataset so that a reduced set of components captures the majority of the variance present in the data. Applying this method in finance traces back to studies by Steeley in 1990 [60] and Litterman and Scheinkman in 1991 [40]. Their pioneering contributions focused on analyzing the dynamics of the yield curve within the US interest rate market. They established that the first three principal components explain over 90% of the historical market volatility during the 1980s. Moreover, these components individually represent a parallel shift, a change in slope, and an adjustment in the curvature of the term structure.

In a different study conducted by Carmona [11], specifically in chapter 2.5, PCA was applied to analyze the daily changes in the US Treasury bond curve from 1995 onwards, covering 1352 trading days. The study also applied PCA to swap rates from May 1998 to March 2000, producing similar outcomes, where the first three components accounted for over 99% of the variance. The following sections delve into a more comprehensive and mathematical exposition of this methodology.

## 4.2. Mathematical Foundations

Previously, spectral decomposition was introduced as a method applicable to any symmetric matrix $A$. This implies its applicability to any covariance matrix $\Sigma$. A positive semi-definite matrix, which is the given case for any covariance matrix, also ensures that $\lambda_i \geq 0$ for all $i$.

We will proceed to present the mathematical foundations of PCA, following the definitions outlined in chapter 3.4 of [26], chapter 1.7 of [10], chapter 6.4 of [44], and chapter 2.5 of [11]. We aim to consolidate the relevant information and contextualize these definitions in a manner beneficial to the objectives of this thesis.

Consider a random vector $X$ characterized by a mean vector $\mu$ and covariance matrix $\Sigma$, expressed in the spectral decomposition form as $\Sigma = ALA^T$. The transformation of the principal components of $X$ is formally defined by the equation:

$$Y = A^T(X - \mu) \quad . \tag{4.2}$$

This transformation can be interpreted as a re-centering and rotation of the original random vector $X$. Each component of the rotated vector, denoted by $Y_i$, corresponds to the $i$'th principal component of $X$, determined by

$$Y_i = y_i^T(X - \mu) \quad , \tag{4.3}$$

where $y_i$ signifies the eigenvector of $\Sigma$ corresponding to the $i$'th ordered eigenvalue. This eigenvector is commonly referred to as the $i$'th loading vector, fundamental in establishing the direction of the $i$'th principal component.

It is trivial that $\mathbb{E}(Y) = 0$, and the covariance matrix of $Y$ is represented by

$$\text{Cov}(Y) = A^T L A = A^T A L A^T A = L \quad . \tag{4.4}$$

This demonstrates that the principal components are uncorrelated and possess variances $\text{Var}(Y_i) = \lambda_i$ for all $i$, aligning with the eigenvalues of the covariance matrix.

An interesting feature is the ordered arrangement of these components based on variance. The first component, $Y_1$, stands as the standardized linear combination of $X$ that exhibits the maximal variance among all possible combinations:

$$\text{Var}(y_1^T X) = \max \text{Var}(a^T X) : a^T a = 1 \quad . \tag{4.5}$$

This ordering by variance persists for $i = 2, \cdots, n$, where $n$ represents the number of dimensions. It discloses subsequent components that are orthogonal to the preceding ones, thus ensuring that they are uncorrelated with each other. To assess the explained variance of $X$, the following relationships serve:

$$\sum_{i=1}^{n} \text{Var}(Y_i) = \sum_{i=1}^{n} \lambda_i = \text{trace}(\Sigma) = \sum_{i=1}^{n} \text{Var}(X_i) \quad . \tag{4.6}$$

The interpretation of $\text{trace}(\Sigma) = \sum_{i=1}^{n} \text{Var}(X_i)$ as a measure of the total variance within $X$ demonstrates that for $k \leq n$, the variance accounted for by the first $k$ principal components can be expressed as:

$$\frac{\sum_{i=1}^{k} \lambda_i}{\sum_{i=1}^{n} \lambda_i} \quad . \tag{4.7}$$

The conceptualization of principal components as factors becomes apparent when we invert the transformation of (4.2):

$$X = \mu + AY = \mu + A_1 Y_1 + A_2 Y_2 \quad , \tag{4.8}$$

where, assuming the partition of $Y$ into vectors $Y_1 \in \mathbb{R}^k$ and $Y_2 \in \mathbb{R}^{n-k}$ indicating $Y_1$ encompasses the first $k$ principal components and $A$ is decomposed into the matrices

$A_1 \in \mathbb{R}^{n\times k}$ and $A_2 \in \mathbb{R}^{n\times(n-k)}$, respectively. Given the assumption that the first $k$ components predominantly explain most of the variance, the other components can be disregarded by setting $\epsilon = A_2Y_2$:

$$X = \mu + AY = \mu + A_1Y_1 + \epsilon \quad . \tag{4.9}$$

This representation resembles a linear factor model, forming the basis for numerous models employed within interest rate modeling, which will be detailed later. Here, $Y_1$ represents the factors, and $A_1$ is the factor loading matrix. Despite $\epsilon$ violating the assumption of a diagonal covariance matrix and having no correlation with $Y_1$, the principal components can be construed as factors and utilized to construct approximate factor models.

## 4.3. PCA on Swap Rates

PCA has been extensively employed in financial settings, particularly in the swap market. Consider a multivariate dataset represented as:

$$x = [x(1), \cdots, x(N)] \quad . \tag{4.10}$$

Here, each column $x(t) = (x_1(t), \cdots, x_n(t))^T$ signifies the increments of swap rates within our maturity spectrum $X(t)$ and $N$ denotes the number of trading days in the provided dataset.

The spectrum $X(t)$ is identically distributed as $x$, exhibiting a mean $\mu = \mathbb{E}[X]$ and a covariance matrix $\Sigma = \text{Cov}[X]$, characterized by the spectral decomposition $\Sigma = ALA^T$. After calculating the empirical mean $\hat{\mu}$, we define the sample covariance matrix as:

$$\hat{\Sigma}ij = \text{Cov}[x_i, x_j] = \frac{1}{N}\sum_{t=1}^{N}(x_i(t) - \hat{\mu}_i)(x_j(t) - \hat{\mu}_j) \quad . \tag{4.11}$$

Utilizing the spectral decomposition, we derive

$$\hat{\Sigma} = \hat{A}\hat{L}\hat{A}^T \quad , \tag{4.12}$$

where $\hat{A}$ represents the matrix of eigenvectors, and $\hat{L} = \text{diag}(l_1, \cdots, l_n)$ is a diagonal matrix comprising ordered eigenvalues.

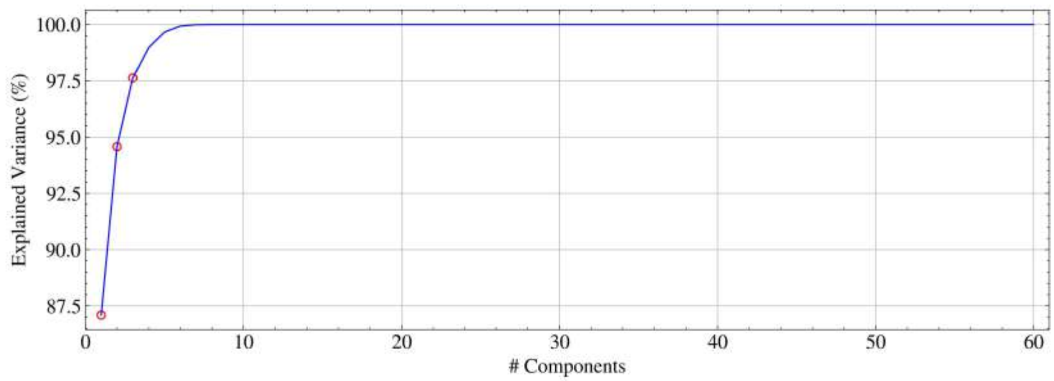


Figure 4.2.: Cumulative Variance Explained by Principal Components

Given the positive semi-definite nature of $\hat{\Sigma}$, we can utilize the previously introduced methodologies to obtain the empirical principal components:

$$y = \hat{A}^T(x - \hat{\mu}) \quad . \tag{4.13}$$

Here, the loadings $\hat{a}_i$ are represented as column vectors of $\hat{A}$. The empirical mean $\hat{\mu}$ and covariance matrix $\hat{\Sigma}$ are standard estimators for the corresponding true parameters, assuming observations are either independent or at least serially uncorrelated. However, the assumption of independence or serial uncorrelation might be debatable for daily swap rates. A common approach is to consider the increments $\delta X(t) = X(t) - X(t-1)$ instead [26], a technique already mentioned before and applied in this analysis. A relevant case study for comparison involving UK forward curves from 1989 to 1992 is elaborated in [52].

## 4.4. Macroeconomic Interpretation of Principal Components

Within the existing literature, significant attention has been directed towards leveraging the informative capacity of the first three principal components to uncover granular aspects of interest rate dynamics across various maturities. For this reason, the introduced Principal Component Analysis (PCA) is now applied to the dataset generated by the Nelson-Siegel-Svensson (NSS) model, as discussed in Chapter 3.

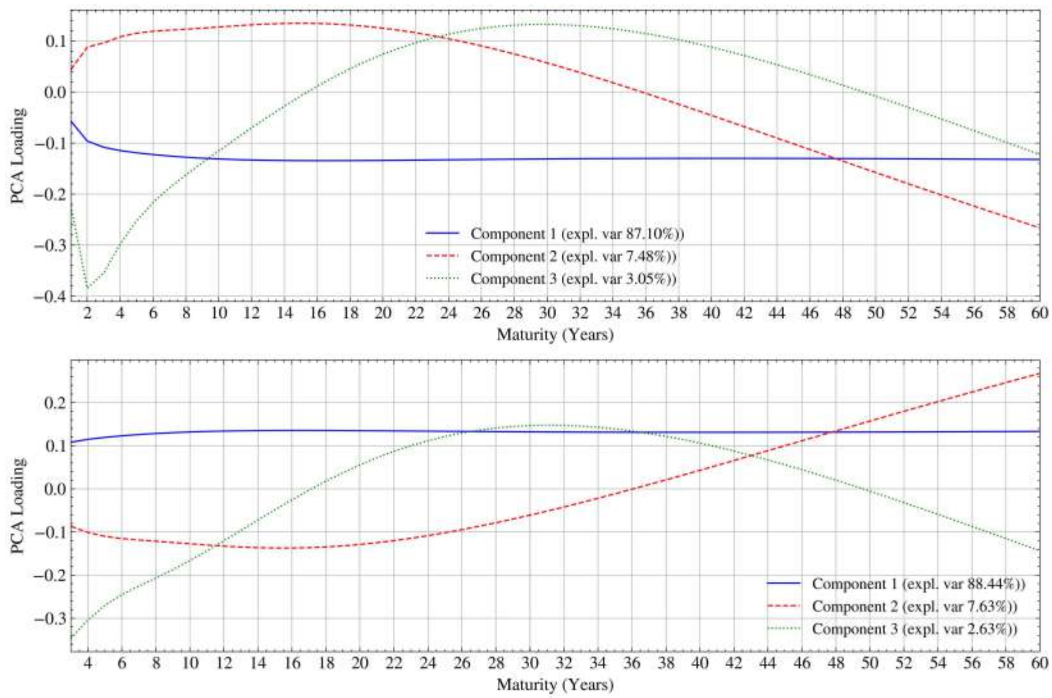


Figure 4.3.: Explained Variance by the First Three Principal Components

Upon inspecting Figure 4.2, it becomes clear that employing three principal components aligns with a comprehensive viewpoint on variance explanation. Specifically, the first three principal components collectively account for approximately 97.63% of the variance in the daily changes of swap rates spanning 1972 to 2023.

We aim to examine the macroeconomic effects of the individual principal components thoroughly. An interesting observation arises if we exclude the initial maturities up to year three. This assumption, based on the volatility considerations of the portfolios to be examined in Chapter 5, as these never enter maturities below three years, leads to an increased explained variance of about 98.70%.

Comparing the two analyses in Figure 4.3 reveals detailed insights into each principal component's changes and their respective contribution to the explained variance. This systematic analysis sets the stage to understand better the complicated dynamics driving the interest rate landscape.

The observed mirroring along the x-axis in the first and second principal components is a computational artifact from the PCA calculations. It is essential to point out that this mirroring effect holds no bearing on the substantive interpretation of the component. In practical terms, this mirroring implies that the factor loadings are simply multiplied by -1 relative to each other. Consequently, while the visual representation may appear inverted, the inherent information and implications encapsulated by the second principal component remain intact and retain their interpretative significance.

The first principal component primarily captures the overarching trend or level inherent in interest rates, reflecting general fluctuations influenced by factors such as central bank policy decisions, current economic conditions, and inflation expectations. This component reflects shifts from central bank interventions, impacting short-term rates through policy adjustments and market operations. Consequently, modifications in the first principal component frequently correspond to strategies implemented in monetary policy to manage economic conditions and regulate inflation.

In contrast, the second principal component delineates the slope or twist observable within the yield curve. This component reflects alterations in the spread between short-term and long-term interest rates, subject to influences from central banks, mainly through changes in monetary policy outlooks or forward guidance. Market sentiments and expectations regarding future interest rate movements, shaped by these policy adjustments, significantly impact the yield curve's slope and, consequently, the second principal component.

The third principal component predominantly captures the curvature evident within the yield curve, indicating variations in the convexity or concavity of the term structure. This component is sensitive to unconventional monetary strategies, such as quantitative easing and liquidity management implemented by central banks. Such measures often target long-term rates, contributing to observable changes in the curvature of the yield curve, thereby reflecting the influence of these policies.

Central bank decisions and their communication strategies are crucial in shaping these principal components. Financial markets closely monitor central bank meetings, policy communications, economic forecasts, and forward guidance as pivotal indicators of potential shifts within these principal components, influencing the broader yield curve dynamics.

In Chapter 5, we will leverage this understanding of macroeconomic decisions and their impact on the swap curve. We aim to analyze the influence of each principal component on two portfolios, facilitating the management and quantification of portfolio risk attributed to specific movements rooted in macroeconomic dynamics. Currently, we focus on testing the PCA on our prepared dataset, seeking to validate the common findings in the literature.

## 4.5. Evaluation and Analysis

In the preceding sections, we delved into the theoretical foundations of Principal Component Analysis (PCA). We underscored the common practice of using the first three components for interpreting daily changes in swap rates. These components are known to effectively encapsulate a significant portion of the variance in such rate movements. Beyond that, we provided a macroeconomic interpretation of these components, offering a visual representation in Figure 4.3 using the specific dataset relevant to this thesis. In this section, we embark on an in-depth analysis of the PCA outcomes applied to the prepared swap rate data.

Our objective is to extract meaningful patterns and interpretations from the PCA outcomes, aiming to apply them in a practical example involving different portfolios with specific exposures to the swap curve in Chapter 5. As highlighted in Figure 4.3, the decision to exclude the first two maturities before conducting PCA proved beneficial due to the high volatility in the initial periods. Consequently, the ensuing analysis focuses on the filtered data, starting with maturity 3.

Chapter 23 of [27] describes that over a given time interval, the behaviors of all points in the yield curve may appear heterogeneous, suggesting the influence of multiple factors. Nevertheless, a more refined understanding suggests that yields corresponding to adjacent times-to-maturity are likely to move together, whereas those with greater temporal

| PC | Variance | Std. Dev. | Expl. Variance | Cum. Expl. Variance |
|---|---|---|---|---|
| | $\lambda_i$ | $\sqrt{\lambda_i}$ | $\frac{\lambda_i}{\sum(\lambda_i)}$ | $\frac{\sum_{i=1}^{k}\lambda_i}{\sum_{i=1}^{n}\lambda_i}$ |
| 1 | 1.019044e-05 | 0.319% | 88.444% | 88.444% |
| 2 | 8.787854e-07 | 0.094% | 7.627% | 96.071% |
| 3 | 3.034384e-07 | 0.055% | 2.634% | 98.704% |
| 4 | 1.296102e-07 | 0.036% | 1.125% | 99.829% |
| 5 | 1.681893e-08 | 0.013% | 0.146% | 99.975% |
| 6 | 2.456158e-09 | 0.005% | 0.021% | 99.996% |
| 7 | 3.466739e-10 | 0.002% | 0.003% | 99.999% |
| 8 | 6.223525e-11 | 0.001% | 0.001% | 100.000% |
| 9 | 6.898086e-12 | 0.000% | 0.000% | 100.000% |
| 10 | 5.319285e-13 | 0.000% | 0.000% | 100.000% |

Table 4.1.: Statistical Examination of First 10 Principal Components

separation exhibit less mutual dependence. In this context, disturbances impacting a single yield tend to spread across the term structure based on the proximity of other points. This observation forms the basis for conducting PCA on the empirical covariance matrix of absolute (or relative) yield returns, as explained here. In alignment with this approach, we computed the daily changes in swap rates and derived the empirical covariance matrix. Additionally, we assume that daily swap rate changes follow a multivariate normal distribution, a premise that aligns with the general behavior observed in these daily movements.

The detailed insights into the results of Principal Component Analysis (PCA) on the swap rates are summarized in Table 4.1. This table thoroughly examines the first ten principal components derived from the filtered swap rates and the key statistical measures. These measures include the variance ($\lambda_i$), standard deviation ($\sqrt{\lambda_i}$), explained variance, and cumulative explained variance. Together, these components shed light on the intrinsic variability embedded in the daily changes of the swap rates, offering a

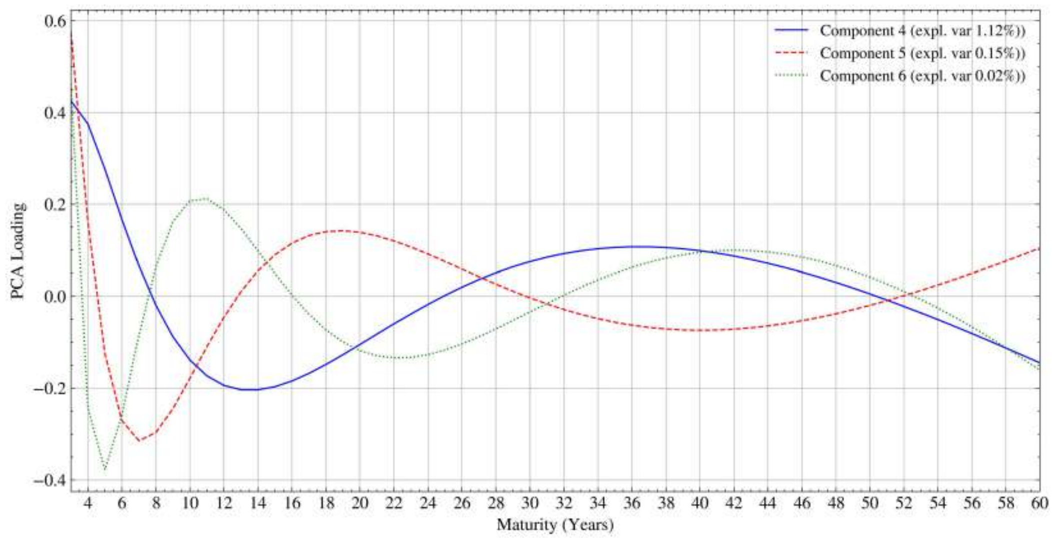


Figure 4.4.: Explained Variance by Principal Components 4, 5, and 6

nuanced understanding of each component's significance within the broader context of overall changes.

The variance of each principal component ($\lambda_i$) reflects the range of information captured by individual components. Complementing this, the standard deviation ($\sqrt{\lambda_i}$) is a normalized metric, quantifying the spread of values around the mean and providing insight into the normalized variability. The explained variance, expressed as a percentage of the total variance, clarifies each principal component's specific contribution to the dataset's overarching variability. Furthermore, the cumulative explained variance accumulates the contributions up to a specified component, offering a full view of the contained information. A differentiated consideration of explained variance is crucial in strategically identifying influential principal components. Components with higher explained variance contribute more significantly to the dataset's overall variability. Therefore, carefully evaluating cumulative explained variance is vital in determining the minimum subset of principal components needed to represent most of the dataset's variability. This cautious selection forms the core of dimensionality reduction, allowing for a more concise representation of the dataset while retaining its essential features.

Given the cumulative explained variance by the first three principal components reaching almost 99%, a reasonable choice is to focus on these components for the analysis. However, a detailed examination of components 4 to 6 remains valuable, as they contribute marginally to the overall variance. Figure 4.4 illustrates these three components, emphasizing their potential impact in real-world applications. It can be important for a practitioner to consider them alongside the primary three components in a comprehensive analysis, as they may exert influence in specific scenarios. An insightful discussion on the concept of tail risk and its relevance in dimension reduction can be found in [62].

After closer inspection, the three principal components reveal substantial fluctuations, which makes them difficult to interpret in a macroeconomic context. A deeper analysis of the most influential fourth component exposes a better distribution of its impact across distinct temporal terms. These terms include very short periods (up to 8 years), medium durations (8 to 25 years), long spans (25 to 51 years), and very long durations (over 51 years). The observed split of influence and the categorization into temporal terms underscore the complex nature of these additional components, necessitating careful consideration of their implications in a broader financial analysis.

Our attention now shifts to the factor loadings derived from PCA, as illustrated in Figure 4.5, corresponding to the first three principal components. Beginning with the period from 1972 to 1989, we observe a substantial influence from the Brownian bridge, implemented in Chapter 2 that differs from the results obtained in the time onwards of 1989. This influence significantly impacts components 2 and 3 during this period, as indicated by a lower frequency of outliers and a reduced density of larger values. Notably, this behavior is not mirrored in component 1. The Brownian bridge's effect on the yield curve, characterized by the curve moving up and down to the same extent across all maturities - particularly at the start of each month - implies that specific shape changes are more pronounced in the month's latter half. This explains the different weighting of the parallel shift and the other two types of change.

At least some caution is advised when interpreting results from this period, especially

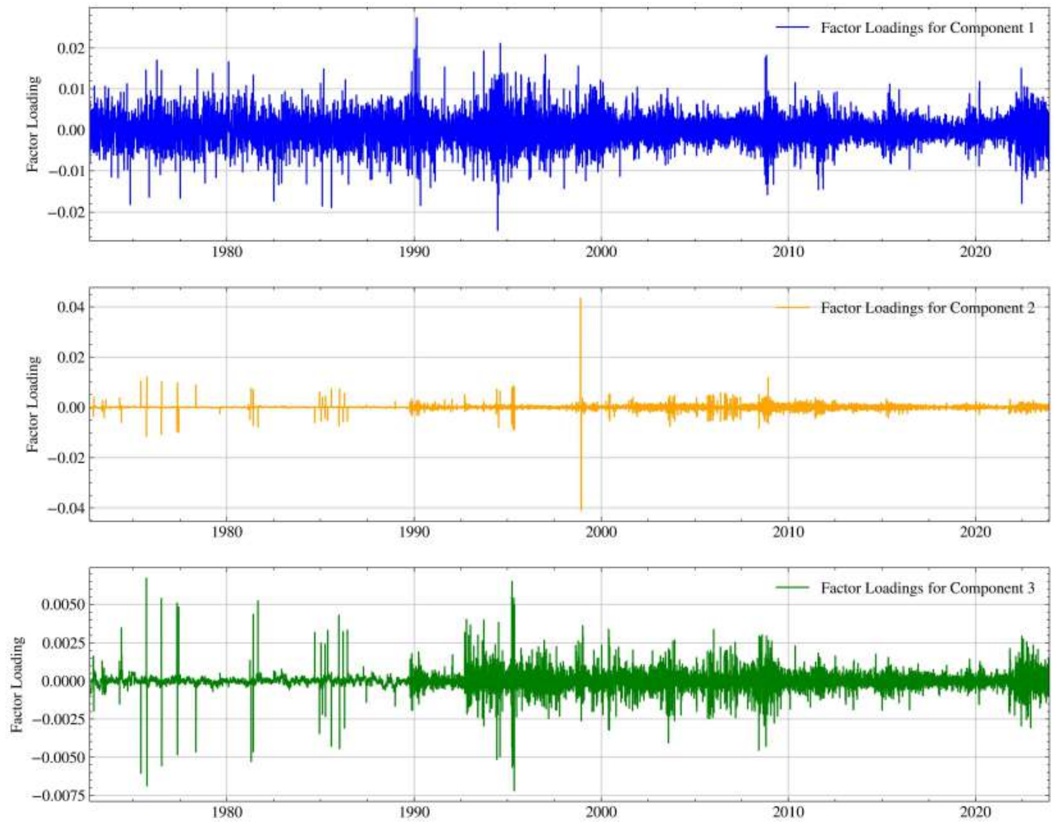


Figure 4.5.: Time-Series Analysis of PCA Factors

concerning their applicability to practical applications. There is potential for refining the Brownian bridge based on PCA results from 1989 onwards. Consequently, the variance explained by the first component may be relatively higher for the entire period than when considering the time from 1989 onwards. When conducting PCA on the data starting from October 1, 1989, the first component explains 85.86% of the variance, while components 2 and 3 explain 9.49% and 3.05%, respectively. The cumulative explained variance by the first three components remains almost the same at 98.40%. While the components' general behavior and macroeconomic interpretation remain consistent, keeping these temporal fluctuations in mind is crucial. Such considerations become especially important when reflecting on the data construction process in Chapter 2 and when applying the

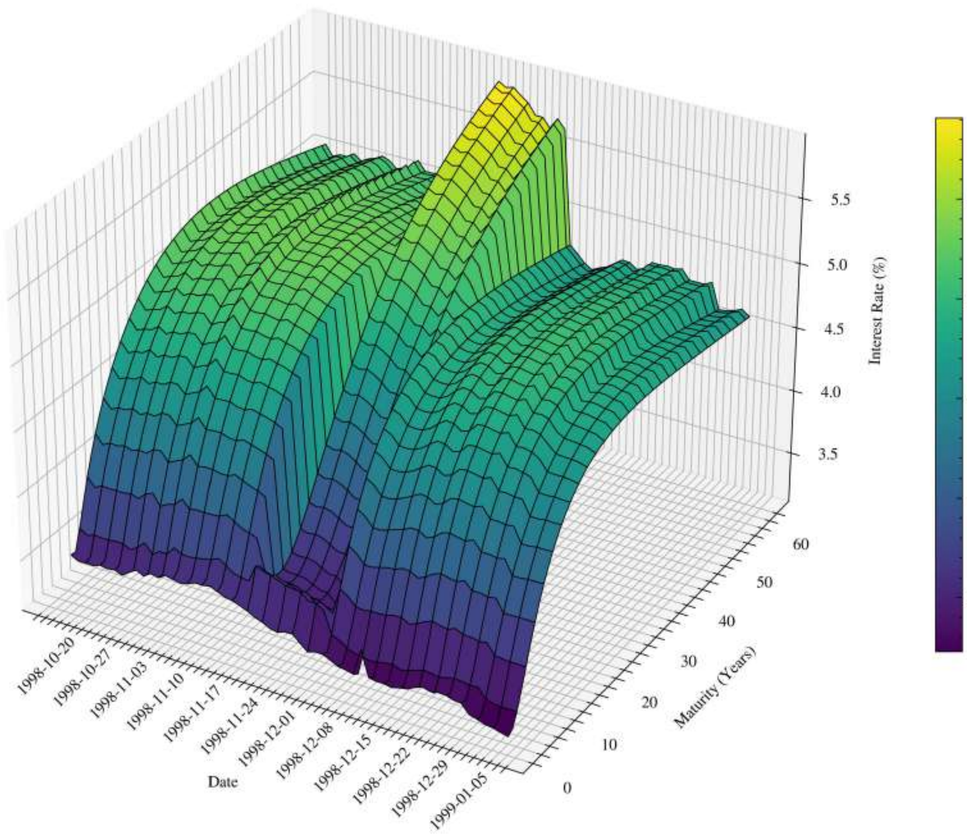


Figure 4.6.: Unusual Period Identified by PCA

results in practical applications.

Turning our attention to the overall behavior of each principal component derived from PCA, we observe that all weights tend to average around zero. This aligns with the overarching concept of daily interest rate movements from a medium to long-term perspective.

Nevertheless, among the general behavior, the factor loadings of component 2 at the end of 1998 stand out. To further investigate this unusual occurrence, we examine the swap rates from October 20, 1998, to January 10, 1999, as shown in Figure 4.6. The noticeable abnormal behavior during this period prompts a closer examination. Given that this time frame aligns with the period just before the introduction of the Euro, it becomes essential to investigate whether this particular event stems from data errors or if it can be contextualized within the macroeconomic landscape of the time.

Efforts to explain the cause behind this irregularity have not provided a clear explanation. One factor to consider is the stability of refinancing rates during the period under consideration. It should be noted that the first European Central Bank (ECB) refinancing rate was only published on December 22, 1998, and therefore had no direct influence. Still, it would have impacted market dynamics if market participants had been uncertain about the direction of monetary policy before this date.

In spite of the currency and financial crises in East Asian emerging markets during the summer of 1997, the market in 1998 appears unaffected, with the Deutsche Bundesbank's semi-annual report[1] for the first half of 1998 reflecting a certain degree of optimism in the financial markets. Regardless, it is noted that the rouble crisis in August 1998 unexpectedly worsened the climate of the financial markets. Yet, the significant decrease in swap rates on November 23, 1998, and the subsequent immediate increase on December 7, 1998, are challenging to explain. It can be considered that events on the previous weekend played a role, as both days were on a Monday.

In 1998, the Bundesbank also conducted three short-term balancing operations for the money market. These operations, including foreign exchange swaps and a quick tender with a five-day term, did not lead to any major changes in the interest rate market at the end of April and the end of October. The intervention at the end of November, involving the liquidation of foreign exchange swaps amounting to DM 4.9 billion with a maturity of nine days, may explain the purpose of this action, which was also intended to ensure the transition to the European Monetary Union (EMU).

In contrast, it is essential to emphasize that comparable effects in German government bonds were not evident then. This casts doubt on the hypothesis that the Bundesbank interventions mentioned are solely responsible for the observed irregularities. Overall, there remains a lack of clarity about the exact causes of the observed movements in

[1] Visit Deutsche Bundesbank's annual report 1998 for more information.

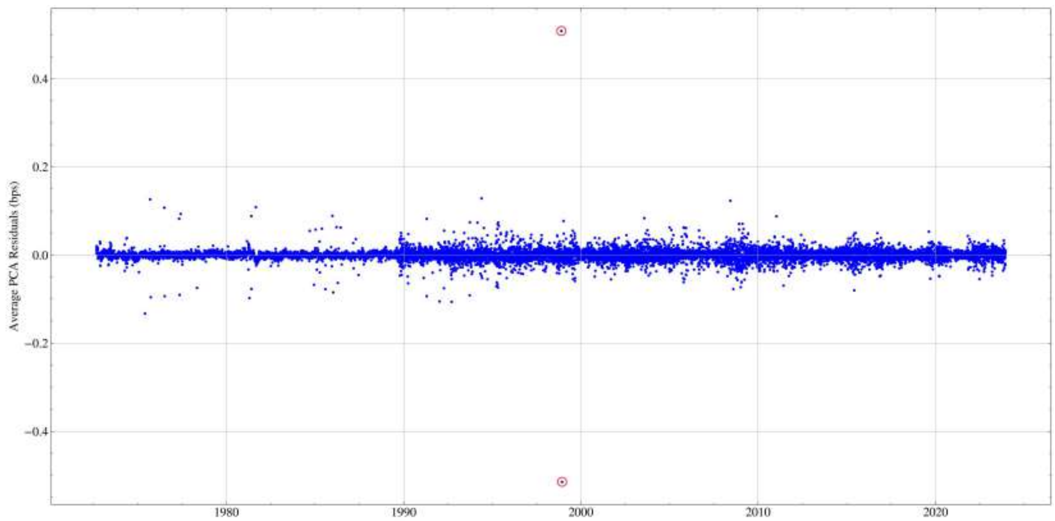


Figure 4.7.: Mean Deviation: Original vs. Reconstructed Swap Rates (First 3 PCs)

swap rates. Despite the explanatory approaches presented, it is not easy to establish a causal relationship. Given this uncertainty, we avoid reaching a definitive conclusion, even though valid arguments exist for addressing this potential data error by employing a Brownian bridge.

After analyzing the economic period in 1998, one can also see the financial crisis from 2007 to 2009, as a density of elevated values can be observed in all three components. This is not surprising, as the fluctuations in the market are relatively high due to the high level of uncertainty among market participants at this time. The same applies to the period in July 2022, when the ECB changed its policy and initiated a turnaround in interest rates. Ten further increases followed this in the most important key interest rates. It was not until October 26, 2023, that the ECB decided for the first time not to raise the key interest rate and reaffirmed this decision on December 14, 2023.

Continuing our analysis, an interesting aspect involves examining reconstructed data using only the first three principal components. In this process, we calculate residuals across all maturities and dates within the historical dataset, obtaining the average residual for each date. This can be visualized in Figure 4.7. Evidently, apparent differences

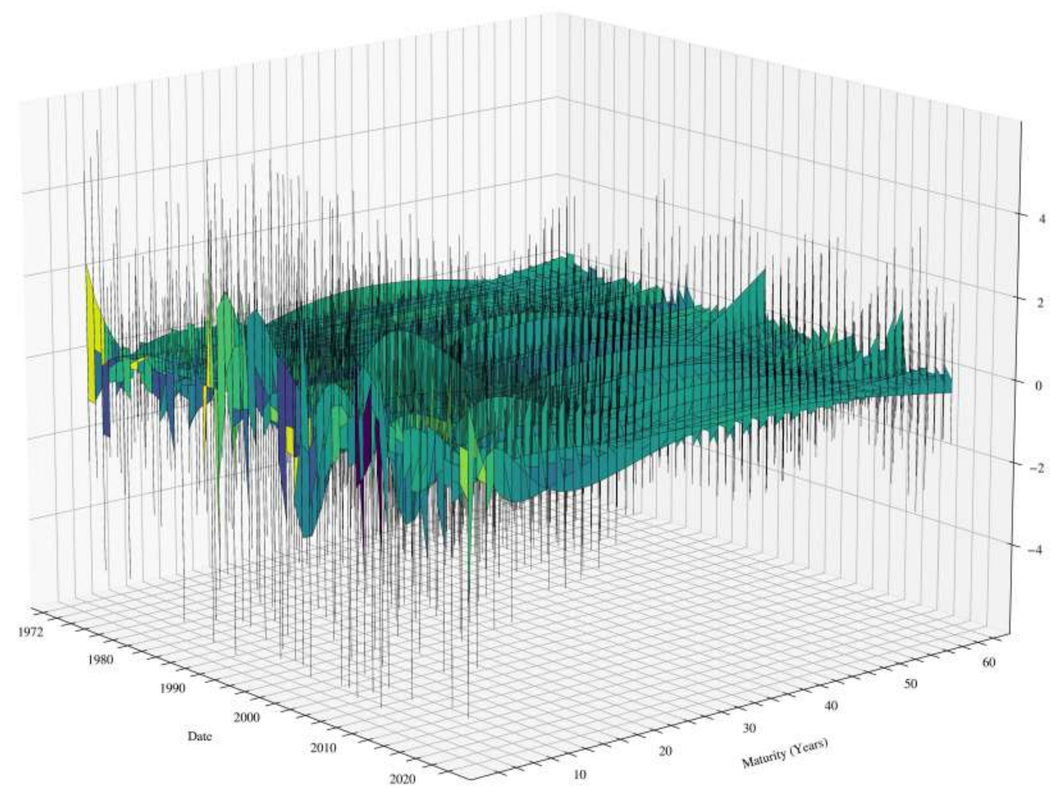


Figure 4.8.: Overall Residuals in Reconstructed Swap Rates

emerge when contrasting data from periods before and after 1989. The discrepancy could be attributed to the lack of intra-monthly data during that period, with the need to generate such data through a more controlled Brownian bridge. Once more, the outliers previously discussed, now highlighted in Figure 4.7, draw attention.

Analyzing this graphical representation provides initial insights, but a more comprehensive understanding is obtained by exploring the complete residual matrix, as illustrated in Figure 4.8. To address outliers, we have visualized the 99% confidence interval here. This visualization reveals wave-like behavior in the residuals across maturities, ranging from -4 to 4 basis points, which can be regarded as relatively small. The observed wave-like pattern can be attributed to the excluded principal components during the analysis. This distinctive pattern emphasizes the importance of considering the excluded principal components, as demonstrated in Figure 4.4. It underscores the necessity of caution when exclusively analyzing daily changes through the perspective of the first three principal components, even though the average residuals per date and the overall residuals consistently remain close to zero.

## 4.6. Conclusion and Future Research

In conclusion, this chapter looked at applying Principal Component Analysis (PCA) to the complex field of swap rates. PCA, a powerful mathematical tool for dimensionality reduction, was explained, highlighting its potential to break down complicated market dynamics into recognizable components.

The analysis of PCA results revealed valuable insights into the behavior of swap rates. A thorough examination was carried out, interpreting each derived principal component within a macroeconomic framework. It is crucial to feature the temporal heterogeneity in data quality before and after October 1989, acknowledging the potential impact on real-world applications.

Furthermore, the intentional choice to exclude the first two maturities, supported by a rationale grounded in market volatility, emerged as a methodological gain. The introduction and interpretation of the additional principal components 4, 5, and 6 added depth to the analysis, shedding light on potential areas for further research and development.

The exploration of an abnormal period at the end of 1998 has shown that outliers and anomalies must be examined very closely. This thorough investigation contributes to a better understanding of the results, promoting a cautious approach when translating findings into real-world applications.

On another note, this chapter recognizes the significance of ongoing refinement and development, particularly in enhancing the quality of the Brownian bridge methodology introduced in Chapter 2. The insights gained from PCA analysis pave the way for many ideas and methods that can be applied in the financial markets, considering both the strengths and limitations.

Continuing the exploration, additional insights from the literature reveal considerations that deepen our understanding of the PCA results. One notable observation, as discussed in the literature, relates to the applicability of PCA in less liquid markets, such as emerging currencies with less active fixed income markets. In these markets, the lower correlation between interest rates can make it challenging to create a transparent and comparable analytical framework similar to what has been accomplished in our study of the highly liquid European swap market.

Another recurrent idea, emphasized in [10], revolves around cases where a single component explains a predominant proportion of the variation. In such instances, a recommended practice involves removing the effect of this dominant component, frequently achieved by subtracting the overall mean rate level. Subsequently, PCA is performed on the transformed data, emphasizing fluctuations around the mean rate level. While this methodology holds potential interest for further research, our primary focus remains on the authentic components of daily changes. The decision to retain the real components becomes particularly crucial as these will serve as the foundation for the real-world application explored in Chapter 5.

In light of the PCA results, the revelation of underlying components unveils the underlying factor structure embedded in interest rate dynamics. The consistency of the "parsimony principle", evident in the factor structure, suggests the benefit of incorporating constraints in interest rate models. While this practice can affect the in-sample fit, it is a robust defense against data mining, leading to more effective out-of-sample modeling [56]. This understanding catalyzes the development of various interest rate models, leveraging factor structures to augment their explanatory power and analytical tractability.

Among the numerous models, the Vasicek model adopts a one-factor approach, attributing interest rate movements to a single source of risk [65]. Similarly, the Ho-Lee model introduces a streamlined one-factor framework to describe interest rate fluctuations [33]. The Cox-Ingersoll-Ross (CIR) model incorporates mean reversion within its one-factor structure, capturing the tendency of interest rates to revert to a long-term average [17]. Advancing beyond single-factor models, the Heath-Jarrow-Morton (HJM) framework introduces multiple factors, offering a more detailed representation of interest rate movements across various maturities [32]. Additionally, affine term structure models capitalize on factor structures by assuming linear relationships between yields and underlying factors, providing analytical tractability and flexibility in capturing interest rate dynamics [18]. The Dynamic Nelson-Siegel model, an extension of the traditional Nelson-Siegel, incorporates factors evolving over time to capture term structure dynamics [14]. This same principle is applied in the Dynamic Nelson Siegel Svensson model [22]. Collectively, these models showcase the incorporation of factor structures into interest rate modeling, contributing to a better understanding of the complexities inherent in interest rate behavior.

In undertaking PCA on European swap rates, it is essential to underscore the methodological approach adopted in this thesis. The sequential execution of tasks allows for a comprehensive analysis encompassing all maturities constructed in Chapter 3. Improving our ability to identify nuanced behaviors across a spectrum of maturities provides a more refined understanding of the underlying dynamics. This wide-ranging analysis is made possible by the large dataset created in Chapter 2 and comprises over 50 years of market data.

The significance of utilizing the entire spectrum of constructed maturities becomes apparent when considering practical applications. The versatility of the analysis makes it possible to investigate at various temporal resolutions, ranging from monthly and weekly to daily maturities. Alternatively, one could focus on specific periods to explore the underlying behavior within distinct macroeconomic environments.

Embracing a cyclical or paradigmatic view of the economy, drawing connections between historical results may be more accessible, creating a narrative that reflects recurring patterns [19]. This enables the isolation of specific economic paradigms for in-depth examination, utilizing PCA to compare historical results with the present global or European economic landscape. Such an approach offers valuable insights for decision-making in the capital market.

# 5. Portfolio Dynamics: Clustering, Sensitivities, and PCA

## 5.1. Introduction

In this thesis, a comprehensive dataset of European swap rates from over 50 years was thoroughly constructed. A continuous yield curve was created that can be adjusted to different time resolutions of maturities - from annual to monthly and even daily. In addition, a Principal Component Analysis (PCA) was performed to uncover underlying patterns with macroeconomic implications.

With this mathematical foundation and extensive dataset, the challenge is to find a practical use case in which all of this can be applied. One interesting avenue that arises from the insights gained in Chapter 4 is to examine different economic paradigms throughout history. By connecting these paradigms, especially in the context of swap curves and their different forms, we will identify and analyze three clusters: Flat, steep, and inverse curves. Each cluster and its average spot curve are then investigated further.

The ensuing information will quantify each principal component's impact on the portfolio sensitivity. This portfolio comprises exposures derived from forward swap rates introduced in Chapter 1. The structural process involves cluster identification, computation of discount factors and forward rates, illustration of portfolio exposures, discussion of simplifying assumptions, and the explanation of delta buckets and their calculations. The integration of PCA into this framework will facilitate the quantification of principal component influence on two exemplary portfolios. The analysis concludes with thoroughly examining these quantities, placing them within a broader macroeconomic context.

## 5.2. Historical Clustering

Cluster algorithms, rooted in the field of unsupervised machine learning, constitute a potent toolkit for unveiling latent structures within seemingly disorganized datasets. By categorizing data points based on shared features, clustering algorithms facilitate the identification of recognizable patterns and trends, offering a comprehensive tool for analyzing the diverse dynamics of historical swap movements.

To systematically explore various clustering possibilities, we adopt the classification presented in [13], organizing them into four domains: Raw-data clustering, filtering methods, adaptive methods, and distance-based methods. Raw-data clustering operates directly on observed data points. Filtering methods, conversely, approximate curves through a finite basis of functions, such as B-splines, to reduce dimensionality. Clustering is subsequently performed using coefficients derived from the basis expansion or functional principle component scores. Adaptive methods seamlessly integrate dimensionality reduction and clustering by treating basis expansion coefficients and functional principle component scores as random variables with cluster-specific probability distributions. Unlike filtering methods, adaptive methods treat these variables as stochastic, providing a more dynamic representation of the functional nature of the curves. Lastly, distance-based methods cluster curves by establishing dissimilarity or distance measures between them without assuming a predefined form for the curves. Depending on the application of these distances, these methods can align with either raw-data or filtering methods, offering flexibility in capturing the similarity characteristics between functional observations.

The objective of clustering is to identify the embedded structure within data when no prior information, apart from the observed values, is available. In our context, we possess some structural information regarding the typical shapes a yield curve takes. Exploiting this information advantage should be mandatory.

Before that, typical clustering approaches commonly used in the field of interest rates are presented, which can be used in the manner described above. A great overview of which clustering methods are widely used in the financial world is given in [63]. We will pick two of the presented algorithms that suit our use case very well and present them shortly.

The first widely recognized approach involves hierarchical clustering algorithms. These methods organize data points into a hierarchical, tree-like structure, unveiling related trends at different levels of granularity. They require either a codependence and similarity metric or some distance or dissimilarity metric to achieve this. They exhibit efficiency in handling clusters that are non-convex, anisotropic, and possess unequal variance. Hierarchical algorithms permit connectivity constraints, facilitating the linking of points even if the centroid is not part of the cluster. However, these approaches may encounter challenges in properly handling elongated clusters. Interestingly, a standard solution to this issue involves using PCA without dimensionality reduction to orthogonalize the features.

In contrast to hierarchical clustering methods, the K-Means clustering method, a centroid-based approach, partitions data into distinct groups or clusters. The objective is to minimize the sum of squared distances between data points and the centroids of their assigned clusters. This can be mathematically expressed as

$$J = \sum_{i=1}^{N} \sum_{k=1}^{K} \mathbb{1}(c_i = k) \cdot \|x_i - \mu_k\|^2 \quad , \tag{5.1}$$

where $\mathbb{1}(c_i = k)$ is an indicator function that equals 1 if $c_i = k$ and 0 otherwise. Here, $x_i = (x_{i1}, x_{i2}, \cdots, x_{iD})$ represents the data points in a $D$-dimensional space, $c_i$ denotes the cluster assignment for each data point, and $\mu_k$ signifies the centroid of cluster $k$. The iterative refinement process in this optimization problem proves particularly effective in identifying periods characterized by similar interest rate regimes. By discerning shifts in cluster assignments over time, analysts can gain insights into the evolution of market sentiment and prevailing economic conditions. Notably, K-Means assumes that clusters are convex, isotropic, and possess similar variance compared to hierarchical approaches. Standardizing features before clustering proves beneficial due to this assumption. Another noteworthy aspect is that within-cluster variance is not a normalized metric. Consequently,

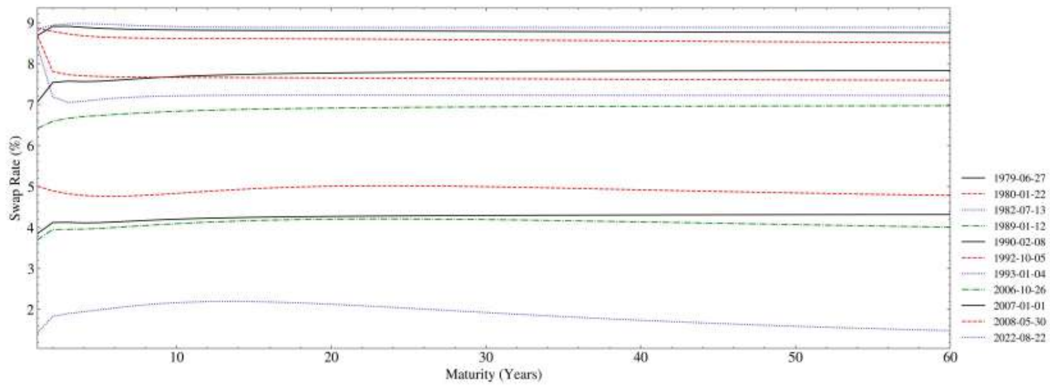


Figure 5.1.: Visualization of Exemplary Flat Spot Curves

when dealing with many features, variances might inflate, potentially biasing outcomes. Here, the utilization of PCA before clustering may be advantageous. Lastly, K-Means always converges, yet the result may be a local minimum. Therefore, running multiple instances in parallel, each with different seed centroids, can aid in confirming the correct clusters.

In conclusion, both approaches can be employed to investigate various shapes regarding historical swap curves. Given the pre-existing knowledge of typical yield curve shapes, the goal is defined as identifying three distinct clusters representing flat, steep, and inverse swap rate curves. Although both introduced algorithms encountered challenges in identifying these clusters, the K-Means algorithm proved beneficial, especially as it allowed for setting the number of clusters beforehand. Despite attempting PCA, the algorithms struggled to find the three distinct shapes for the entire dataset. Instead, two steep shapes were identified, with differences in the first 15 years of maturity, splitting into one convex and one concave steepening in these early maturities, followed by the inverse cluster.

Consequently, the identification of the flat curves involved an initial filtering step. Defining the characteristics of a flat yield curve was crucial for this analysis. To accomplish this, a practical approach is chosen in which the differences between the maturities 2 and 10, 2 and 20, and 2 and 30 are calculated. Flat curves were filtered based on these

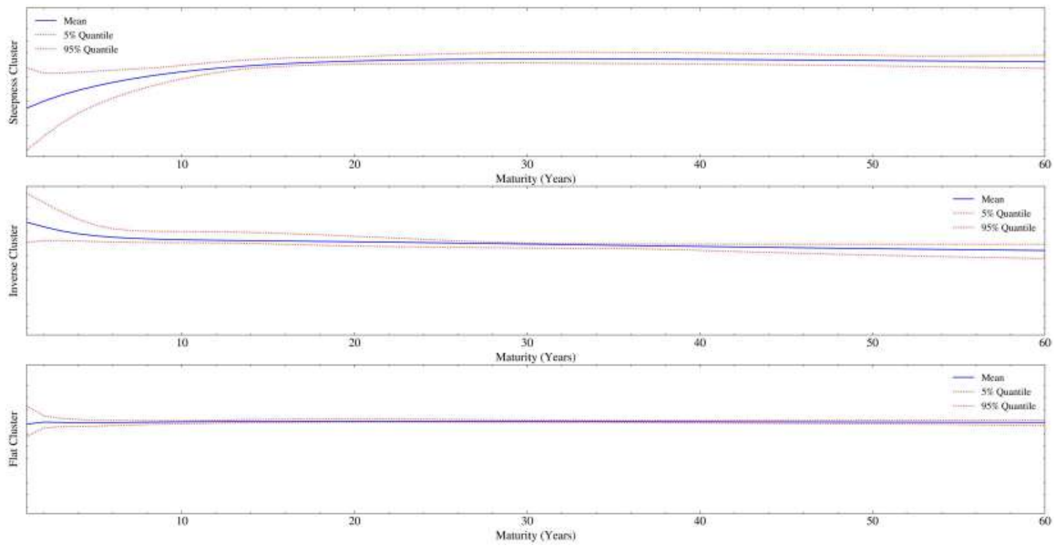


Figure 5.2.: History's 3 Identified Clusters

differences, requiring that all differences fall below 25 basis points and above -10 basis points. The choice of these boundaries reflects their significant impact on the strategic aspects of the subsequent portfolio analysis. Additionally, the inverse cluster is less frequent than the steep cluster, necessitating careful recognition of this scenario. This filtration process resulted in 911 trading days classified under a flat yield curve cluster. For each year where a flat curve was identified, an exemplary date was selected and visualized in Figure 5.1.

The K-Means algorithm has proven advantageous for extending the cluster analysis to the remaining swap curves. It is important to note that the previously introduced preprocessing steps must be considered. Initially, the mean of each date was subtracted, and each date was divided by its standard deviation to ensure standardization of the data, as this benefits the assumptions of K-Means. Furthermore, only the initial 30 maturities were implemented to mitigate the problem's dimensionality. This choice is justified by the observation that the primary market movements predominantly occur in the earlier maturities. Through the adaptation of this implementation and the multiple executions of the algorithm with different seed centers, two recognizable clusters could be

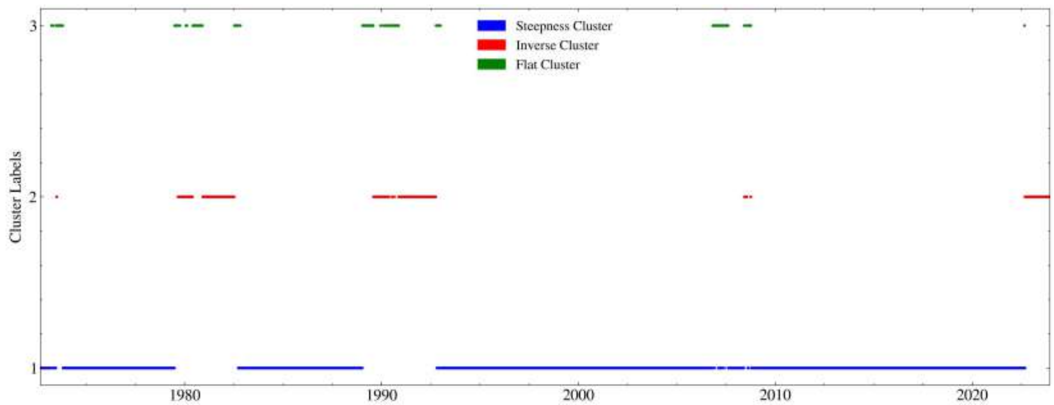


Figure 5.3.: Cluster Assignments Over Time

identified, which align with the relevant aspects of the posed inquiry. In summary, Figure 5.2 portrays the average curve of each cluster, where the mean of the curve for each date was subtracted for visualization purposes, along with their respective 90% confidence intervals.

Finally, Figure 5.3 illustrates the historical distribution of the three identified clusters. The visualization confirms the anticipated pattern: During the transition from the steep to the inverse cluster and vice versa, there is an intermediate period where flat yield curves predominate. Overall, the steep cluster prevailed in 80.86% of time, the inverse cluster in 12.33%, and the flat cluster, as we previously defined, in 6.81% of time.

In summing up, this section has provided an overview of various data preparation methods applicable to clustering. Two clustering algorithms were tested to address the specific problem of classifying different yield curves based on their shape over more than 50 years. The final approach involved filtering out relatively flat curves and utilizing the K-Means algorithm to identify two clusters representing steep and inverse yield curves. The examination of average curves and their confidence intervals demonstrates the success of the clustering, particularly in capturing the temporal distribution and adhering to the logical sequence of having flat curves as transitional phases between the other two clusters. However, there is room for improvement, especially in the way flat curves are filtered out, which was only applied in a very practical way.

For future research, a robust identification of highly persistent interest rate regimes can be found in [50]. An interesting approach is also the approach in [67], which identifies historical data segments with similar patterns to those observed in the present. This could be used to turn the results of historical analyses into implications for the present. Nevertheless, the three clusters identified here form a basis for further analysis in this chapter.

## 5.3. Key Components of Portfolio Derivatives

This section delves into the essential components that form the basis for the upcoming portfolio analysis. Building upon the concepts introduced in Section 1.1, where we outlined the fundamental ideas and calculations, we now possess thoroughly prepared swap rates across various maturities, providing the desired granularity.

To derive the necessary discount factors, we employ the bootstrapping method. Leveraging the formulas (1.18), (1.19), and (1.10), we sequentially calculate the discount factors. Subsequently, Equation (1.21) comes into play, enabling the computation of forward rates.

The derivatives selected for our analysis combine several forward swaps, for instance, the 2s20s Forward Steepener. This means taking a long position on the 20-year forward swap while simultaneously shorting the 2-year forward swap. Such combinations are widespread in the market, providing a suitable choice for our analysis.

For the sake of simplicity in our subsequent analysis, we assume that these forward swap rates are already convexity-adjusted. The details of convexity adjustment for constant maturity swaps are explained in [36].

## 5.4. Quantifying Portfolio Sensitivities

In the fixed income market, a key issue revolves around understanding price sensitivity to interest rate fluctuations, which essentially captures the derivative of present value concerning interest rates. A standard metric used for this purpose is the concept of PV01, which denotes the present value of a one basis point shift in interest rates and is often referred to as risk.

Building upon the previously introduced present value calculation of Section 1.1, we express PV01 as

$$\mathrm{PV01} = \frac{\Delta P}{\Delta s} \quad , \tag{5.2}$$

where $\Delta P$ represents the change in the present value of the derivative, and $\Delta s$ signifies the change in the interest rate in basis points. While considering convexity becomes crucial in more substantial rate movements and for longer maturities, for calculating PV01, a straightforward approach suffices [45]. To calculate PV01, we employ the present value computation for a specific instrument, such as a 2s20s Forward Steepener, with an effective date in 5 years. We obtain the desired sensitivity measure by shifting the underlying swap curve by one basis point and recalculating the present value. This is appropriate as the present value of the 2s20s Forward Steepener is zero at the outset. In addition, the choice between an upward or downward shift of 1 basis point or a symmetrical approach with a shift in both directions and averaging proves to be practically interchangeable.

For the Forward Steepener, initiating a $\Delta$-neutral position can be mandatory to ensure that its PV01 is zero at the outset. Achieving this neutrality involves appropriately setting the notional value of each forward swap using their PV01. Let us denote the notional value of the 20-year forward swap as $N_{\mathrm{fwd}_{20}} = 100\,\mathrm{EUR}$. Following this, the notional value of the 2-year forward swap, denoted as $N_{\mathrm{fwd}_2}$, can be defined as:

$$N_{\mathrm{fwd}_2} = 100\,\mathrm{EUR} * \frac{\mathrm{PV01}_{\mathrm{fwd}_{20}}}{\mathrm{PV01}_{\mathrm{fwd}_2}} \quad . \tag{5.3}$$

Here, $\mathrm{PV01}_{\mathrm{fwd}}$ represents the PV01 for the respective forward swap. This shows how, in general, the portfolio's positioning can be chosen so that a $\Delta$-neutral stance is taken and is, therefore, no longer influenced by a parallel shift in the underlying swap curve. However, for our analyses, we use the assumption that the forward rates are already convexity adjusted. This means that both notional values can simply be set to the same value, and $\Delta$-neutrality is already given. This applies to every portfolio that will be analyzed in the following.

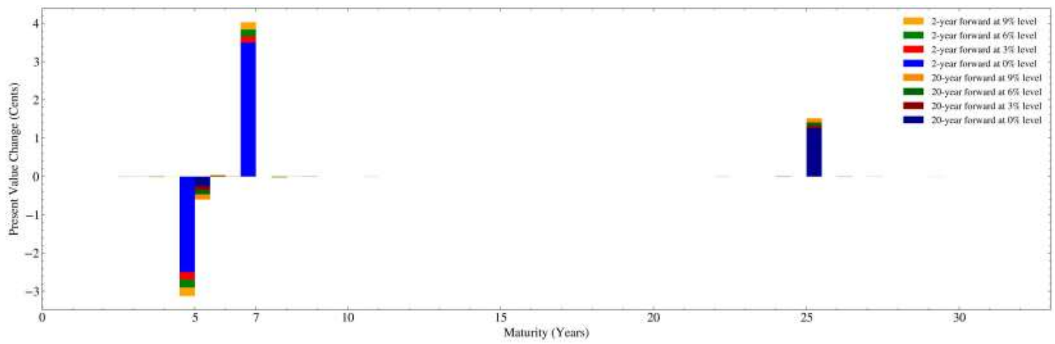


Figure 5.4.: Delta Buckets for 2-Year and 20-Year Forward Swap, 5-Year Effective Date

Derived from the idea of PV01, another approach is logical, which does not shift the entire curve by one basis point but only a single interest rate at a time. The calculation of so-called delta buckets is another key measure for quantifying the effects of individual swap rate changes [45]. These buckets serve as a tool for assessing the interest rate risk associated with a security or portfolio by examining its sensitivity to small changes in individual rates along the yield curve. Each delta bucket encapsulates the responsiveness to a one basis point alteration in the corresponding rate.

To illustrate, consider a flat curve. Employing the 2s20s Forward Steepener with an effective date in five years, denoted as $\text{FRS}_{(2s20s,5)}$, results in the sensitivities shown in Figure 5.4. The figure also shows that when altering the interest level to 0%, 6%, or 9%, a clear trend can be seen in which the sensitivity adjusts according to the changed interest rate level. This phenomenon serves as a critical consideration in the subsequent analysis.

## 5.5. Analyzing Portfolio Sensitivities

We can apply the previously developed concepts to an actual portfolio with all the tools at our disposal. In this analysis, we will leverage the extended dataset, which includes government bonds and swap rates, from Chapter 2. This dataset was thoroughly interpolated in Chapter 3 to encompass all maturities ranging from 1 to 60 years. Subsequently, we employed Principal Component Analysis (PCA), explained and contextualized in Chapter 4, to distill underlying patterns. These principal components will be vital in analyzing different interest rate movements here. Chapter 5 delved into additional facets, unveiling the discovery of three distinct clusters, the introduction of the 2s20s Forward Steepener, and the incorporation of Delta Buckets.

For the following analysis, we will examine a specific portfolio of five 2s20s Forward Steepener positions labeled as follows:

$$\text{pf}_{2s20s} = \{\text{FRS}_{(2s20s,6)}, \text{FRS}_{(2s20s,7)}, \text{FRS}_{(2s20s,8)}, \text{FRS}_{(2s20s,9)}, \text{FRS}_{(2s20s,10)}\} \quad , \tag{5.4}$$

where the tenors are set to 6, 7, 8, 9, and 10 years, respectively. Such a portfolio can be seen as an alternative investment, and its idea is to develop a positive market value over time - referred to often as roll.

The strategic consideration underlying this selection is to initially establish all five positions in a $\Delta$-neutral manner and allow them to evolve until the shortest-running position matures at an effective date in five years. Upon closure, a new position with an effective date in ten years will be opened, regardless of the prevailing macroeconomic environment or the current shape of the swap curve. Indeed, the strategy outlined is rather simplistic, as it overlooks considerations related to different clusters or varying macroeconomic environments, factors that would be crucial in practical scenarios. Despite its simplicity, it is noteworthy that historically, this portfolio has proven profitable, particularly when employed in the steep swap rate cluster, which has been predominant in 80.86% of the period since 1972.

### 5.5.1. Analysis of the 2s20s Portfolio

In the first phase of our analysis, we opt for a flat yield curve characterized by an interest level of 3%. Subsequently, we will contrast these findings with yield curves exhibiting either a steep or inverse profile, considering varying interest rate levels.

The ensuing step involves the computation of forward rates, constructing the 2s20s Portfolio outlined in Equation (5.4) by using forward swaps and computing their delta

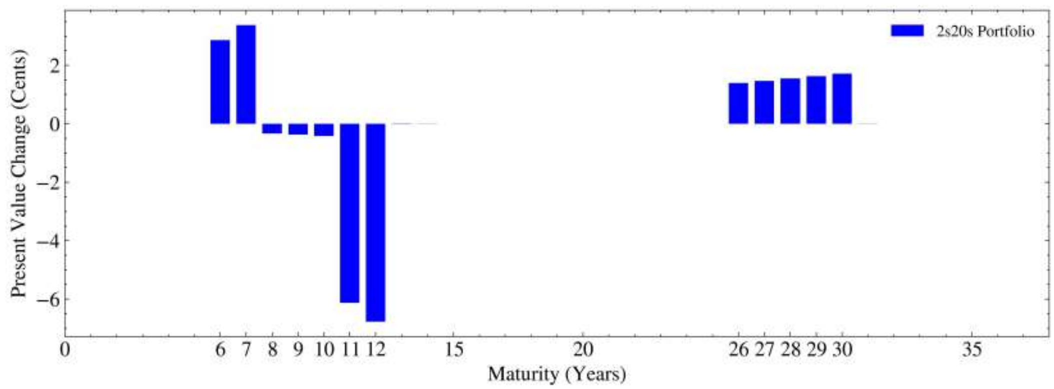


Figure 5.5.: Delta Buckets for 2s20s on Flat Spot Curve at 3% Interest Level

buckets, as previously illustrated. To clarify the notional value used for the portfolio analysis, the 20-year forward swap is consistently set to a value of 100 EUR representing the total, with the corresponding 2-year forward swap adjusted for $\Delta$-neutrality according to the equation (5.3). Since we assume convexity-adjusted forward rates, we know that the notional value is also 100 EUR for the 2-year forward swap.

A closer examination of the delta buckets specifically for $\text{FRS}_{(2s20s,5)}$ in Figure 5.4, considering an appropriately adjusted effective date, reveals that specific sensitivities counterbalance each other. This counterbalancing effect is evident in Figure 5.5, illustrating the delta buckets of the 2s20s Portfolio. Positive sensitivities are apparent for short maturities (6 and 7 years) and longer maturities (26 to 30 years), while negative sensitivities manifest at maturities 12 and 13, representing the most significant sensitivities for this portfolio. Furthermore, the offsetting effect is evident for maturities 8, 9, and 10. As previously discussed, the sum of all sensitivities equals zero, signifying that an exact parallel shift in the swap curve would not impact the present value of the portfolio.

Up to this point, our analysis has predominantly revolved around a flat yield curve. However, to enhance the realism of our investigation, we will now consider the average curve of each cluster, as computed in Section 5.2 and displayed in Figure 5.2. Setting the average of each curve to an interest level of 3%, we visualize all three curves in Figure 5.6.

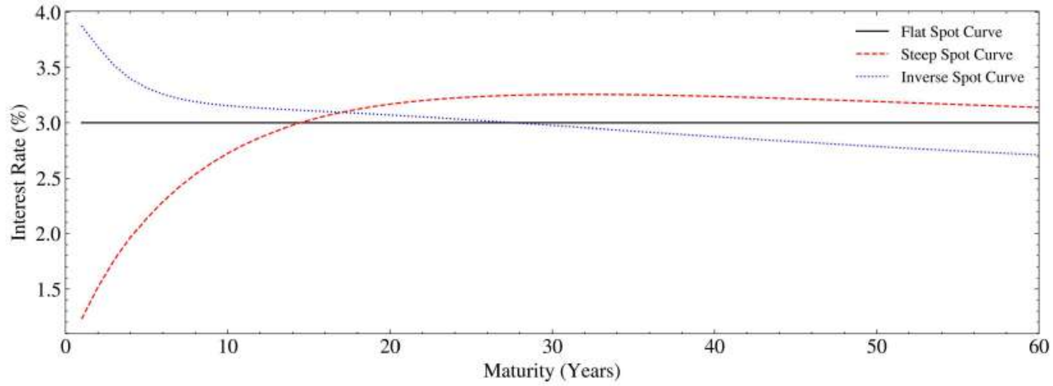


Figure 5.6.: Average Spot Curves in Different Clusters

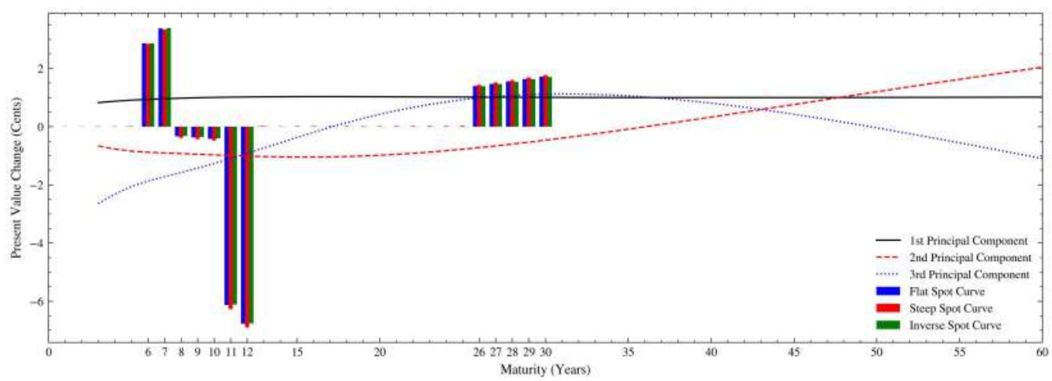


Figure 5.7.: Delta Buckets for 2s20s Portfolio

The three delta buckets corresponding to each underlying spot curve are presented in Figure 5.7. It is crucial to grasp that the values presented are denominated in Cents. This implies that a one basis point shift in maturity, for instance, at maturity seven, corresponds to an impact of approximately three Cents or EUR 0.03 on the portfolio. This detail is noteworthy as it directly impacts risk and exposure control decisions.

Upon close examination of the three distinct delta buckets, subtle differences emerge, particularly in the context of the shortest and longest maturities. These discrepancies can be attributed to discount factor variations resulting from swap rate fluctuations across different sections. A plausible inference is that, in a steep yield curve environment,

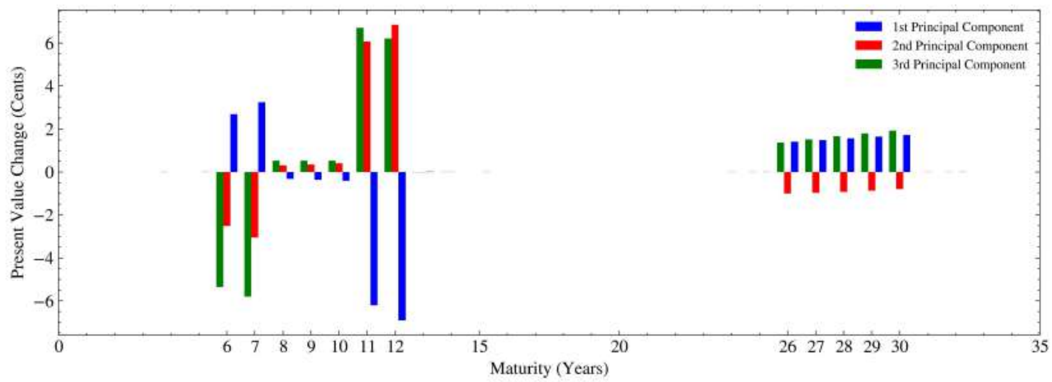


Figure 5.8.: Delta Buckets for 2s20s Portfolio with PCA Shifts

there is a slightly heightened sensitivity at longer maturities and a diminished sensitivity in the earlier ones, and vice versa for the inverse cluster.

To establish a conceptual link between macroeconomic behavior and its influence on the portfolio's present value, we utilize the three principal components derived in Chapter 4. As previously observed, these components were included in Figure 5.7. For interpretability, the principal components were normalized by the mean of the first component. This normalization ensures that the average parallel shift, which the first component signifies, is set to 1, while the other components are expressed in relative terms. As a result, this normalization facilitates the subsequent analysis and interpretation of their impact.

Furthermore, our understanding of how the components' movements impact the portfolio becomes clearer. Considering positive and negative factor loadings, looking at these effects in both directions is crucial. By multiplying the components by the values of the delta buckets, we gain insights into how these components affect the portfolio value.

The visual representation in Figure 5.8 provides a nuanced view of how each principal component influences different sections along the maturity axis and how they relate to each other. The prior normalization of the principal components makes interpreting the absolute values in Cents more feasible. One might consider this as specific maturities representing a one basis point shift, while others undergo a two or even three basis point shift. Importantly, this is always in the correct relative terms of the respective principal component, aiding in the interpretation of macroeconomic effects.

As explained in Chapter 4, the first principal component encapsulates the broader trend of interest rates. It is evident that the delta buckets multiplied by the first principal component yield nearly identical delta buckets as before. This is a trivial outcome, considering the component was normalized to represent a one basis point shift in all values. An exception might be made for maturities lower than five years; however, given our preference to avoid sensitivities in these early years due to volatility considerations, we assert that the first principal component has negligible impact on the present value. This is underpinned by our understanding that the sum of all delta buckets of the portfolio is zero, as described earlier in the context of $\Delta$-neutrality.

The second principal component is commonly referred to as the slope, while the third component is associated with the curvature of the yield curve. It is interesting to observe in Figure 5.8 that, in shorter maturities, both components exhibit a reinforcing effect, whereas the third component generates a more substantial sensitivity in very short maturities (6 and 7 years). Simultaneously, both components diverge when it comes to longer maturities (26 to 30 years).

In particular, the effects of the second component reflect real scenarios in which surprising decisions by central banks to change interest rate policy affect shorter maturities but have an even greater impact on longer maturities, as they reflect market expectations regarding future adjustments by the central bank. The portfolio's sensitivity to such scenarios is evident. Figure 4.5 in Chapter 4, illustrating the factors of each principal component over the analyzed historical data, suggests that both the second and third components show outliers during the 2007-2009 financial crisis and the recent crisis influenced by the pandemic and wars. The sum of the corresponding delta buckets for each component is insightful to measure the total influence of each component. This sum is 3.83 Cents for the second principal component, while for the third component, it is 11.64 Cents. These values will be visually compared to another portfolio in Figure 5.12.

Shifting our focus, we delve into the influence of the interest level, as explored in the previous analysis in Section 5.4, where the sensitivity for each maturity increased with a

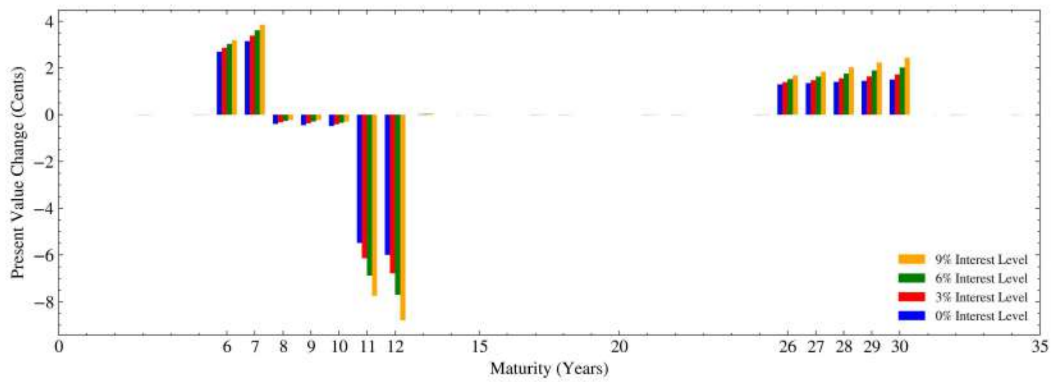


Figure 5.9.: Delta Buckets for 2s20s Portfolio on Flat Spot Curves

rise in the interest level. We again investigate this using the four flat curves with different interest levels. The outcomes, showcased in Figure 5.9, reveal an intriguing pattern. Interestingly, the interest rate level appears to impact not the relative behavior of each delta bucket in relation to each other but rather the absolute sensitivity of the portfolio to changes in individual maturities. It can be easily explained by considering the $\Delta$ neutrality, which must nevertheless be given for the underlying interest rates. Still, this observation suggests that, for risk management reasons, it might make sense to use less leverage in a high-interest rate environment than in a low-interest rate environment. It is noteworthy that the sensitivity for maturities 7, 8, and 9 decreases due to the offsetting of the 2-year and the 20-year forward curves, which effectively reduces the sensitivity in this scenario.

### 5.5.2. Analysis of the Fly Portfolio

Having examined various yield curve shapes and interest levels, along with their impacts on delta buckets and principal components, we turn our attention to another widespread combination of forward swaps in the fixed income market - the Forward Fly. This Fly involves taking a long position twice in the 20-year forward swap and shortening both the 10-year and 30-year forward swaps. If we were not assuming convexity-adjusted forward rates, we would set the notional of the 20-year forward swap to EUR 100 in each case

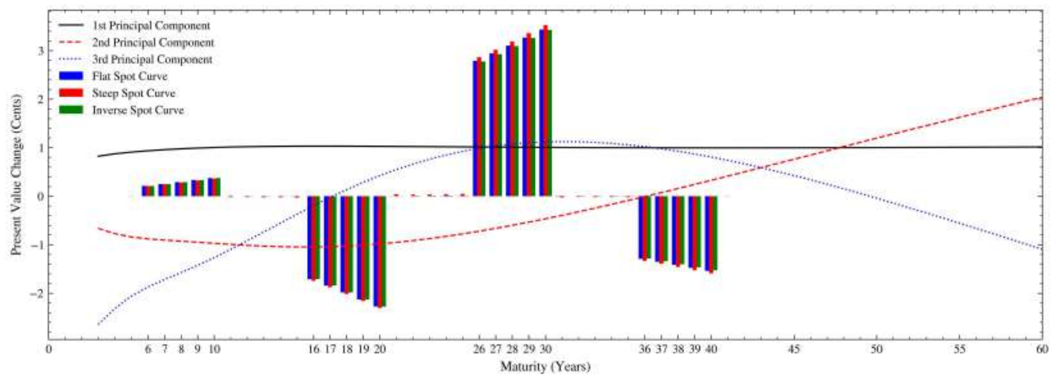


Figure 5.10.: Delta Buckets for Fly Portfolio

and adjust the 10-year forward swap and the 30-year forward swap accordingly to obtain two $\Delta$-neutral positions. Due to our simplifying assumption, all notional values are set to EUR 100 again.

For this Fly, we define a second portfolio:

$$\mathrm{pf}_{Fly} = \{\mathrm{FRS}_{(Fly,6)}, \mathrm{FRS}_{(Fly,7)}, \mathrm{FRS}_{(Fly,8)}, \mathrm{FRS}_{(Fly,9)}, \mathrm{FRS}_{(Fly,10)}\} \quad . \qquad (5.5)$$

This new portfolio inherently alters the appearance of the delta buckets and the influence of the three principal components. The delta buckets for the three different clusters and the principal components are illustrated in Figure 5.10. Initially, we observe the maturities to which the portfolio is now sensitive. Interestingly, the lower sensitivity to shorter maturities, where the most vital fluctuations are usually observed, is very noticeable. It should also be pointed out that there are a total of 20 underlying derivative positions in this portfolio.

Examining the three principal components in comparison, we notice that their influence is now distributed differently. Striking here is the curvature of the third component and the way the delta buckets are distributed. It looks like the effect of the component is reduced due to the three different sensitivity blocks at the longer maturities. Upon examining the three principal components in comparison, it becomes evident that their influence on sensitivity is distributed differently. Particularly noteworthy is the curvature of the third component and how the delta buckets are distributed. The component's

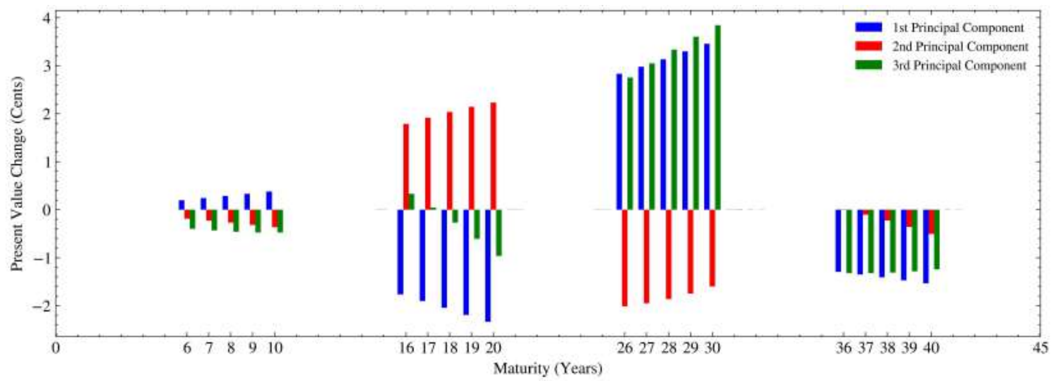


Figure 5.11.: Delta Buckets for Fly Portfolio with PCA Shifts

effect appears somewhat diminished due to the presence of the three distinct sensitivity blocks at longer maturities.

Once again, the detailed examination of the relative effects of each principal component on different maturities is revealed by multiplying the normalized components with the delta buckets, as visualized in Figure 5.11. Notably, the absolute sensitivity for each component in one bucket is lower than that for the 2s20s Portfolio, where sensitivities reached up to 6 Cents. Several interesting effects emerge from this illustration. First, it is evident that the second component appears to be neutralized by maturities 16 to 20 on one side and 26 to 30 on the other. As a result, only sensitivities at the short and very long ends of the maturity spectrum would play a significant role despite reinforcing each other. As suggested earlier, the last three blocks neutralize the third component. However, a closer look reveals that the sensitivities in maturities 26 to 30 cannot be fully balanced, indicating a significant influence of these maturities on the third component.

It is interesting to examine the sum of all individual delta buckets for each principal component within the context of the Fly Portfolio. Assuming a flat spot curve with an interest level of 3%, Figure 5.12 illustrates the present value change of the Fly Portfolio, providing a comparative analysis with the changes observed for the 2s20s Portfolio. Several noteworthy observations emerge from this comparison. Strikingly, the second component of the Fly Portfolio exhibits an opposite and lower overall sensitivity compared

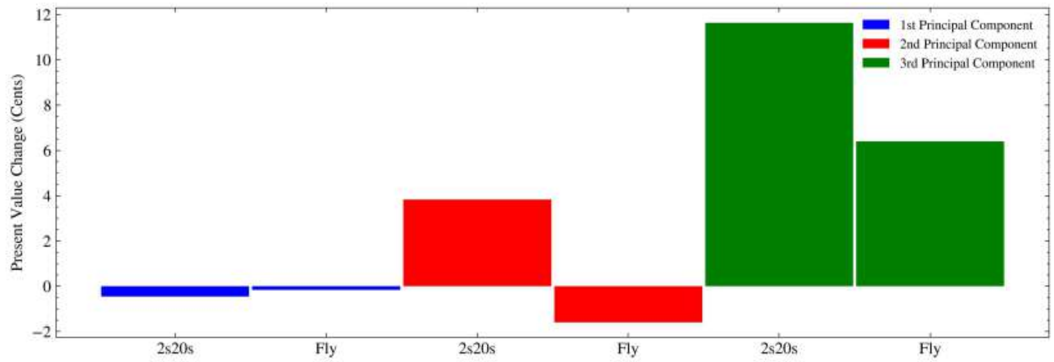


Figure 5.12.: Present Value Change for 2s20s-Fly Portfolio with PCA Shifts

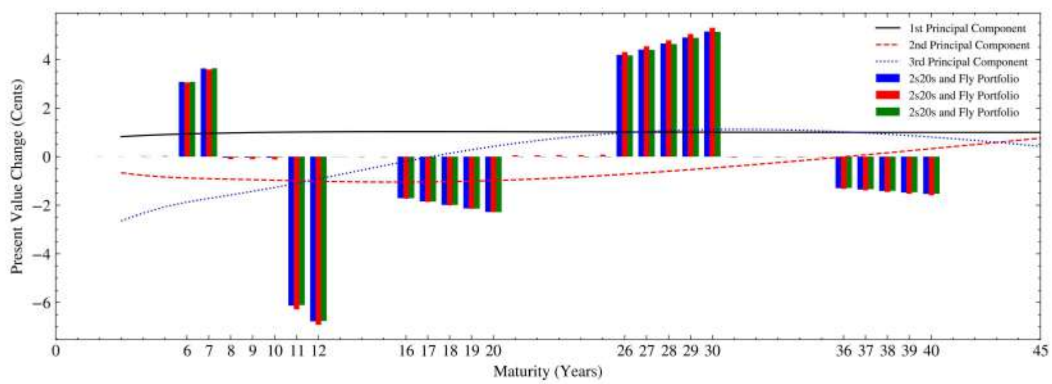


Figure 5.13.: Delta Buckets for combined 2s20s-Fly Portfolio

to the 2s20s Portfolio. Moreover, the third component is significantly less influential on the overall present value of the Fly Portfolio, being almost half as impactful as observed for the 2s20s Portfolio. This suggests that the Fly Portfolio demonstrates a lower exposure to these effects when considering the cumulative sensitivity to various components or typical movements in the swap curve. This implies a reduced sensitivity to common market interventions, such as those initiated by central banks.

### 5.5.3. Analysis of the combined 2s20s-Fly Portfolio

A logical progression is to combine both portfolios and assess their collective exposures. Assuming a notional value of 100 EUR for each of the 30 underlying derivative positions

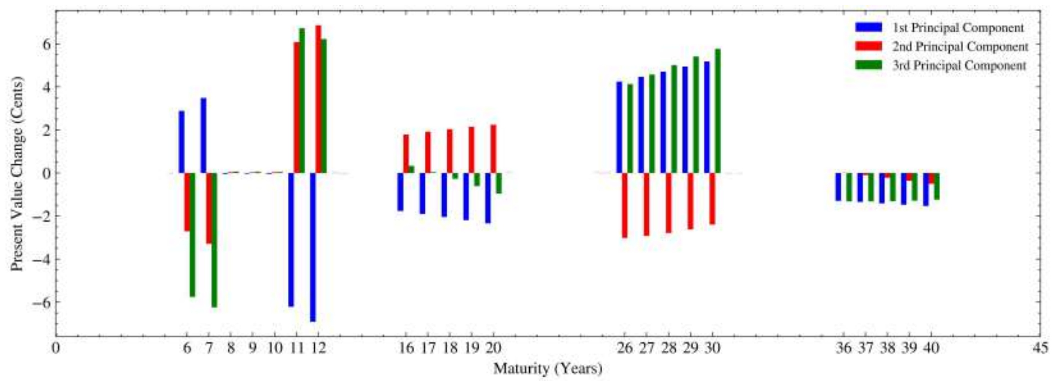


Figure 5.14.: Delta Buckets for combined 2s20s-Fly Portfolio with PCA Shifts

in total leads to the familiar visualization technique shown in Figure 5.13, showcasing the delta buckets and principal components.

Upon multiplying these components, as previously demonstrated and assuming a flat spot curve of 3% again, the outcomes presented in Figure 5.14 emerge. Although this visualization is informative, it becomes increasingly difficult to immediately see all the relative effects of the individual components. For the first principal component, the known offsetting of sensitivities is clear. A similar effect is observed for the second component, even though the sensitivities for maturities 11 and 12, as well as 16 to 20, slightly dominate the combined portfolio's exposure in this component. Regarding the last principal component, it is apparent that the portfolio has significant exposure to longer maturities of 26 to 30, exerting a neutralizing effect on shorter maturities where maturities 6 and 7 offset the sensitivity of maturities 11 and 12.

In terms of the present value change for this consolidated portfolio, the sum of all delta buckets with PCA shifts is retaken, resulting in the outcomes displayed in Figure 5.15. The numerical results align with expectations, as the delta buckets and their corresponding effects are simply aggregated, reflecting the combined impact of each principal component. It is crucial to note that the notional value for all derivatives in this portfolio is higher than before.

Indeed, the combination of both portfolios results in a notable reduction in sensitivity

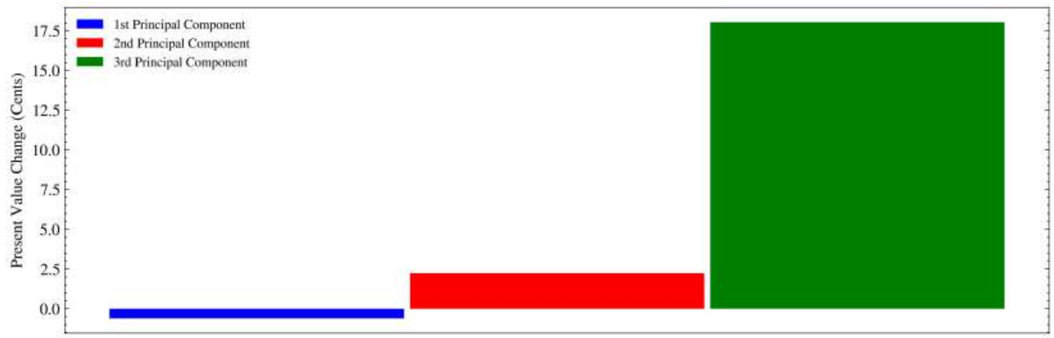


Figure 5.15.: Present Value Change for combined 2s20s-Fly Portfolio with PCA Shifts

to the second principal component. Considering how much each principal component explained in terms of the variance in the daily changes of the swap rates, this combined portfolio appears reasonable, especially given its diminished exposure to the second component. However, it is noteworthy that the exposure to the third component remains high. These insights directly affect a portfolio manager when deciding how to allocate and leverage the total notional value. It underscores the importance of understanding and managing the exposure to different risk factors for effective portfolio management.

## 5.6. Conclusion and Future Research

In this chapter, we initiated the exploration by identifying flat, steep, and inverse swap rate clusters within the historical dataset created in this thesis. We introduced the construction of portfolios incorporating forward swaps and elaborated the methodology for measuring sensitivities in these portfolios. A practical application was then developed independently of the literature, in which the principle components are used with regard to different portfolio sensitivities.

In our analysis, we considered convexity-adjusted forward rates. In practical applications, explicit calculation of convexity adjustments is essential. This involves calculating the costs of replicating a linear payoff using swaptions added to the forward rates.

Exploring further combinations of portfolios for customized portfolio construction tailored to different clusters, specific macroeconomic environments, or expectations remains for future research. The possibilities are vast, constrained primarily by the liquidity of the derivatives in the market. For instance, one could devise a portfolio deliberately engineered to exhibit minimal or even no sensitivity to the third principal component. Similarly, a portfolio could be crafted to simultaneously have the lowest possible exposure across all principal components. These endeavors can contribute to developing strategic portfolios that align with specific risk preferences or market conditions.

One idea would be to start at maturity 3 when doing the PCA, but also to set the boundaries of this axis precisely to the sensitives of the portfolios so that an even higher explained variance can be obtained. As already mentioned in Chapter 4, the effect of the fourth principal component - and possibly further components - should also be investigated.

On top of that, it would be interesting to compare the used approach here to the concept of Principal Component Duration as introduced in [51]. They show how the principal components can be used to construct hedges that neutralize the risk, similar to what we have already suggested. This book also introduces the idea of using factor models, as used in Chapter 3 in the form of the NSS model, to find ways to construct hedges.

Moreover, a practitioner could thoroughly analyze historical data, delving into the effects of each principal component and their factor loadings, e.g., in each of the three clusters. This in-depth analysis might identify indicators that serve as signals for particular shifts in the swap curve, each with its known implications for the portfolio. Consequently, this methodology not only aids in formulating strategic portfolios but also offers the potential to uncover early warning indicators. These indicators could play a crucial role in adjusting portfolio leverage or indicating when it is opportune to reposition the portfolio in response to evolving market dynamics.

# 6. Conclusion and Future Research

**Conclusion** The main objective of this thesis was to advance the application of principal components in the analysis of portfolios and to establish a link between macroeconomic events and their impact on the swap curve, thereby influencing portfolio dynamics. To achieve this, a large database was created in which government bonds and swaps on the European market were brought together to create an extended historical scope. A Brownian bridge was used to convert monthly bond data into a daily format and ensure a seamless transition from bonds to swaps in October 1989. This fundamental step was crucial in providing a robust dataset for later analyses.

The prior development of a comprehensive yield curve further laid the groundwork for the investigation. This provided the framework for the subsequent investigation of the principal components and their interaction with macroeconomic factors.

The application of Principal Component Analysis (PCA) to the swap curve in conjunction with its macroeconomic interpretation confirmed the results, which are consistent with the analyses in the existing literature, although the literature often only analyzed maturities of up to 10 or 25 years. This agreement confirms the robustness of the methodology used.

Independently of the existing literature, an innovative approach involving clustering historical data was introduced. This was followed by a quantitative analysis of the sensitivity of sample portfolios to the first three principal components. The results of this approach highlight the significant influence of the individual components. These findings underscore the possibility for portfolio managers to control the sensitivity of their portfolios to general swap rate changes through careful analysis and strategic decision-making.

**Chapter 2** In Chapter 2, the chosen approach aimed to expand the dataset by including Deutsche Mark swaps and German government bonds. This decision was based on the consideration that a larger dataset offers greater potential for in-depth analysis. By combining Deutsche Mark swaps and German government bonds, we wanted to take advantage of the amount of information contained in these financial instruments.

The expectations underlying this approach were based on the existing literature, highlighting the similarities in the evolution of government bond yields and swap rates. In addition, examples from the literature illustrated the utility of Deutsche Mark swaps as an extension of Euro swaps, further supporting the feasibility of our chosen methodology. The decision to focus on Deutsche Mark swaps was supported by the importance of the German economy at the time, making it a central player in the European financial landscape and a very liquid market.

The results of this methodology confirmed our expectations. The correlation between the bond data and the interest rate swaps was over 99% in the period after 1998, confirming the validity of the dataset extension to include government bonds. The inclusion of Deutsche Mark swaps was underpinned by the close alignment of the swap curves in the 1998/99 transition period. In essence, the results of Chapter 2 confirm the effectiveness of our approach to extending the dataset for further analyses.

**Chapter 3** In Chapter 3, the methodology for constructing the yield curve was a central aspect, with the choice between cubic interpolation and the Nelson-Siegel-Svensson (NSS) model at the center of the analysis. The decision to investigate these approaches was motivated by the fact that they are widely used in financial markets, as evidenced by the literature documenting their use by different countries and market participants. The main objective was to use a method that enables the calculation of individual sensitivities across all maturities and, thus, specific portfolio analyses.

Cubic interpolation was expected to be more accurate as it retains the original data points. However, this retention could cause problems in the shape of the first two derivatives and, in turn, in calculating discount factors and consequently in determining forward rates - especially for older historical datasets. On the other hand, the NSS model should ensure smoothness at the expense of precision, particularly given the optimization process involved. Using the Adam optimizer with an extensive number of 200,000 epochs was expected to reduce the problems associated with finding an optimum and provide a robust and reliable yield curve.

The results were broadly in line with the original expectations. Analytically, the expected trade-off between precision and smoothness was confirmed and visually demonstrated, with comparisons to existing literature providing additional validation. The successful implementation of the Adam Optimizer further strengthened the reliability of the NSS model. However, the critical decision point arose when the wider application of the yield curve in the following analyses, such as PCA or clustering, was considered. It became clear that it was wise to sacrifice some precision to obtain smoother curve shapes. This was even more important when dealing with bond data limited to maturities of up to 10 years, which required additional calculations for longer maturities. Unlike cubic interpolation, the NSS model has proven to smooth out inaccurate longer run times, which runs through each data point without such adjustments. At its core, the results of Chapter 3 confirmed the analytical expectations but also provided a clear guideline for selecting the appropriate methodology based on the specific requirements of the later analyses.

**Chapter 4** In Chapter 4, the focus shifted to applying PCA to the swap curve due to a large body of literature demonstrating its utility. The overall aim was to use PCA to uncover underlying patterns in the swap curve and establish a link between these patterns and macroeconomic scenarios or influences.

The expectations guiding this approach were that the first three principal components could be interpreted as parallel shift, slope, and curvature change, respectively. Furthermore, these components were expected to account for a significant proportion of the variance, specifically when performing PCA on the daily changes of the yield curve.

The results not only met but exceeded these expectations. The first three principal components were successfully interpreted as representing parallel shift, slope, and curvature change, which closely matched the existing literature. Further investigations looked at the next components and their influence on the daily changes, allowing a more detailed understanding of the dynamics. The creative approach of excluding the first three years of the swap curve for fine-tuning the PCA resulted in a higher variance explanation and smoother components, contributing to a more accurate interpretation. The close similarity of the component shapes to those found in the literature, despite the longer historical period and the incorporation of additional maturities of up to 60, further confirmed the robustness of the results.

Another aspect introduced in this chapter was the interpretation of factor loadings, which allowed for a deeper examination of historical events and the identification of specific periods, such as the notable period in late 1998, through the factor loadings of the second component. This analysis provided valuable insights into the relationships between macroeconomic events and yield curve dynamics. In addition, this chapter highlights the limitations of the Brownian bridge in mimicking daily changes. Identifying areas where the Brownian bridge was less effective contributed to a refined understanding of its application while highlighting its superiority over alternative methods, such as linear interpolation.

In conclusion, Chapter 4 not only confirmed the expected results of PCA for a yield curve but also extended the analysis to include factor loadings, comparisons of historical events, and a critical evaluation of the effectiveness of the Brownian bridge. This thorough approach enriched the understanding of the relationship between the swap curve and macroeconomic influences.

**Chapter 5** Chapter 5 explored the practical challenges of incorporating PCA and the swap curve in the context of portfolio analysis. The idea of this approach can be traced back to the future research concepts formulated towards the end of Chapter 4, where the intention was to deepen the analysis of unlike economic paradigms. As part of this proposition, clustering swap rate curves emerged. The central question was how to quantitatively measure the differences within these clusters and use this information for portfolio analysis. The final solution was to use delta buckets to analyze the sensitivities of the portfolio.

It was expected that the interest rate level would impact the overall sensitivity of the portfolio and that the different average curves of each cluster would have distinct degrees of sensitivity. Given the delta neutrality of each portfolio, it was also expected that the first principal component would have no impact. As a unique combination of techniques, the analysis was based on minimal baseline expectations and left room for exploring and quantifying its impacts.

The results of the portfolio analysis were consistent with the expectations. The level of interest rates did indeed affect the portfolio's sensitivity to changes in an interest rate, while the overall relative behavior remained consistent across all delta buckets. The results for the average curve of each cluster were slightly weaker than expected. Still, they showed recognizable differences, especially when comparing the sensitivity of the inverse and steep curves at extremely short and long maturities.

There was significant confirmation in relation to the first principal component, as it was quantified and confirmed to have no impact on the portfolio, which was in line with initial expectations. However, the most convincing findings came from analyzing the different portfolios and their sensitivity to the principal components. In particular, the Fly portfolio showed a lower sensitivity to the third component, and the ability to quantify and compare the impact of each component on different portfolios provided valuable insights for further application.

In addition, the combination of the two portfolios revealed an interesting dynamic, showing an opposite effect on the sensitivity to the second principal component while enhancing the impact of the third component. These results confirmed expectations, deepened the understanding of portfolio behavior in response to principal components, and offered practical insights for portfolio managers. In conclusion, Chapter 5 successfully overcame the challenge of incorporating PCA and the swap curve into portfolio analysis and revealed nuanced insights into the sensitivity of portfolios to various principal components.

**Future Research** In concluding this master's thesis, the research has provided valuable insights and paved the way for future portfolio analysis and yield curve dynamics research. The findings highlight several directions practitioners and researchers could consider to refine methods and gain a deeper understanding.

One notable recommendation is to fine-tune the Brownian bridge or explore alternative methods to increase the realism of daily movements, specifically in the context of PCA results. Improving the modeling of daily movements is a crucial factor for more accurate and insightful analyses.

In addition, research into alternative techniques for constructing yield curves beyond cubic interpolation and the NSS model is encouraged. A comparative analysis of the residuals obtained by reconstructing data with the first three principal components using different construction techniques, including the study of monotonic convex interpolation, could contribute to more robust and refined results.

The proposal to extend the analysis to other markets, such as the United States, is also a promising way forward. Daily data is available in the US from 1962 onwards, so there is an opportunity to gain a broader and more complete understanding of yield curve dynamics. The proposed use of a Brownian bridge can then be used again to transition from bonds to swaps.

The portfolio analysis presented in Chapter 5 opens the door for further research. It might be worthwhile to develop new portfolios, run optimization problems over the space of possible derivative combinations, and look for different optimal portfolios based on specific desired exposures to principal components. Considering the potential influence of the fourth principal component on the daily changes adds an additional layer of complexity that could improve the analysis.

The detailed analysis of the diverse clusters is also promising for future research. Conducting a PCA for each cluster or examining the factor loadings in more detail could reveal patterns that could serve as early indicators of macroeconomic change and provide valuable insights for practitioners.

Simulations with different interest rate models are another promising approach. Examining the established principal components and their impact on portfolios in different scenarios using various models could improve understanding of the correlation between interest rate dynamics and portfolio returns. This analysis can help to construct a more resilient portfolio for the future.

Finally, introducing the concept of principal component duration offers a convincing way of hedging against non-parallel shifts in yield curves. Examining this alternative approach to principal component hedging can provide practitioners with additional risk management tools.

In summary, the conclusions and outlook of this master's thesis highlight the potential for refinements and enhancements in various aspects of portfolio analysis, yield curve modeling, and risk management. The recommendations outlined here provide a roadmap for practitioners and researchers to advance the field of financial mathematics, macroeconomics, and portfolio management and deepen their understanding of the complex dynamics of financial markets.

# Bibliography


[1] K. J. Adams and D. R. Van Deventer, "Fitting yield curves and forward rate curves with maximum smoothness", *The Journal of Fixed Income*, vol. 4, no. 1, pp. 52–62, 1994.

[2] L. Andersen and V. Piterbarg, *Interest Rate Modeling Volume 1: Foundations and Vanilla Models*. Atlantic Financial Press, 2010.

[3] L. Andersen, "Discount curve construction with tension splines", *Review of Derivatives Research*, vol. 10, no. 3, pp. 227–267, 2007.

[4] L. Bartolini, "Foreign exchange swaps", *New England Economic Review*, pp. 11–13, 2002.

[5] A. Belke and T. Polleit, *Monetary economics in globalised financial markets*. Springer Science & Business Media, 2010.

[6] M. Bianchetti, "Two curves, one price: Pricing & hedging interest rate derivatives decoupling forwarding and discounting yield curves", *One Price: Pricing & Hedging Interest Rate Derivatives Decoupling Forwarding and Discounting Yield Curves*, 2008.

[7] R. R. Bliss, "Testing term structure estimation methods", Working Paper, Tech. Rep., 1996.

[8] D. Brigo and F. Mercurio, *Interest rate models-theory and practice: with smile, inflation and credit (Section 1.4)*. Springer, 2006, vol. 2.

[9] W. T. Carleton and I. A. Cooper, "Estimation and uses of the term structure of interest rates", *The Journal of Finance*, vol. 31, no. 4, pp. 1067–1083, 1976.

[10] R. Carmona and M. R. Tehranchi, *Interest rate models: an infinite dimensional stochastic analysis perspective*. Springer Science & Business Media, 2007.

[11] R. A. Carmona, *Statistical analysis of financial data in S-Plus*. Springer, 2004.

[12] O. Castello and M. Resta, "Modeling the yield curve of brics countries: Parametric vs. machine learning techniques", *Risks*, vol. 10, no. 2, p. 36, 2022.

[13] A. S. Cheam and M. Fredette, "On the importance of similarity characteristics of curve clustering and its applications", *Pattern Recognition Letters*, vol. 135, pp. 360–367, 2020.

[14] J. H. E. Christensen, F. X. Diebold, and G. D. Rudebusch, "The affine arbitrage-free class of nelson-siegel term structure models", *Capital Markets: Asset Pricing & Valuation*, 2007.

[15] J. H. Christensen, F. X. Diebold, and G. D. Rudebusch, *An arbitrage-free generalized nelson–siegel term structure model*, 2009.

[16] K. J. Cohen, R. L. Kramer, and W. H. Waugh, "Regression yield curves for us government securities", *Management science*, vol. 13, no. 4, B–168, 1966.

[17] J. C. Cox, J. E. Ingersoll Jr, and S. A. Ross, "A theory of the term structure of interest rates", in *Theory of valuation*, World Scientific, 2005, pp. 129–164.

[18] Q. Dai and K. J. Singleton, "Specification analysis of affine term structure models", *The journal of finance*, vol. 55, no. 5, pp. 1943–1978, 2000.

[19] R. Dalio, *Principles for navigating big debt crises*. Simon and Schuster, 2022.

[20] P. De Grauwe, *Economics of the monetary union*. Oxford University Press, USA, 2020.

[21] R. B. De Rezende and M. S. Ferreira, "Modeling and forecasting the yield curve by an extended nelson-siegel class of models: A quantile autoregression approach", *Journal of Forecasting*, vol. 32, no. 2, pp. 111–123, 2013.

[22] F. X. Diebold and G. D. Rudebusch, *Yield curve modeling and forecasting: the dynamic Nelson-Siegel approach (Chapter 2)*. Princeton University Press, 2013.

[23] P. F. Du Preez and E. Maré, "Interpolating yield curve data in a manner that ensures positive and continuous forward curves", *South African Journal of Economic and Management Sciences*, vol. 16, no. 4, pp. 395–406, 2013.

[24] M. E. Echols and J. W. Elliot, "Forecasting versus allocational efficiency in bank asset planning an integrated evaluation", *Journal of Bank Research*, vol. 6, no. 4, pp. 283–295, 1976.

[25] E. F. Fama and R. R. Bliss, "The information in long-maturity forward rates", *The American Economic Review*, pp. 680–692, 1987.

[26] D. Filipovic, *Term-Structure Models. A Graduate Course.* Springer, 2009.

[27] G. Fusai and A. Roncoroni, *Implementing models in quantitative finance: methods and cases.* Springer, 2008, vol. 1.

[28] P. S. Hagan and G. West, "Interpolation methods for curve construction", *Applied Mathematical Finance*, vol. 13, no. 2, pp. 89–129, 2006.

[29] P. S. Hagan and G. West, "Methods for constructing a yield curve", *Wilmott Magazine, May*, pp. 70–81, 2008.

[30] J. Handa, *Monetary economics (Part 4).* Routledge, 2002.

[31] J. Healy, "Equivalence between forward rate interpolations and discount factor interpolations for the yield curve construction", 2020.

[32] D. Heath, R. Jarrow, and A. Morton, "Bond pricing and the term structure of interest rates: A new methodology for contingent claims valuation", *Econometrica: Journal of the Econometric Society*, pp. 77–105, 1992.

[33] T. S. Ho and S.-B. Lee, "Term structure movements and pricing interest rate contingent claims", *the Journal of Finance*, vol. 41, no. 5, pp. 1011–1029, 1986.

[34] J. C. Hull, *Options futures and other derivatives (Chapter 4).* Pearson Education India, 2003.

[35] I. T. Jolliffe, "Principal component analysis and factor analysis", 1986.

[36] N. Karouzakis, J. Hatgioannides, and K. Andriosopoulos, "Convexity adjustment for constant maturity swaps in a multi-curve framework", *Annals of Operations Research*, vol. 266, pp. 159–181, 2018.

[37] N. Kazemie, *Mispricing due to nelson-siegel-svensson model*, 2014.

[38] T. Koller, M. Goedhart, D. Wessels, *et al.*, *Valuation: measuring and managing the value of companies.* john Wiley and sons, 2010, vol. 499.

[39] A. Lakhany, A. Pintar, and A. Zhang, "Calibrating the nelson-siegel-svensson model by genetic algorithm", 2021.

[40] R. B. Litterman and J. Scheinkman, "Common factors affecting bond returns", *The journal of fixed income*, vol. 1, no. 1, pp. 54–61, 1991.

[41] J. H. McCulloch, "Measuring the term structure of interest rates", *the Journal of Business*, vol. 44, no. 1, pp. 19–31, 1971.

[42] J. H. McCulloch, "An estimate of the liquidity premium", *Journal of Political Economy*, vol. 83, no. 1, pp. 95–119, 1975.

[43] J. H. Mcculloch and H. C. Kwon, "U.s. term structure data, 1947-1991", 1993.

[44] A. J. McNeil, R. Frey, and P. Embrechts, *Quantitative risk management: concepts, techniques and tools-revised edition.* Princeton university press, 2015.

[45] P. Miron and P. Swannell, *Pricing and hedging swaps (Section 4.3 and Chapter 8).* Euromoney Inst Investors Plc, 1991.

[46] A. d'Almeida Monteiro, "Estimating interest rate curves by support vector regression", *Econometric Reviews*, vol. 29, no. 5-6, pp. 717–753, 2010.

[47] L. Muthoni *et al.*, "In search of the best zero coupon yield curve for nairobi securities exchange: Interpolation methods vs. parametric models", *Journal of Mathematical Finance*, vol. 5, no. 04, p. 360, 2015.

[48] L. Muthoni, S. Onyango, and N. O. Ongati, "Construction of nominal yield curve for nairobi securities exchange: An improvement on monotone preserving r(t)t interpolation method", 2015.

[49] K. Pearson, "Principal components analysis", *The London, Edinburgh, and Dublin Philosophical Magazine and Journal of Science*, vol. 6, no. 2, p. 559, 1901.

[50] S. Peluso, A. Mira, and P. Muliere, "Robust identification of highly persistent interest rate regimes", *International Journal of Approximate Reasoning*, vol. 83, pp. 102–117, 2017.

[51] P. Priaulet, F. J. Fabozzi, and L. Martellini, "Advanced bond portfolio management", 2006.

[52] R. Rebonato, *Interest-rate option models: understanding, analysing and using models for exotic interest-rate options*. Wiley, 1996.

[53] R. Rebonato, *Bond pricing and yield curve modeling: A structural approach (Section 2.2.1)*. Cambridge University Press, 2018.

[54] A. Sadr, *Interest rate swaps and their derivatives: A practitioner's guide (Chapter 1-3)*. John Wiley & Sons, 2009, vol. 510.

[55] D. G. Schweikert, "An interpolation curve using a spline in tension", *J. Math. Phys*, vol. 45, no. 3, pp. 312–317, 1966.

[56] M. B. Seasholtz and B. Kowalski, "The parsimony principle applied to multivariate calibration", *Analytica Chimica Acta*, vol. 277, no. 2, pp. 165–177, 1993.

[57] G. S. Shea, "Pitfalls in smoothing interest rate term structure data: Equilibrium models and spline approximations", *Journal of Financial and Quantitative Analysis*, vol. 19, no. 3, pp. 253–269, 1984.

[58] G. S. Shea, "Interest rate term structure estimation with exponential splines: A note", *Journal of Finance*, vol. 40, pp. 319–325, 1985.

[59] S. E. Shreve *et al.*, *Stochastic calculus for finance II: Continuous-time models (Section 4.7)*. Springer, 2004, vol. 11.

[60] J. M. Steeley, "Modelling the dynamics of the term structure of interest rates", *Economic and Social Review*, 1990.

[61] L. E. Svensson, *Estimating and interpreting forward interest rates: Sweden 1992-1994*, 1994.

[62] N. N. Taleb, "Statistical consequences of fat tails: Real world preasymptotics, epistemology, and applications (chapter 3-6)", 2020.

[63] G. Tang, R. Tian, and B. Wu, "An overview of clustering methods in the financial world", in *7th International Conference on Financial Innovation and Economic Development (ICFIED 2022)*, Atlantis Press, 2022, pp. 524–529.

[64] L. Van Der Maaten, E. O. Postma, H. J. van den Herik, *et al.*, "Dimensionality reduction: A comparative review", *Journal of Machine Learning Research*, vol. 10, no. 66-71, p. 13, 2009.

[65] O. Vasicek, "An equilibrium characterization of the term structure", *Journal of financial economics*, vol. 5, no. 2, pp. 177–188, 1977.

[66] O. A. Vasicek and H. G. Fong, "Term structure modeling using exponential splines", *The Journal of Finance*, vol. 37, no. 2, pp. 339–348, 1982.

[67] T. Wei and B. Wang, "A novel curve clustering method for functional data: Applications to covid-19 and financial data", *Analytics*, vol. 2, no. 4, pp. 781–808, 2023.

[68] J. Wiseman, "The magpie yield curve model", J.P. Morgan - Fixed Income Research, Tech. Rep., 1998.

[69] J. Wiseman, "The magpie yield curve model at sg", Societe Generale Cross Asset Research - Fixed Income, Tech. Rep., 2012.

# A. Appendix

## A.1. Implementation of the Nelson Siegel Svensson Model

```
# Import all Packages
import jax
import jax.numpy as jnp
from jax import grad, jit
from jax.example_libraries import optimizers

# Define the Nelson Siegel Svensson Function
@jax.jit
def nss(params, t):
    beta0, beta1, beta2, beta3, tau1, tau2 = params
    term1 = beta0
    term2 = beta1 * ((1 - jnp.exp(-t / tau1)) / (t / tau1))
    term3 = beta2 * (((1 - jnp.exp(-t / tau1)) / (t / tau1))
            - jnp.exp(-t / tau1))
    term4 = beta3 * (((1 - jnp.exp(-t / tau2)) / (t / tau2))
            - jnp.exp(-t / tau2))
    return term1 + term2 + term3 + term4

# Define the Loss Function
@jax.jit
```

```
def loss(params, t, y):
    y_pred = nss(params, t)
    return jnp.mean((y_pred - y)**2)

# Define the Update Function for the Optimizer
@jax.jit
def update(i, opt_state, t, y):
    params = get_params(opt_state)
    gradient = grad(loss)(params, t, y)
    return opt_update(i, gradient, opt_state)

# Preparation Steps
date_column = swaprates.index
t = jnp.array(swaprates.columns.astype(int))
all_parameter = []

# Loop through each Date and fit the NSS Model
for i in range(len(swaprates)):
    row = jnp.array(swaprates.iloc[i])
    mask = jnp.logical_not(jnp.isnan(row))
    t_mask = t[mask]
    row_mask = row[mask]
    epoch_results = []
    params = jnp.array([0.1, 0.5, 0.0, 1.0, 1.0, 5.0])
    opt_init, opt_update, get_params = optimizers.adam()
    opt_state = opt_init(params)

    # Training Loop
    for epoch in range(200000):
```

```
        opt_state = update(epoch, opt_state, t_mask, row_mask)
        params = get_params(opt_state)
        loss_value = loss(params, t_mask, row_mask)
    all_parameter.append(params)
```

## A.2. Code

| | |
|---|---|
| Chp2_01_Calculate_Longer_Maturities.ipynb | All notebooks from the 2nd Chapter |
| Chp2_02_Linear_Interpolation_vs_Brownian_... | All notebooks from the 2nd Chapter |
| Chp2_03_Proximity_Approach.ipynb | All notebooks from the 2nd Chapter |
| Chp2_04_Correlation_Bonds_Swaps.ipynb | All notebooks from the 2nd Chapter |
| Chp3_01_Cubic_Interpolation.ipynb | All notebooks from the 3rd Chapter |
| Chp3_02_NSS_Model_JAX.ipynb | All notebooks from the 3rd Chapter |
| Chp3_03_Cubic_vs_NSS_Analysis.ipynb | All notebooks from the 3rd Chapter |
| Chp4_01_PCA_Swap_Rates.ipynb | Notebook from the 4th Chapter |
| Chp5_01_Cluster_Analysis.ipynb | All notebooks from the 5th Chapter |
| Chp5_02_Portfolio_Analysis.ipynb | All notebooks from the 5th Chapter |

Figure A.1.: Overview of All Python Jupyter Notebooks

The analysis code used in this thesis is accessible in the designated GitHub repository, which is organized according to the individual chapters of the thesis in a total of ten Jupyter Notebooks as seen in Figure A.1. It can be accessed via the following link: https://github.com/G-Sell-09/masterthesis. Users with data on government bonds or swaps can run each notebook in turn, perform the analyses explained in this thesis, and create the corresponding graphs. To gain access to the repository, simply contact the author of the thesis.

# Eidesstattliche Erklärung

Hiermit versichere ich an Eides statt, dass ich die vorliegende Arbeit selbstständig und ohne die Benutzung anderer als der angegebenen Hilfsmittel angefertigt habe. Alle Stellen, die wörtlich oder sinngemäß aus veröffentlichten und nicht veröffentlichten Schriften entnommen wurden, sind als solche kenntlich gemacht. Die Arbeit ist in gleicher oder ähnlicher Form oder auszugsweise im Rahmen einer anderen Prüfung noch nicht vorgelegt worden. Ich versichere, dass die eingereichte elektronische Fassung der eingereichten Druckfassung vollständig entspricht.[1]

Ort, Datum Unterschrift

[1] I hereby declare in lieu of an oath that I have written this thesis independently and without the use of any sources other than those indicated. All passages taken verbatim or in spirit from published and unpublished works are identified as such. The thesis has not yet been submitted in the same or similar form or in extracts as part of another examination. I hereby confirm that the electronic version submitted corresponds in full to the print version submitted.